Metal ion catalysis of s-nitrosothiol decompositions

Helen R. Swift

METAL ION CATALYSIS OF S-NITROSOTHIOL DECOMPOSITIONS

by

Helen R. Swift, B.Sc. (Hons.)

(Graduate Society)

A thesis submitted for the degree of Doctor of Philosophy in the Department of Chemistry, University of Durham
December 1996

METAL ION CATALYSIS OF S-NITROSOTHIOL DECOMPOSITIONS

by Helen R. Swift

A thesis submitted for the degree of Doctor of Philosophy in the Department of Chemistry, University of Durham, December, 1996.

ABSTRACT

Most S-nitrosothiols (RSNO) are unstable in aqueous solution and decompose to release nitric oxide. This is catalysed by copper ions. A mechanistic study of NO formation from S-nitrosoglutathione (GSNO), the nitroso derivative of the most abundant thiol in the body, was carried out. This relatively stable S-nitrosothiol decomposed in the presence of reduced glutathione and copper ions. The products were identified as nitric oxide and oxidised glutathione, observed as a complex of copper. The role of reduced glutathione was two fold. Firstly, it reduced Cu^{2+} to produce the active Cu^{+} catalytic species and regenerated the catalyst from the oxidised glutathione complex. Spectrophotometric kinetic measurements, under pseudo first order conditions ([GSNO]>>[Cu^{2+}]) showed no conventional order with respect to nitrosothiol. This was attributed to the inconstant concentration of available copper during reaction due to the ability of reduced glutathione to complex Cu^{+} and oxidised glutathione to complex Cu^{2+}.

An investigation of thiol induced decomposition of GSNO and other more stable nitrosothiols showed the reaction to be first order with respect to thiol and nitrosothiol. The rate equation was determined and has been explained in terms of a radical mechanism involving rate limiting attack of the thiyl radical on the RS-NO bond.

The decomposition of S-nitrosothiols via the mercuric ion was also investigated. Reactions were stoichiometric rather than catalytic, and the products determined to be $H_2NO_2^{+}$ and $RSHg^{+}$. The rate equation was established and the reaction found to be first order in S-nitrosothiol and Hg^{2+}. Second order rate constants obtained for a variety of nitrosothiols showed no dependency of the rate of the reaction on the structure of R. A mechanism was proposed involving direct attact of the Hg^{2+} ion on S of the nitroso group, reflecting the high affinity of the metal ion for the sulfur atom. Similarly, an investigation into Ag^{+} mediated S-nitrosothiol decomposition showed the reaction to be stoichiometric. Nitric oxide was not a product of this reaction.

ACKNOWLEDGEMENTS

I would like to take this opportunity to thank my supervisor, Prof. D. Lyn H. Williams, for his advice and guidance throughout this Ph.D., and Colin Greenhalgh for his help with the computer software and for keeping all the machines well maintained.

Special thanks to my colleague, Andy Dicks, for the many useful lab. discussions, his time spent proof reading this thesis and his help and encouragement over the last two years. I would also like to thank my other fellow workers; Simon Lord, Alex Eberlin, Ian Robotham, Jonathan Barnett and Gaynor Duffield for making my time in Durham so enjoyable.

I would like to thank Denise, Joan, Tracy, Sam, Sandra, Marie, Lynne, Irene and Judith, collectively known as the Hetton Hotshots Netball Club, for a great season (and the many enjoyable Friday nights spent in Sunderland!).

I am indebted to my family who have encouraged and supported me every step of the way, and to Bertha, for always being there.

Last but not least, thanks to Samantha Wheale and Theresa Regan for their unremitting help and support over the last few years.

I would like to thank Durham University for funding this research.

DECLARATION

The material in this thesis is the result of research carried out in the Department of Chemistry, University of Durham, between October 1993 and September 1996. It has not been submitted for any other degree and is the author's own work, except where acknowledged by reference.

STATEMENT OF COPYRIGHT

to my mum

CONTENTS

Chapter 1:

Introduction

Chapter 1: Introduction

1.1 The Physiological Role Of Nitric Oxide

1.1.1 Introduction

Nitric oxide is a colourless gas at room temperature with a bp. of -151.8^{0}C and mp. of -163^{0}C. Its solubility in water at 25^{0}C and 1atmosphere is 1.8x10^{-3}mol dm^{-3} which does not change with pH. Its structure can be represented by the canonical forms shown in fig. 1.1.

Figure 1.1

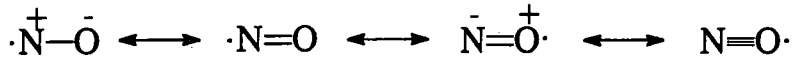

The unpaired electron reduces the bond order to 2.5 (bond order is c.a. 3 in NO^+) but as the electron density is distributed over the whole molecule, dimerisation is not normally observed. Car exhaust emissions of nitric oxide are a major source of air pollution due to the partial oxidation of NO to NO_2 resulting in photochemical smogs. Additionaly, the depletion of the ozone layer via nitric oxide released by engines of supersonic aircraft has become increasingly worrying.

However, the discovery of the physiological importance of nitric oxide in the late 1980s has lead to a renewed interest in this molecule and has opened a completely new area of NO research, reviewed by Moncada *et al*[1] and Butler *et al*[2].

1.1.2 Endothelium Derived Relaxing Factor

Acetylcholine (to name but one) is known to cause the relaxation of blood vessels. Furchgott *et al*[3] were the first to demonstrate that the presence of endothelial cells was obligatory for this action. It was shown that relaxation was mediated by a substance, later labelled endothelium derived relaxing factor (EDRF), which was produced by the cells in response to stimuli. EDRF, which has a half life of only seconds in aqueous solution[4], stimulates the enzyme, guanylate cyclase. This enzyme catalyses the conversion of guanosine triphosphate (GTP) (1.1) to cyclic guanosine

monophosphate (cGMP) (1.2). The increased levels of cGMP due to enzyme activation by EDRF causes smooth muscle relaxation[1].

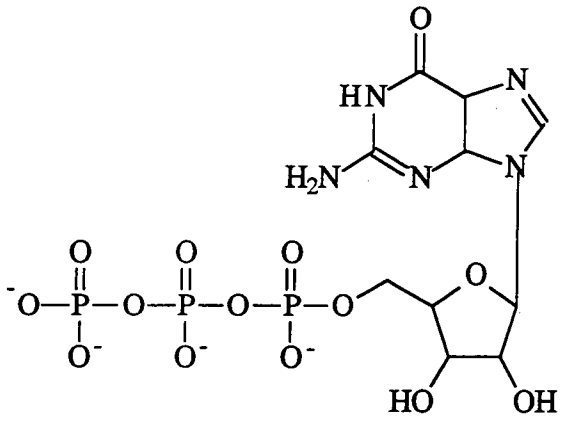

(1.1)

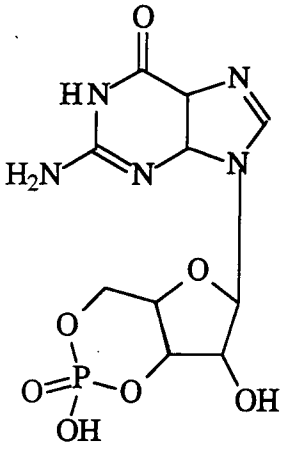

(1.2)

In 1987, EDRF, produced from stimulated cells, was subjected to a chemiluminescent assay for NO[5]. The assay was the reaction of NO with ozone[6] (scheme 1.1).

$$NO + O_3 \longrightarrow NO_2^* + O_2$$

$$NO_2^* \longrightarrow NO_2 + hv$$

scheme 1.1

Not only was it detected but the concentration of NO was sufficient to account for the observed relaxation. A comparison of their biological reactivity showed EDRF and

NO to be indistinguishable, and explained why the vasodilatory action of EDRF was inhibited by haemoglobin[7] (since NO reacts with haemoglobin) and prolonged by superoxide dismutase[8] (this enzyme removes the superoxide ion which is known to react with NO). However, the actual identity of EDRF is still a matter of some controversy. Many people disbelieve that this simple gaseous molecule can act as a physiological messenger molecule, especially as its reaction with molecular oxygen in solution appears to be favourable ($-d[NO]/dt = k[O_2][NO]^2$ where $k = 9 \times 10^6$ mol^{-2} dm^6 s^{-1} at 25°C [9])(eqn. 1.1).

$$4NO + O_2 + 2H_2O \longrightarrow 4NO_2^- + 4H^+$$

(eqn. 1.1)

However, even in aqueous solutions, where $[O_2] \sim 1 \times 10^{-4}M$, the half life of NO is several hours; sufficiently stable to act as a messenger molecule. However, the potency of EDRF was shown to be more like that of low molecular weight nitrosothiols, such as S-nitrosocysteine, than NO[10]. In 1991, Vanin[11] proposed that EDRF could in fact be a di-nitrosyl iron complex (DNIC) and later observed[12] the vasodilatory response of rat aorta to DNIC. However, Feelisch *et al*[13] later showed that both nitrosothiol and DNIC were less susceptible to vasorelaxant inhibition by haemoglobin. By observing the relaxing actions of these compounds on de-endothelialised rabbit aortic rings, found S-nitrosocysteine too potent to be EDRF and DNIC equipotent, but with a much longer lasting effect than EDRF. They maintained that NO was still the most likely candidate for EDRF. However, whatever EDRF is, it is clear that the biological effects of EDRF are mediated ultimately by nitric oxide.

1.1.3 Biosynthesis Of Nitric Oxide

Nitric oxide is synthesised, *in vivo*, from the amino acid, L-arginine[14]. The synthesis is catalysed by the enzyme, nitric oxide synthase (NOS). L-arginine is oxidised by this enzyme to produce NO and L-citrulline[15] as shown in eqn. 1.2.

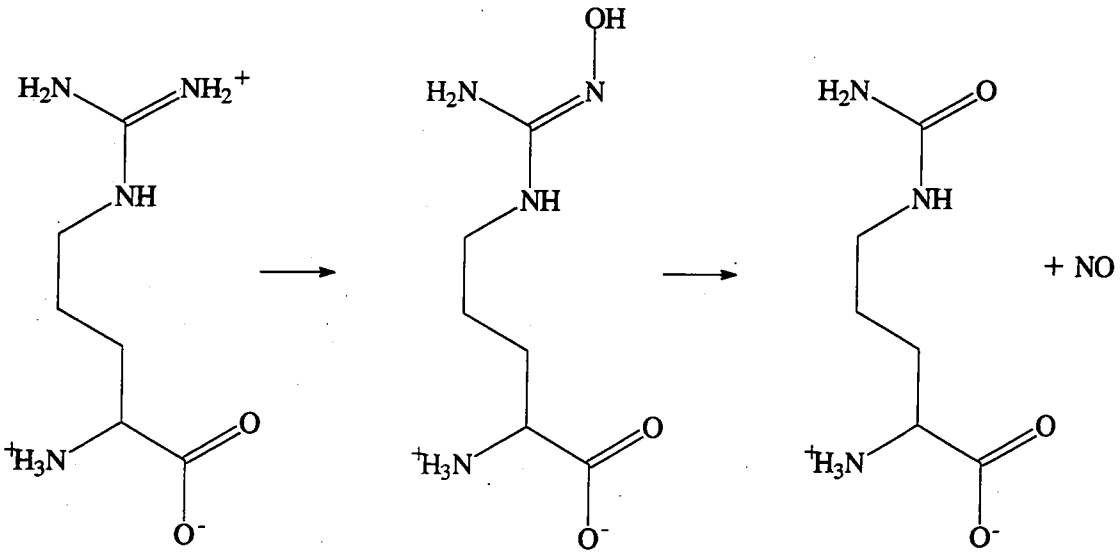

(eqn. 1.2)

Hydroxylation of L-arginine forms the enzyme bound N^9-hydroxy-L-arginine intermediate which subsequently undergoes a three elctron oxidation followed by carbon- nitrogen bond cleavage. The enzyme is enantiomerically substrate specific and can be inhibited by using derivatives of L-arginine such as N-monomethyl-L-arginine (L-NMMA) and N-nitro-L-arginine methyl ester[16] ((1.3) and (1.4)).

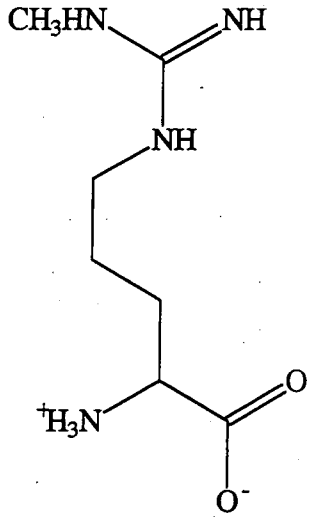

(1.3)

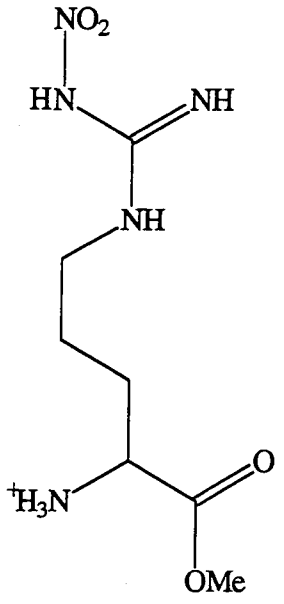

(1.4)

To date, two types of NOS have been isolated; a constitutive enzyme found in the endothelium, brain and platelets, and an inducible enzyme isolated from

macrophages (discussed later). The constitutive enzyme, meaning it is present all the time, rapidly responds to stimuli to produce picomoles of nitric oxide. NADPH, Ca^{2+} and calmodulin (a protein which binds calcium ions) are associated with its activation. To avoid constriction of arteries, it appears NO is produced continuously via this enzyme[2]. Figure 1.2 gives a diagrammatic representation of the processes involved in smooth muscle relaxation and includes the mode of action of vasodilators which will be discussed in section 1.3.

Figure 1.2

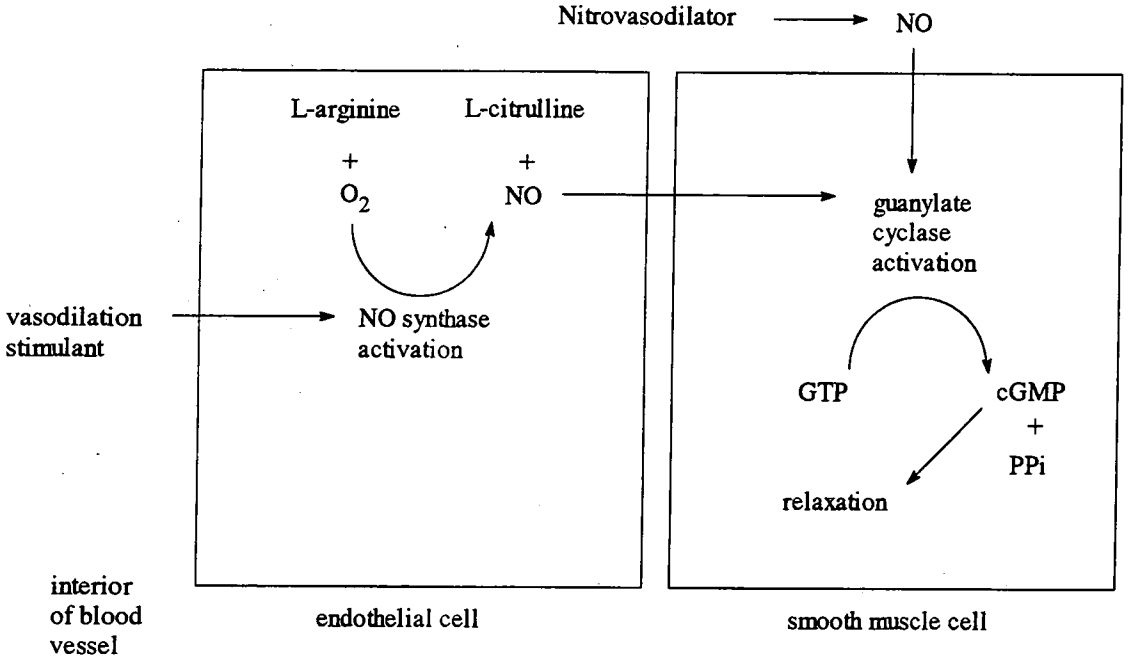

1.1.4 Regulation of Platelet Aggregation

Platelets are granules which naturally occur in blood plasma. When a blood vessel bursts, platelets aggregate and adhere to the cell wall to stop bleeding. This action is controlled internally via nitric oxide which acts as a form of feedback[17]. Platelets produce NO from L-arginine in response to stimuli such as adenosine 5'-diphosphate arachidonic acid and thrombin. NO activates guanylate cyclase and the resulting increased levels of cGMP attenuate platelet aggregation[18]. The mechanism by which this is done is, as yet, unknown. Endothelial cells in the surrounding area also release NO, along with prostacyclin. They act in synergy to prevent adhesion of aggregated platelets to the vessel wall as well as disaggregating aggregated platelets[19].

1.1.5 Neurotransmission

Electrical impulses are carried throughout the body via nerve cells which interact with each other at junctions called synapses. Chemical neurotransmitters, such as acetylcholine, glutamate and aspartate operate across these junctions and pass on impulses from one nerve cell to the next. Increased levels of cGMP have been associated with this activity[20] and a form of NO synthase isolated from rats forebrain[21]. It is believed that upon stimulation, the presynaptic nerve releases a neurotransmitter which diffuses across the synapse and activates the post synaptic nerve cell. NO synthase is activated and NO produced. NO diffuses back to the presynaptic nerve and surrounding nerve cells where guanylate cyclase is activated to increase levels of cGMP. The biological consequences of this are not yet understood but NO has been labelled a retrograde messenger and could also be linked to long term memory[22].

1.1.6 Macrophage Cytotoxicity

Macrophages are part of the body's immune system which does not require recognition of a foreign substance in order to eradicate it. Cytokines (e.g. interferon-l, tumour necrosis factor, interleukin-1 and -2) cause macrophage reproduction and stimulate the cells to envelop foreign matter, which is subsequently killed via cell release of cytotoxic substances. This process is known as phagocytosis. It was observed that urinary NO_3^- levels increased in response to macrophage stimulation and ^{15}N-labelled L-arginine experiments showed that NO_3^- was derived from the amino acids terminal guanidino nitrogen atoms[23]. With the discovery of the synthesis of NO from L-arginine[14], it was evident that NO was the precursor to NO_3^-.

The apparent toxicity of NO is not fully understood, but could be due to its reaction with $O_2^{-}\cdot$, also produced by macrophages, resulting in the formation of NO_2 and $OH\cdot$ (scheme 1.2) which can destroy cell membranes and DNA.

$$NO + O_2^- \longrightarrow ONOO^-$$

$$ONOO^- + H^+ \longrightarrow ONOOH$$

$$ONOOH \longrightarrow NO_2 + OH\cdot$$

scheme 1.2

Nitric oxide synthase, isolated from macrophages, has been shown to differ from that found in endothelial cells[1]. Production of the enzyme is *induced* when macrophages are activated, and produces *nanomoles* of NO over a longer time period. The enzyme is calmodulin *independent* but NADPH dependent and can be inhibited by derivatives of L-NMMA[16]. Overproduction of NO can lead to septic shock, i.e. blood vessel dilation and hypertension, and can lead to death[2]. NO synthase selective inhibitors may therefore become useful in the treatment of this condition.

1.2 S-Nitrosothiols

1.2.1 Introduction

S-Nitrosothiols (thionitrites) are the sulfur analogues of the organic nitrites, and are of the general formula RSNO. They are generally unstable to decomposition although several have been isolated. These include t-butylthionitrite[24], triphenylmethylthionitrite[25] and the nitroso derivatives of the amino acids, N-acetylpenicillamine[26] (1.5) and glutathione[27](1.6).

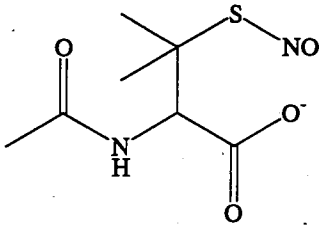

(1.5)

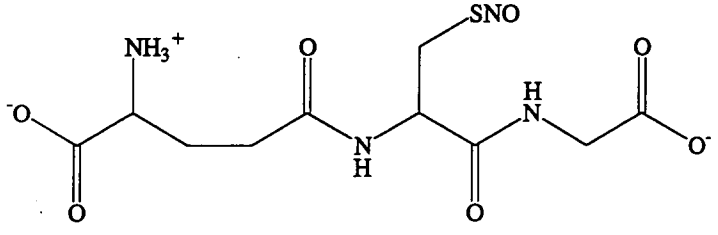

(1.6)

More recently the following nitrosothiols have been synthesised and isolated[28].

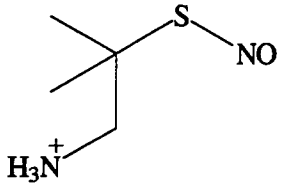

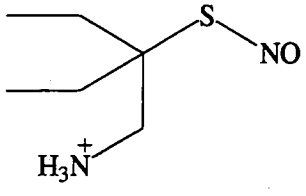

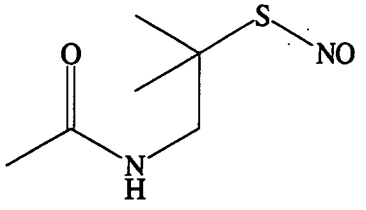

Nitrosothiols show two characteristic UV-Vis absorption peaks at c.a 340nm (ε~10^3 mol^{-1} dm^3 cm^{-1}) and at either 540nm (primary and secondary nitrosothiols) or 590nm (tertiary compounds) where ε~10 mol^{-1} dm^3 cm^{-1}. These absorption bands are assigned to the $n_O \rightarrow \pi^*$ (340nm) and $n_\Pi \rightarrow \pi^*$ (540/590nm) electronic transitions[29].

1.2.2 Nitrosation

Nitrosation describes the electrophilic addition of NO^+ to a compound. Nitrosation of primary aliphatic and aromatic amines with a range of nitrosating agents, XNO (e.g. ClNO), leads to the formation of unstable nitrosamines and ultimately to the diazonium ion (scheme 1.3).

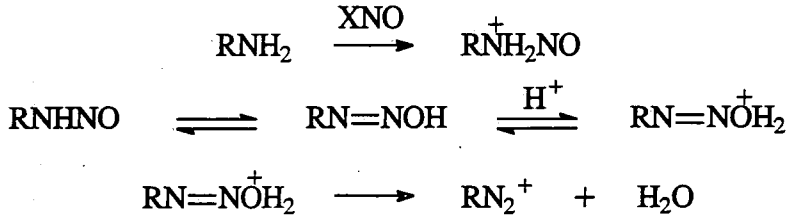

scheme 1.3

The first step is rate limiting and is followed by rapid proton transfer and loss of water to give the diazonium ion. This ion is very reactive. Loss of N_2 results in the deamination products. However aromatic diazonium ions are much more stable. The salts can be isolated and used as intermediates in many industrial synthetic pathways.

In the case of secondary amines the nitrosamine is much more stable due to the absence of an α-hydrogen. The diazonium ion is not formed (eqn. 1.3).

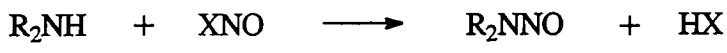

(eqn. 1.3)

Tertiary amines also undergo nitrosation. However, in this case elimination of the nitroxyl radical to give the iminium ion is rate limiting[30] (see scheme 1.4).

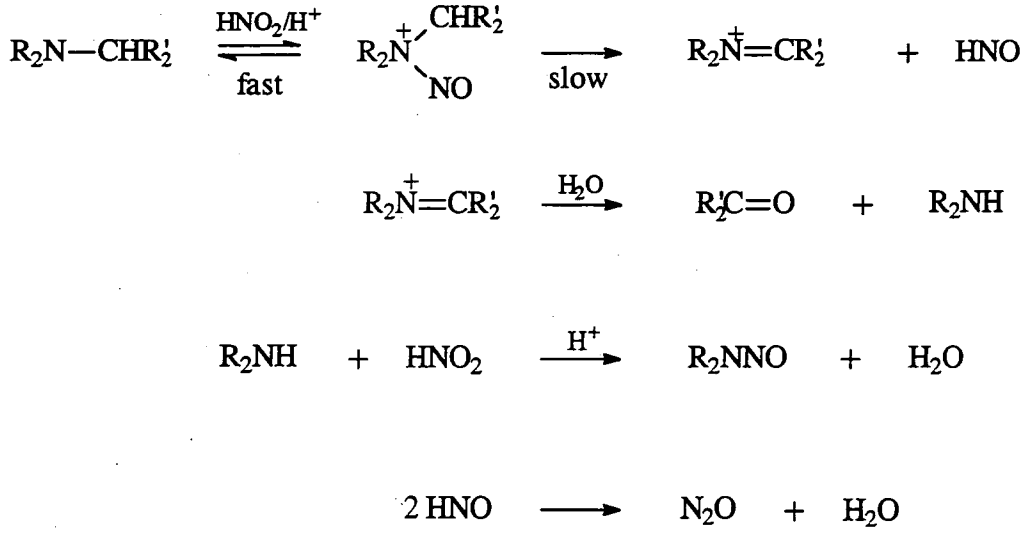

scheme 1.4

Hydrolysis of this ion yields a carbonyl compound and a secondary amine which undergoes normal rapid nitrosation to produce the nitrosamine.

C-Nitrosation involves the replacement of a hydrogen atom by the nitroso group resulting in the formation of monomers, dimers and oximes. Monomers are generally unstable and dimerise (eqn. 1.4).

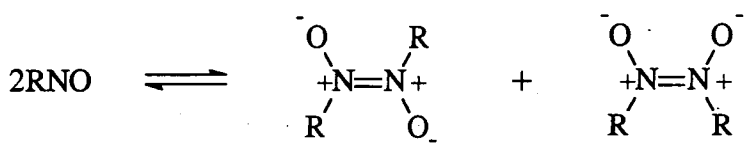

(eqn. 1.4)

Isomerisation affords the oxime (eqn. 1.5) which is both acid and base catalysed in solution.

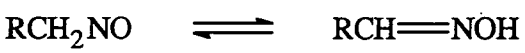

(eqn. 1.5)

O-Nitrosation of alcohols by HNO_2 yields alkyl nitrites (eqn. 1.6).

$$ROH + HNO_2 \rightleftharpoons RONO + H_2O$$

(eqn. 1.6)

The reaction is reversible but the product can be easily removed by distillation as the boiling point of the alkyl nitrite is much less than that of the alcohol. Allen[31] proved this reaction to be indeed O-nitrosation and not nucleophilic attack by the nitrite ion using optically active alcohols. The kinetics of the reaction have been determined and will be discussed later.

S-Nitrosation of thiols yields the S-nitrosothiol (eqn. 1.7).

$$RSH + XNO \longrightarrow RSNO + HX$$

(eqn. 1.7)

Nitrosyl chloride, dinitrogen tetroxide, dinitrogen trioxide, alkyl nitrites and nitrous acid are all effective nitrosating agents. Reports suggest[32] that nitric oxide itself is a nitrosating agent. This has been proved not to be the case[33]. Any nitrosation that is observed under these conditions is due to the formation of N_2O_3 via the reaction of NO with molecular oxygen. However, in basic conditions with the rigorous exclusion of oxygen, nitrosation can occur due to the reaction of NO with the thiolate ion followed by rapid protonation and radical coupling (scheme 1.5)[34].

$$RSH + B^- \rightleftharpoons RS^- + BH$$

$$RS^- + NO^{\cdot} \longrightarrow RS{-}\dot{N}{-}O^- \overset{H^+}{\rightleftharpoons} RS{-}\dot{N}{-}OH$$

$$2\,RS{-}\dot{N}{-}OH \longrightarrow RS{-}\overset{HO}{N}{-}\overset{OH}{N}{-}SR \longrightarrow RSSR + HON{=}NOH$$

$$HON{=}NOH \longrightarrow N_2O + H_2O$$

scheme 1.5

Kinetics of S-nitrosation will be discussed later.

1.2.3 Nitrous Acid

Any nitrite salt in aqueous acid yields nitrous acid, the most commonly used nitrosating agent for S-nitrosation of thiols. It has a pK_a value of 3.1[35] and is unstable to decomposition (eqn. 1.8).

$$3HNO_2 \rightleftharpoons 2NO + HNO_3 + H_2O$$

(eqn. 1.8)

Fig. 1.3 shows the two isomers of nitrous acid[36].

Figure 1.3

The trans isomer is prevalent in solution being the more stable of the two. The bond lengths are N=O, 1.2Å; O-N, 1.46Å and H-O, 0.98Å.

At low pH and high concentrations of nitrous acid an equilibrium shown in eqn. 1.9 produces significant concentrations of N_2O_3.

$$2HNO_2 \rightleftharpoons N_2O_3 + H_2O$$

(eqn. 1.9)

Dinitrogen trioxide is also a nitrosating agent. The mechanism of nitrosation of general substrate, S via N_2O_3 is shown in scheme 1.6[37].

$$2HNO_2 \underset{}{\overset{K}{\rightleftharpoons}} N_2O_3 + H_2O$$

$$N_2O_3 + S \xrightarrow{k} \overset{+}{S}—NO + NO_2^-$$

scheme 1.6

$$\text{Rate} = k[N_2O_3][S]$$

Therefore,

$$\text{Rate} = kK[HNO_2]^2[S]$$

(eqn. 1.10)

The rate equation (eqn. 1.10) shows a second order dependence on nitrous acid and first order on substrate. With particularly reactive substrates (e.g. ascorbic acid, azide ion or the thiosulfate ion) or at very high concentrations of substrate, the rate of reaction with substrate can become greater than the hydrolysis of N_2O_3 such that the rate determining step becomes the formation of N_2O_3 (eqn. 1.11).

$$2HNO_2 \xrightarrow{k} N_2O_3 + H_2O$$

(eqn. 1.11)

$$\text{Rate} = k[HNO_2]^2$$

(eqn. 1.12)

The rate equation (eqn. 1.12) is then second order with respect to HNO_2 but zero order in substrate.

S-Nitrosation of thiols, however, is generally carried out at lower concentrations of nitrous acid and at a higher pH. Under these conditions another nitrosating agent prevails. The rate equation (eqn. 1.13) now becomes first order in substrate and HNO_2, and the reaction shows acid catalysis.

$$\text{Rate} = k[HNO_2][S][H^+]$$

(eqn. 1.13)

Two possible mechanisms can be proposed to explain the rate equation, both of which involve a pre-equilibrium forming a nitrosating species followed by attack on the substrate[38]. Two different equilibrium reactions have been suggested, one involving the formation of the nitrous acidium ion (eqn. 1.14) and the other involving the nitrosonium ion (eqn. 1.15).

$$HNO_2 + H^+ \rightleftharpoons H_2NO_2^+$$

(eqn. 1.14)

$$H_2NO_2^+ \rightleftharpoons NO^+ + H_2O$$

(eqn. 1.15)

In aqueous solution it is very difficult to determine which species is the nitrosating agent.

1.2.4 Kinetics Of Nitrosation

When describing the kinetics of nitrosothiol formation, a comparison of alcohol and thiol nitrosation is constructive.

1.2.4.1 Alcohol Nitrosation

Alkyl nitrite formation (RONO) from nitrous acid and the corresponding alcohol is very rapid but not quantitative. Aldred *et al*[39] measured the observed first order rate constant for the reaction of ROH with HNO_2 ([ROH] > > [HNO_2]) at various [ROH]. A plot of k_{obs} against [ROH] was linear (confirming a first order dependence of ROH on the rate equation) with a positive slope and intercept. This is characteristic of a reversible reaction; first order in both directions where the observed first order rate constant, k_0 is the sum of those for the forward and reverse reaction (see eqns. 1.16 and 1.17).

$$ROH + HNO_2 \underset{k_{-1}}{\overset{k_1}{\rightleftharpoons}} RONO + H_2O$$

(eqn. 1.16)

$$k_{obs} = k_1[ROH] + k_{-1}$$

(eqn. 1.17)

Measurements of different acidities indicate that eqn. 1.13 is obeyed and thus indicates that the well known mechanism involving $H_2NO_2^+$ (or NO^+) is occurring. Values for the third order rate constant, k_2 (eqn. 1.18) for the forward reaction and the second order rate constant, k_{-2} (eqn. 1.19) for the back reaction have been determined for a series of alcohols.

$$Rate = k_2[ROH][HNO_2][H^+]$$

(eqn. 1.18)

$$Rate = k_{-2}[RONO][H^+]$$

(eqn. 1.19)

k_{-2} values are almost the same for each alcohol whereas k_2 decreases along the series MeOH > EtOH > Pr^iOH > Bu^tOH which indicates a steric control on the rate constant rather than an electronic one.

1.2.4.2 Thiol Nitrosation

Investigations of the nitrosation of cysteine[40], 3-mercaptopropionic acid[41] and N-acetylpenicillamine[39] have demonstrated that the rate law (eqn. 1.13) holds for S-nitrosation suggesting a mechanism of nitrosation involving $H_2NO_2^+$ (or NO^+) also. Reactions are much more rapid due to the greater nucleophilicity of the sulfur atom compared to oxygen. Rate constants measured for the nitrosation of the more reactive thiols are very similar despite their difference in structure[42] and are close to the encounter control limit of 7000 mol^{-2} dm^6 s^{-1}, [43]. The N-acetylated derivatives of cysteine and penicillamine are much more reactive possibly due their ability to

stabilise the positive charge on S in the transition state via the interaction with the carbonyl group (see fig. 1.4).

Figure 1.4

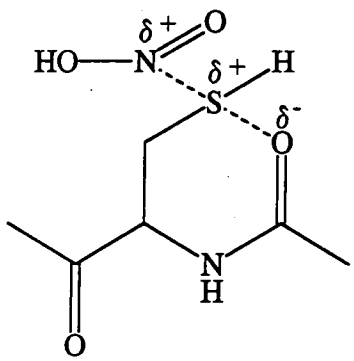

This could also account for the reactivity of glutathione. First order rate plots (k_{obs} against [RSH]) did not show an appreciable positive intercept indicating the reaction is virtually irreversible. Since denitrosation is acid catalysed, it is likely that the first step in the back reaction is rapid reversible protonation at the sulfur atom of RSNO (or the oxygen atom in the case of RONO) (eqn. 1.20).

$$RSNO + H^+ \rightleftharpoons RS\overset{+}{H}NO \xrightarrow{H_2O} RSH + H_2NO_2^+$$

(eqn. 1.20)

As sulfur sites are generally several orders of magnitude less basic than their oxygen counterparts, the virtual irreversibilty of thiol nitrosation is probably due to the reduced basicity of the RSNO. However, Herves *et al*[44] have now measured the equilibrium constants for the nitrosation of penicillamine and cysteine to be ~10^6 mol^{-1} dm^3 using a thiol assay. The importance of the reversibility of S-nitrosation is highlighted in section 1.2.5.4.

1.2.4.3 Nucleophilic Catalysis

In general, nitrosation is strongly catalysed by a range of nucleophilic species e.g. Cl^- and Br^- [43]. Kinetic studies of the catalytic nitrosation of many reactants (e.g. amines) showed that the first order rate constant was linearly dependent on Y^- (Y^-= Br^-,Cl^-). It is likely that nitrosation occurs via the nitrosyl halide where the fourth order rate constant is defined by eqn. 1.21.

$$\text{Rate} = k_3[RNH_2][HNO_2][H^+][Y^-]$$

(eqn. 1.21)

NOCl is found to be more reactive than NOBr due to the greater electronegativity of Cl^-.

Nitrosation of thiols is also catalysed by nucleophiles[42]. The rate is defined by eqn. 1.22 which incorporates a term for acid catalysed nitrosation also observed.

$$\text{Rate} = k_3[H^+][HNO_2][RSH] + k_2K_{YNO}[RSH][H^+][Y^-][HNO_2]$$

(eqn. 1.22)

Values of k_2 for any one thiol decrease in the order ClNO > BrNO > ONSCN as expected from electronegativity arguments. For the most reactive thiols, k_2 values lie within a small range suggesting that these reactions are encounter-controlled. If [RSH] is increased, a plot of k_{obs} against [RSH] (where d/dt $[HNO_2]$= $k_{obs}[HNO_2]$ and k_{obs} is defined by eqn. 1.23) begins to develop a downward curvature.

$$k_{obs} = k_3[H^+][RSH] + k_2K_{YNO}[RSH][H^+][Y^-]$$

(eqn. 1.23)

This curvature can be explained by a change in the rate determining step. At high [RSH], the reaction between RSH and YNO becomes so rapid that formation of YNO

becomes rate limiting. Now the general expression for k_{obs} is given by eqn. 1.24 where k_1 and k_{-1} are the rate constants for the formation and decomposition of YNO respectively.

$$k_{obs} = \frac{k_1 k_2 [H^+][Y^-][RSH]}{k_{-1} + k_2[RSH]} + k_3[H^+][RSH]$$

(eqn. 1.24)

At sufficiently high [RSH], for a sufficiently reactive thiol the first term will be reduced to $k_1[H^+][Y^-]$ and k_{obs} will become independent of [RSH].

1.2.5 Reactions Of S-Nitrosothiols

1.2.5.1 Thermolysis/Photolysis

If S-nitroso-N-acetylpenicillamine is refluxed in methanol, after 2hrs the colour disappears and the disulfide product can be collected and identified[26]. Photolytic decomposition of S-nitrosothiols also yields the disulfide (eqn. 1.25)[45].

$$2RSNO \xrightarrow{h\nu/\Delta} RSSR + 2NO$$

(eqn. 1.25)

Singh *et al*[46] have detected the thiyl radical as an intermediate in this reaction. A biological application of photolytic RSNO decomposition was recently demonstrated[47] when cells incubated with S-nitrosoglutathione (GSNO) prior to irradition were killed, via nitric oxide, released by the nitrosothiol. The possible use of GSNO as a photochemotherapeutic agent was proposed.

1.2.5.2 Acid Catalysed Decomposition

As previously discussed, thiol nitrosation is a virtually irreversible reaction due to the low basicity of the nitrosothiol. Therefore, forcing conditions are required before denitrosation can be observed. In highly acidic conditions (1-4M) and in the presence of a nitrous acid trap (N_3^-) denitrosation of S-nitroso-N-acetylpenicillamine has been observed[48]. Generally a nucleophile (Br^-) better than the solvent is also required. With $[H^+] >> [RSNO]$, the observed first order rate constant, k_{obs}, increases with $[HN_3]$ until a plateau is reached. At this point denitrosation is irreversible, the mechanism of which is given in scheme 1.7.

$$RSNO + H^+ \overset{K}{\rightleftharpoons} \overset{+}{R}SHNO$$

$$\overset{+}{R}SHNO + Br^- \underset{k_{-1}}{\overset{k_1}{\rightleftharpoons}} RSH + NOBr$$

$$NOBr + HN_3 \xrightarrow{k_2} N_2 + N_2O + Br^- + H^+$$

scheme 1.7

The rate equation is described by eqn. 1.26 where h_0 is the Hammett acidity function.

$$\frac{-d[RSNO]}{dt} = Kh_0k_1[Br^-][RSNO] - \frac{k_{-1}Kh_0k_1[RSH][Br^-][RSNO]}{k_2[HN_3] + k_{-1}[RSH]}$$

(eqn. 1.26)

Therefore k_{obs} (defined by $-d/dt\ [RSNO] = k_{obs}[RSNO]$) is given by eqn. 1.27.

$$k_{obs} = \frac{k_2Kh_0k_1[Br^-][HN_3]}{k_{-1}[RSH] + k_2[HN_3]}$$

(eqn. 1.27)

At high $[HN_3]$, $k_2[HN_3] >> k_{-1}[RSH]$ and therefore,

$$k_{obs} = k_1 K h_0 [Br^-]$$

(eqn. 1.28)

A plot of k_{obs} against $[Br^-]$ is linear with a slope=$k_1 K h_0$ (hence giving a measure of the second order rate constant).

1.2.5.3 Metal Ion Decomposition

Nitrosothiols can be reduced by the Hg^{2+} metal ion (eqn. 1.29).

$$RSNO + H_2O \xrightarrow{Hg^{2+}} RSH + HNO_2$$

(eqn. 1.29)

This reaction has been used for analysis of the thiol group by Saville[49]. More recently, decomposition has been observed in the presence of Cu^{2+} [50] (eqn. 1.30).

$$2RSNO \xrightarrow{Cu^{2+}} RSSR + 2NO$$

(eqn. 1.30)

As this involves the release of NO, catalysis via this ion has great biological significance and is dealt with separately in the next section. Fe^{2+} and Ag^+ ions also induce decomposition. However, decomposition is not observed in the presence of Zn^{2+}, Ca^{2+}, Mg^{2+}, Ni^{2+}, Co^{2+}, Cr^{3+} or Fe^{3+}.

1.2.5.4 Copper Ion Catalysed Decomposition

The release of NO from S-nitrosothiols in aqueous buffered solution (pH 7.4) is catalysed by copper ions. Two articles recently published give an excellent review of this subject[51]. Nitric oxide, released from the decomposition of S-nitroso-N-acetylpenicillamine can be quantitatively detected directly using an NO specific electrode and via the nitrite ion, and the formation of disulfide shown by HPLC.

Over a range of $[Cu^{2+}]$, which may differ from one nitrosothiol to the next, the rate of decomposition can be described by eqn. 1.31.

$$\text{Rate} = k[Cu^{2+}][RSNO]$$

(eqn. 1.31)

A plot of k_{obs} (where $-d/dt\ [RSNO] = k_{obs}[RSNO]$ and $k_{obs} = k[Cu^{2+}]$) against $[Cu^{2+}]$ is linear, with a small intercept due to reaction catalysed by Cu^{2+} ions present naturally in the distilled water-buffer components. The value of the second order rate constant (k) greatly depends on the structure of R and was initially explained in terms of the formation of a six membered ring intermediate involving the bi-dentate coordination of the Cu^{2+} ion to the N atom of the -SNO group and either the amino or carboxylate group (1.7 and 1.8)[52].

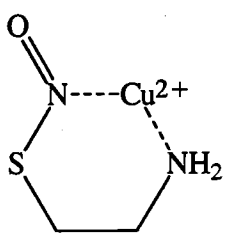

(1.7)

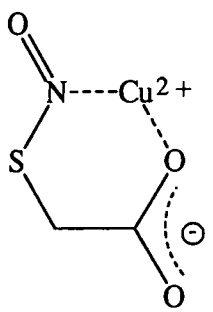

(1.8)

N-acetylation of the amino group drastically reduces the rate of reaction due to the delocalisation of the N atom lone pair onto the carbonyl group. Competitive chelation of the copper ion causes a reduction in the value of k when a carboxylic acid group is introduced. The addition of an extra methylene group reduces k as formation of a seven membered ring intermediate proves less favourable. The occurrence of two

methyl groups on the carbon atom adjacent to the nitrosothiol increases the rate of reaction and is known as the "gem-dimethyl effect". This describes the electron donating properties of the two methyl groups enhancing the electron density around S, and the conformational constraints these groups impose on the molecule which hold the coordinating groups within close proximity of each other. For example, the second order rate constants for S-nitrosocysteine and S-nitrosopenicillamine decomposition are 24500 and 67000 mol^{-1} dm^3 s^{-1} respectively. Nitrosothiols which do not possess a second functional group in the vicinity of the nitroso group cannot react with Cu^{2+}. Similarly, esterification of the carboxylic acid results in complete stability of RSNO. Increasing the chain length by one CH_2 group reduces reactivity and inclusion of a methyl group and a further $CH_2CO_2^-$ group increases the reactivity probably as a result of the steric constraints they impose on the molecule.

Coordination with the SNO group is shown to be via nitrogen however, structures involving coordination via S can be envisaged in all cases.

Outside this window of $[Cu^{2+}]$ where the reaction is first order in RSNO and Cu^{2+}, zero order kinetics and an induction period prior to reaction can sometimes be observed. This can be explained if it is taken that Cu^+ is the true catalytic species[53]. Cu^{2+} is reduced by the thiolate ion (specifically added or naturally present due to the slight reversibilty of the nitrosation reaction[44]) as shown in scheme 1.8.

$$RS^- + Cu^{2+} \rightleftharpoons X \longrightarrow RS^{\cdot} + Cu^+$$

$$RSNO + Cu^+ \rightleftharpoons Y \longrightarrow RS^- + Cu^{2+} + NO$$

$$2RS^{\cdot} \longrightarrow RSSR$$

scheme 1.8

Intermediate X is probably $RSCu^+$ and Y either (1.7) or (1.8), depending on the nitrosothiol but with Cu^+ coordination rather than Cu^{2+}. If $[RS^-]_0 >> [Cu^{2+}]_0$, where $[RS^-]_0$ is the initial concentration of thiolate ion and $[Cu^{2+}]_0$ the initial concentration of Cu^{2+}, then rapid formation and regeneration of Cu^+ occurs and hence the rate equation is first order (eqn. 1.32) where $k_{obs} = k[Cu^+]$.

$$\frac{-d[RSNO]}{dt} = k_{obs}[RSNO]$$

(eqn. 1.32)

However, for the more reactive nitrosothiols, formation of Cu^+ becomes rate limiting and a zero order reaction is observed. In either case if the $[RS^-]$ is too low initially (i.e. not specifically added to the solution) an induction period is observed which is thought to be due to time spent generating RS^- via hydrolysis of RSNO (eqn. 1.33).

$$RSNO + 2OH^- \longrightarrow RS^- + NO_2^- + H_2O$$

(eqn. 1.33)

Copper has been implicated in the mechanism of *in vivo* decomposition of nitrosothiols and will be discussed later. The mechanism of copper ion catalysis described above was given credibility when it was reported that protein bound Cu^{2+} could serve as a Cu^+ source for the decomposition of S-nitrosocysteine[54].

1.2.5.5 Transnitrosation

The primary products from the transfer of the NO group from a nitrosothiol to a thiol was first spectroscopically observed by Meyer *et al*[55] and later by Arnelle *et al*[56] (eqn. 1.34). Kinetic studies[57] of the reaction of S-nitroso-N-acetylpenicillamine with thioglycolic acid, and S-nitrosocysteine with thiomalic acid show the reaction to occur readily in aqueous solution at $pH > 8$, and the rate equation to be first order in RSNO and RS^-.

$$RSNO + R'S^- \rightleftharpoons RS^- + R'SNO$$

(eqn. 1.34)

The rate of reaction is too high for the formation of NO as an intermediate to be a possibility, and is unchanged in the presence of EDTA. The reactivity of the thiolate ion is governed by steric, as opposed to electronic effects[58]. Electron withdrawing groups on the nitrosothiol however promote transnitrosation i.e second order rate constants for the reaction of CH_3CH_2SNO, $HOCH_2CH_2SNO$ and ClC_6H_4SNO with N-acetylcysteine are 84, 432 and 1016 $mol^{-1}\ dm^3\ s^{-1}$ respectively. Nitrosothiol-thiol exchange may be of physiological importance (see later).

1.3 NO Releasing Compounds (Nitrovasodilators)

1.3.1 Introduction

The physiological importance of NO has previously been discussed. Medical disorders believed to be due to a natural deficiency of NO can be treated with drugs which can generate NO *in vivo*. $NO_{(g)}$ itself has been shown to cause smooth muscle relaxation of the lungs via inhalation[59]. However, the formation of the highly toxic gas, NO_2, via its reaction with O_2 or via disproportionation of NO, limits the use of gaseous NO as a nitrovasodilator. Glyceryl trinitrate (GTN)(1.9) has been used in the treatment of angina for over a century but has limited use as it is short acting and the patient can develop a tolerance if its use is prolonged[60].

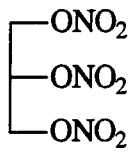

(1.9)

The search for better NO donor drugs has created a new class of compound called nitrovasodilators. They vary greatly in structure but all serve to mimic the actions of endogenous NO by activating soluble guanylate cyclase and thus raising levels of cGMP (see section 1.1). There follows a description of each class of nitrovasodilator and the chemical pathways believed to be involved in NO formation.

1.3.2 S-Nitrosothiols

S-Nitrosothiols (see section 1.2) have been shown to cause the dilation of vascular smooth muscle[61] and to inhibit the aggregation of platelets[62]. The activation of soluble guanylate cyclase by these compounds has also been observed. As authentic nitric oxide also demonstrates these activities, it is logical to assume that the vasodilatory actions of these compounds can be attributed to their decomposition and subsequent formation of NO (see section 1.2.5). However, the potency of RSNO is apparently not directly linked to its chemical stability[63]. This lead to the conclusion that NO production alone could not account for the biological activity of RSNO. However, since these observations, extensive study on the mechanism of RSNO

decomposition in aqueous solution has been undertaken (see section 1.2.5.4). These results show that decomposition is copper ion catalysed and is greatly affected by the concentration of thiol. Neither of these factors were taken into account in earlier measurements of the stability of RSNO and thus care must be taken over the interpretation of these results. The mechanism of NO release by nitrosothiols, *in vivo*, still remains unresolved, but reports do suggest that it is mediated by copper ions[64]. As most nitrosothiols studied are amino acids, they are ionic and hence decomposition is generally thought to occur at the cell wall[65] and may involve transnitrosation to form a less stable nitrosothiol[66].

Nitrosothiols, which are less prone to produce tolerance in patients[60, 67], also show a certain degree of tissue selectivity[68]. This arterioselectivity provides a lead into the treament of one type of NO deficiency, without the side effects on the rest of the body.

The discovery of the natural occurrence of stable nitroso derivatives of sulfhydryl groups in proteins lead to the belief that these plasma S-nitrosoproteins may act as a store of nitric oxide[69]. Quantitative tests showed that human plasma contains c.a. 7μM S-nitrosothiol, 85% of which is S-nitroso-serum albumin[70]. The level of S-nitrosoprotein drops if endogenous production of NO is inhibited. Furthermore, nitric oxide and authentic EDRF have been shown to react with protein thiol groups, *in vitro*, to form S-nitrosoproteins which are much more stable than low-molecular-weight nitrosothiols (e.g. S-nitrosocysteine) and nitric oxide. Therefore, their role as endogenous reserves of NO seems plausible. As albumin circulates as a mixed disulfide with low-molecular-weight thiols[71], release of NO from these S-nitrosoproteins has been explained in terms of transnitrosation from the protein forming a more unstable S-nitrosothiol which, in turn, decomposes to release NO. Simon *et al*[72] later showed that this type of transnitrosation can occur, and explained the observed antiaggregating properties of these S-nitrosoproteins.

1.3.3 Organic Nitrates and Nitrites

The vasodilatory properties of organic nitrates and nitrites have been known for over 100yrs. However, the mode of action of these compounds has only recently been discovered.

The first real step forward in the understanding of the mechanism of the vasodilatory action of organic nitrates was made by Needleman *et al*[73] who found that the vaso-relaxant properties of GTN (1.9) required the presence of thiol groups in

tissue. Gruetter *et al*[74] later showed that GTN stimulated cGMP formation which inferred nitric oxide formation. Indeed, NO production from GTN in the presence of thiol was later reported[75]. However, a systematic study showed that whereas all thiols will react with organic nitrates to produce the NO_2^- and NO_3^- ions, only certain thiols produce NO also[76]. Scheme 1.9 shows the probable reaction between organic nitrates and thiols producing thionitrates which, in the case of cysteine and N-acetylcysteine, rearrange to release NO[77].

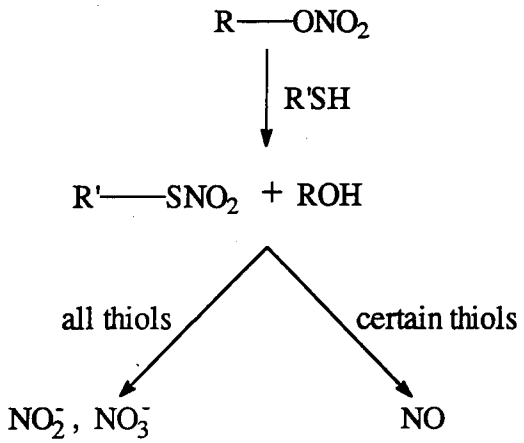

scheme 1.9

More recent studies have shown that thionitrates *are* formed as intermediates in the thiol mediated release of NO from GTN[78] and a systematic study on the decomposition of $^tBuSNO_2$ in aqueous solution at pH 7.4 has given rise to a possible mechanism involving rearrangement of the thionitrate to a sulfenyl nitrite and subsequent rapid homolysis (scheme 1.10).

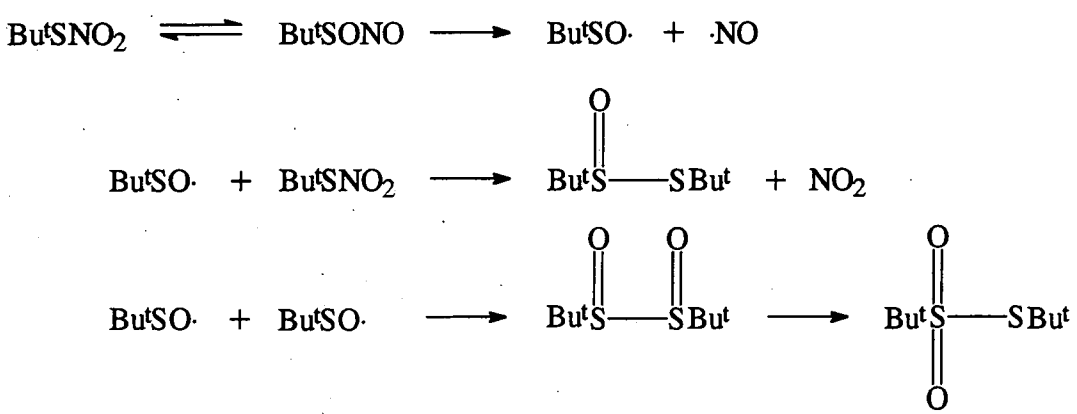

scheme 1.10

NO release from this compound was detected using an NO specific electrode. Perhaps the thionitrate intermediates produced NO in earlier studies but the assay was not sensitive enough to detect it. The carbon containing products of the reaction were identified as being di-*t*-butylthiosulfinate and di-*t*-butylthiosulfonate only. The absence of ^{t}BuSH and ^{t}BuS^{t}Bu as reaction products eliminated the possibility of both heterolytic decomposition to give NO_2^+ and the thiol, and homolytic fission to give NO_2 and the thiyl radical. Unfortunately ^{t}BuSNO_2 did not stimulate soluble guanylate cyclase. Cysteine and N-acetylcysteine are the only thiols which are known to release NO from GTN *and* cause enzyme activation[79]. It has thus been suggested that the carboxylate group of cysteinyl thionitrate is essential for enzyme activation.

RSH is oxidised to disulfide during GTN metabolism hence the reduction in the concentration of endogenous sources of thiol could be a reason for the tolerance a patient acquires if use of organic nitrates is prolonged. In fact, partial reversal of organic nitrate tolerance upon the treatment of patients with N-acetylcysteine has been reported[80]. A second enzymatic pathway for NO formation from GTN has also been mentioned and the down regulation of these enzymes may also be responsible for this tolerance[77].

Unlike organic nitrates, organic nitrites can react with *any* thiol to release NO via the formation of an S-nitrosothiol intermediate (see scheme 1.11)[33].

$$\mathrm{RONO} + \mathrm{RSH} \longrightarrow \mathrm{RSNO} + \mathrm{ROH}$$

$$2\mathrm{RSNO} \longrightarrow \mathrm{RSSR} + 2\mathrm{NO}$$

scheme 1.11

The extent of NO formation depends on the rate of formation and decomposition of RSNO. *In vitro* studies has shown that, as well as thiols, the biological reductones ascorbic acid (1.10) and catechol (1.11) can also facilitate the release of NO from organic nitrites[81].

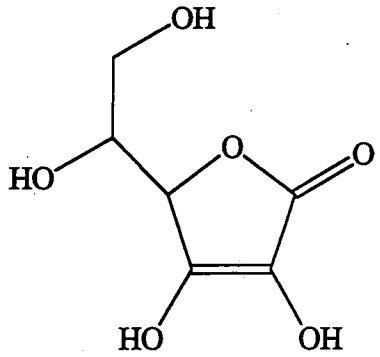

(1.10)

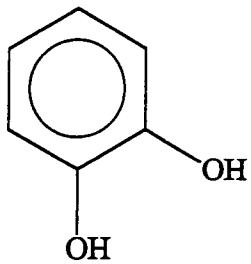

(1.11)

A mechanism was proposed involving nitrosation of the dianion (see scheme 1.12) followed by homolytic cleavage of the O-NO bond to give NO and a radical anion which would be further oxidised to dehydroascorbic acid by another molecule of RONO.

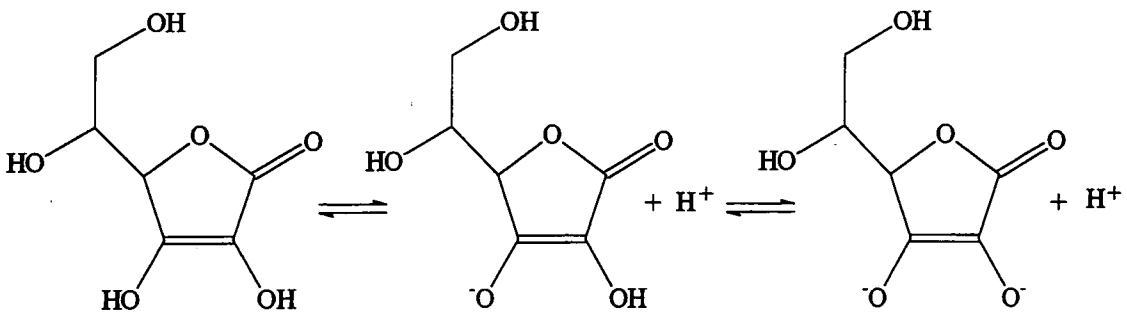

scheme 1.12

1.3.4 Metal Nitrosyl Compounds

There are a number of metal nitrosyls which can donate NO. For example, sodium nitroprusside (1.12) is often used to induce low blood pressure during surgery[2].

$$Na_2[Fe(CN)_5NO]$$

(1.12)

NO release from this compound can be brought about by photolysis[82] or via a slower non-photochemical pathway thought to involve thiols[83].

Heptanitrosyl-tri-μ3-thioxotetraferrate (1-) (1.13), also known as Roussin's Black Salt (RBS), is another metal nitrosyl compound with vasodilatory properties[84].

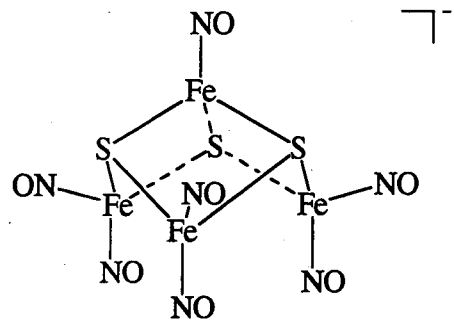

(1.13)

Studies of its NO mediated vasodilatory action showed that the anion can invoke immediate relaxation of precontracted arteries, and can be sustained for a long period of time. The lasting effect of this compound is attributed to its unusual lipid solubility which allows it to diffuse into endothelial and smooth muscle cells and remain there, slowly releasing NO.

RBS is photosensitive and will liberate large amounts of NO in response to light[85]. Photorelaxation is intensity dependent and is due to activation of guanylate cyclase via liberated NO. Cellular respiration had also been shown to be inhibited by the photolysis of RBS[86].

The mechanism of NO release from RBS is still not well understood. Due to the electron-precise nature of the complex it is presumed that addition or removal of an electron will cause disintegration of the Fe-S framework and NO release. In the case of photovasodilation, a photon of energy is imagined to do the same or may upset the balance of equilibrium between RBS and its two closely related derivatives (see scheme 1.13).

$$[Fe_2S_2(NO)_4]^{2-} \rightleftharpoons [Fe_4S_3(NO)_7]^{-} \rightleftharpoons Fe_4S_4(NO)_4$$

scheme 1.13

1.3.5 Furoxans

The furoxans are a group of heterocyclic compounds showing vasodilatory properties associated with NO production and activation of soluble guanylate cyclase[34]. In a similar fashion to organic nitrites, these compounds react with any thiol to form unstable nitrosothiols, which subsequently decompose to release NO (see scheme 1.14).

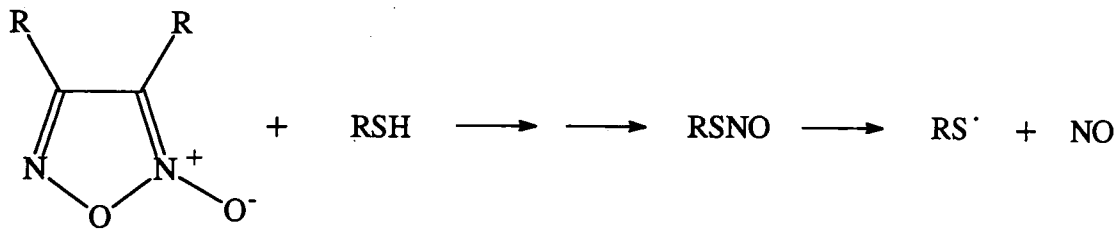

scheme 1.14

1.4 Conclusion

In this chapter, the role of nitric oxide as an essential messenger molecule has been discussed. The synthesis and reactions of S-nitrosothiols have been examined, and the group of compounds presented as potential pro-drugs of NO. Understanding the mechanism is important if the NO releasing properties of S-nitrosothiols is to be harnessed to selectively target areas of the body suffering from NO deficiency.

The aim of my Ph.D. was to investigate *in vitro* NO release from probably the most biologically important S-nitrosothiol, S-nitrosoglutathione, and to investigate possible catalysis of NO formation via metals other than copper.

References

1. S.Moncada, R.M.J.Palmer, E.A.Higgs, *Pharmacol. Rev.*, 1991, **43**, 109.

2. A.R.Butler, D.L.H.Williams, *Chem. Soc. Rev.*, 1993, 233.

3. R.F.Furchgott, J.V. Zawadzski, *Nature*, 1980, **288**, 373.

4. T.M.Griffith, D.H.Edwards, M.J.Lewis, A.C.Newby, A.H.Henderson, *ibid*, 1984, **308**, 645.

5. R.M.J.Palmer, A.G.Ferrige, S.Moncada, *ibid*, 1987, **327**, 524, L.J.Ignarro, G.M.Buga, K.S.Wood, G.Chaudhuri, *Proc. Nat. Acad. Sci., USA*, 1987, **84**, 9265.

6. M.J.Downes, M.W.Edwards, T.S.Elsey, C.L.Walters, *Analyst,* 1976, **101**, 742.

7. W.Martin, G.M.Villani, D.Jothianandan, R.F.Furchgott, *J. Pharmacol. Exp. Ther.*, 1985, **232**, 708.

8. R.J.Gryglewski, R.M.J.Palmer, S.Moncada, *Nature*, 1986, **320**, 454.

9. M.Fontecave, J.Pierre, *Bull. Soc. Chim. Fr.*, 1994, **131**, 620.

10. P.R.Myers, R.L.Minor, R.Guerra, J.N.Bates, D.G.Harrison, *Nature*, 1990, **345**, 161.

11. A.F.Vanin, *FEBS*, 1991, **289**, 1.

12. Y.P.Vedernikov, P.I.Mordvintcev, I.V.Malenkova, A.F.Vanin, *Eur. J. Pharmacol.*, 1992, **211**, 313.

13. M.Feelisch, M.tePoel, R.Zamora, A.Deussen, S.Moncada, *Nature*, 1994, **368**, 62.

14. R.M.J.Palmer, D.S.Ashton, S.Moncada, *ibid*, 1988, 10.

15. M.A.Marletta, P.S.Yoon, R.Iyengar, C.D.Leaf, J.S.Wishnok, *Biochem.*, 1988, **27**, 8706.

16. S.Moncada, E.A.Higgs, H.F.Hodson, R.G.Knowles, P.Lopez-Jaranillo, T.McCall, R.M.J.Palmer, M.W.Radomski, D.D.Rees, R.Schulz, *J. Cardiovas. Pharmacol.*, 1991, **17** (Supp. 3), 1.

17. M.W.Radomski, R.M.J.Palmer, S.Moncada, *Br. J. Pharmacol.*, 1987, **92**, 181.

18. M.W.Radomski, R.M.J.Palmer, S.Moncada, *Proc. Natl. Acad. Sci., USA*, 1990, **87**, 5193. M.W.Radomski, R.M.J.Palmer, S.Moncada, *Br. J. Pharmacol.*, 1990, **101**, 325.

19. M.W.Radomski, R.M.J.Palmer, S.Moncada, *Br. J. Pharmacol.*, 1987, **92**, 639.

20. J.Garthwaite, *TINS*, 1991, **14**, 60.

21. R.G.Knowles, M.Palacios, R.M.J.Palmer, S.Moncada, *Proc. Natl. Acad. Sci., USA*, 1989, **86**, 5159.

22. M.Baringa, *Science*, 1991, **254**, 1296.

23. R.Iyengar, D.J.Stuehr, M.A.Marletta, *Proc. Natl. Acad. Sci., USA*, 1987, **84**, 6369.

24. G.Kresze, U.Uhlich, *Chem. Ber.*, 1959, **92**, 1048.

25. H.Rheinboldt, *Ber.*, 1926, **59**, 1311.

26. L.Field, R.V.Dilts, R.Ravichandran, P.G.Lenhert, G.E.Carnahan, *J. Chem. Soc. Chem. Commun.*, 1978, 249.

27. T.W.Hart, *Tet. Lett.*, 1985, **26**, 2013.

28. B.Roy, A.du Molinet d'Hardemare, M.Fontecave, *J. Org. Chem.*, 1994, **59**, 7019.

29. J.Barrett, D.F.Debenham, J.Glauser, *Chem. Commun.*, 1965, 248.

30. P.A.S.Smith, R.N.Loeppky, *J. Am. Chem. Soc.*, 1967, **89**, 1147.

31. A.D.Allen, *J. Chem. Soc.*, 1954, 1968.

32. L.J.Ignarro, B.K.Barry, D.Y.Gruetter, J.C.Edwards, E.H.Ohlsten, C.A.Gruetter, W.H.Baricos, *Biochem. Biophys. Res. Commun.*, 1980, **94**, 93.

33. M.Feelisch, *J. Cardiovas. Pharmacol.*, 1991, **17** (Supp.3), 25.

34. W.A.Pryor, D.F.Church, C.K.Govindan, G.Crank, *J. Org. Chem.*, 1982, **47**, 156.

35. J.Tummavuori, P.Lumme, *Acta Chem. Scand.*, 1968, **22**, 2003; P.Lumme, P.Lahermo, J.Tummavuori, *ibid*, 1965, **19**, 9; P.Lumme, J.Tummavuori, *ibid*, 1965, **19**, 617.

36. K.Jones, *Comprehensive Inorganic Chemistry*, Vol. 2, Eds. J.C.Bailor, H.J.Emeleus, R.Nyholm, A.F.Trotman-Dickenson, Pergamon Press, New York, 1973, 329.

37. J.H.Ridd, *Quart. Rev.*, 1961, **15**, 418.

38. E.D.Hughes, C.K.Ingold, J.H.Ridd, *J. Chem. Soc.*, 1958, **65**, 88.

39. S.E.Aldred, D.L.H.Williams, M.Garley, *J. Chem. Soc. Perkin Trans. 2*, 1982, 777.

40. P.Collings, K.Al-Mallah, G.Stedman, *ibid*, 1975, 1734.

41. L.R.Dix, D.L.H.Williams, *ibid*, 1984, 109.

42. P.A.Morris, D.L.H.Williams, *ibid*, 1988, 513.

43. D.L.H.Williams, *Nitrosation*, Cambridge University Press, 1988.

44. P.Herves, D.L.H.Williams, *Chem. Commun.*, in the press.

45. J.Barrett, L.J.Fitzgibbons, J.Glauser, R.H.Still, P.N.W.Young, *Nature*, 1966, **211**, 848.

46. R.J.Singh, N.Hogg, J.Joseph, B.Kalyanaraman, *J. Biol. Chem.*, 1996, **271**, 18596.

47. D.J.Sexton, A.Muruganandam, D.J.McKenny, B.Mutus, *Photochem. Photobiol.*, 1994, **59**, 463.

48. S.S.Al-Kaabi, D.L.H.Williams, R.Bonnet, S.L.Ooi, *J. Chem. Soc. Perkin Trans. 2*, 1982, 227.

49. B.Saville, *Analyst*, 1958, **83**, 670.

50. J.McAninly, D.L.H.Williams, S.C.Askew, A.R.Butler, C.Russell, *J. Chem. Soc. Chem. Commun.*, 1993, 1758.

51. D.L.H.Williams, *Chem. Commun.*, 1996, 1085; D.L.H.Williams, *Transition Met. Chem.*, 1996, **21**, 1.

52. S.C.Askew, D.J.Barnett, J.McAninly, D.L.H.Williams, *J. Chem. Soc. Perkin Trans. 2*, 1995, 741.

53. A.P.Dicks, H.R.Swift, D.L.H.Williams, A.R.Butler, H.H.Al-Sa'doni, B.G.Cox, *ibid*, 1996, 481.

54. A.P.Dicks, D.L.H.Williams, *Chem. & Biol.*, 1996, **3**, 655.

55. D.J.Meyer, H.Krammer, N.Ozer, B.Coles, B.Ketterer, *FEBS Letts.*, 1994, **345**, 177.

56. D.R.Arnelle, J.S.Stamler, *Arch. Biochem. Biophys.*, 1995, **318**, 279.

57. D.J.Barnett, J.McAninly, D.L.H.Williams, *J. Chem. Soc. Perkin Trans. 2*, 1994, 1131.

58. D.J.Barnett, A.Rios, D.L.H.Williams, *ibid*, 1995, 1279.

59. J.Pepka-Zaba, T.W.Higenbottam, A.T.Dinh-Xuan, D.Stone, J.Wallwork, *Lancet*, 1991, **338**, 1173.

60. J.A.Bauer, H.Fung, *J. Pharmacol. Exp. Ther.*, 1991, **256**, 249.

61. L.J.Ignarro, H.Lippton, J.C.Edwards, W.H.Baricos, A.L.Hyman, P.J.Kadowitz, C.A.Gruetter, *ibid*, 1981, **218**, 739.

62. B.T.Mellion, L.J.Ignarro, C.B.Myers, E.H.Ohlstein, B.A.Ballot, A.L.Hyman, P.J.Kadowitz, *Mol. Pharmacol.*, 1983, **23**, 653.

63. W.R.Mathews, S.W.Kerr, *J. Pharmacol. Exp. Ther.*, 1993, **267**, 1529.

64. B.Mayer, A.Schrammel, P.Klatt, D.Koesling, K.Schmidt, *J. Biol. Chem.*, 1995, **270**, 17355; M.P.Gordge, D.J.Meyer, J.Hothersall, G.H.Neild, N.N.Payne, A.Noronha-Dutra, *Br. J. Pharmacol.*, 1995, **114**, 1083.

65. M.W.Radomski, D.D.Rees, A.Dutra, S.Moncada, *Br. J. Pharmacol.*, 1992, **107**, 745; E.A.Kowaluk, H.Fung, *J. Pharmacol. Exp. Ther.*, 1990, **255**, 1256.

66. S.C.Askew, A.R.Butler, F.W.Flitney, G.D.Kemp, I.L.Megson, *Bioorg. Med. Chem.*, 1995, **3**, 1; J.E.Freedman, B.Frei, G.N.Welch, J.Loscalzo, *J. Clin. Invest.*, 1995, **96**, 394.

67. J.D.Horowitz, E.M.Antman, B.H.Lorell, W.H.Barry, T.W.Smith, *Ther. Prev. Pharmacol.*, 1983, **68**, 1247.

68. R.J.MacAllister, A.L.Calver, J.Riezebos, J.Collier, P.Vallance, *J. Pharmacol. Exp. Ther.*, 1995, **273**, 154.

69. J.S.Stamler, D.I.Simon, J.A.Osborne, M.E.Mullins, O.Jaraki, T.Michel, D.J.Singel, J.Loscalzo, *Proc. Natl. Acad. Sci., USA,* 1992, **89**, 444.

70. J.S.Stamler, O.Jaraki, J.Osborne, D.I.Simon, J.Keaney, J.Vita, D.J.Singel, C.R.Valeri, J.Loscalzo, *ibid,* 1992, **89**, 7674.

71. P.C.Jocelyn, *Biochemistry of the SH Group*, 1972, Academic Press, London, p.p. 253.

72. D.I.Simon, J.S.Stamler, O.Jaraki, J.F.Keaney, J.A.Osborne, S.A.Francis, D.J.Singel, J.Loscalzo, *Arteriosclerosis and Thrombosis*, 1993, **13**, 791.

73. P.Needleman, E.M.Johnson, *J. Pharmacol. Exp. Ther.*, 1973, **184,** 709.

74. C.A.Gruetter, P.J.Kadowitz, L.J.Ignarro, *Can. J. Physiol. Pharmacol.*, 1981, **59**, 150.

75. L.J.Ignarro, J.C.Edwards, D.Y.Gruetter, B.K.Barry, C.A.Gruetter, *FEBS Letts.*, 1980, **110**, 275.

76. M.Feelisch, E.Noack, *Eur. J. Pharmacol.*, 1987, **142**, 465.

77. M.Feelisch, *Eur. Heart J.*, 1993, **14** (Supp. 1), 123.

78. D.R.Cameron, A.M.P.Borrajo, B.M.Bennett, G.R.J.Thatcher, *Can. J. Chem.*, 1995, 73, 1627; J.D.Artz, K.Yang, J.Lock, C.Sanchez, B.M.Bennett, G.R.J.Thatcher, *Chem. Commun.*, 1996, 927.

79. M.Feelisch, E.A.Noack, *Eur. J. Pharmacol.*, 1987, **139**, 19.

80. J.Abrams, *Am. J. Med.*, 1991, **91** (Supp. 3c), 106.

81. J.Ramon Leis, A.Rios, *J. Chem. Soc. Chem. Commun.*, 1995, 169.

82. F.W.Flitney, G.Kennovin, *J.Physiol.*, 1987, **392**, 43P.

83. A.R.Butler, A.M.Calsy-Harrison, C.Glidewell, P.E.Sorensen, *Polyhedron*, 1988, **7**, 1197.

84. F.W.Flitney, I.L.Megson, D.E.Flitney, A.R.Butler, *Br. J. Pharmacol.*, 1992, **107**, 842.

85. E.K.Mathews, E.D.Seaton, M.J.Forsyth, P.P.A.Humphrey, *ibid*, 1994, **113**, 87.

86. R.D.Hurst, R.Chowdhury, J.B.Clark, *J. Neurochem.*, 1996, **67**, 1200.

Chapter 2:

Copper Ion Induced Decomposition of S-Nitrosoglutathione

2.1 Introduction

Glutathione (γ-glutamylcysteinylglycine, GSH) is a sulfhydryl tripeptide made up of the amino acids, glutamate (glu), cysteine (cys), and glycine (gly) (2.1).

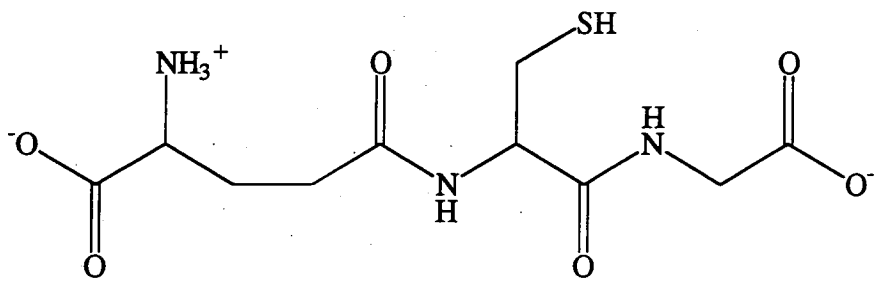

glu cys gly

(2.1)

The glutamate-cysteine peptide bond is unusual in that it involves the γ-carboxyl group of the glutamate amino acid. The four pK_a values are 2.34 (glu-CO_2H), 3.48 (gly-CO_2H), 8.63 (glu-NH_2) and 9.43 (cys-SH)[1]. Therefore, at physiological pH GSH exists as a zwitterion. The glycine carboxyl group is also deprotonated. It is the most abundant thiol in the body with a concentration of ~ 5mM in animal cells[2]. The reduced and oxidised (GSSG) forms act as a sulfhydryl buffer (GSH/GSSG ~ 500) to maintain the integrity of red blood cells. GSH also acts as an antioxidant by reacting with hydrogen peroxide and other organic peroxides produced from aerobic processes within the cell.

GSH can be nitrosated to form S-nitrosoglutathione (GSNO) which may act as an endogenous carrier of NO, released from NO drugs, due to the natural abundance of the thiol and its ease of nitrosation, and thus may prolong the biological activity of NO. GSNO itself is a potent vasodilator[3] and inhibitor of platelet aggregation[4]. Indeed, clinical tests for its use in the inhibition of platelet aggregation during heart surgery[5] and the treatment of high blood pressure in pregnant women[6] have been reported, but the mechanism of NO release from this compound is unknown. Kowaluk *et al*[3] found that degradation of GSNO alone could not account for its vasodilatory properties and proposed that enzymes associated with the cell membrane catalysed NO formation. Radomski *et al*[4] observed GSNO induced inhibition of platelet aggregation as a direct consequence of raised levels of cGMP and similarly

proposed that an enzyme present in platelet membranes is activated to release NO from GSNO when the platelets are stimulated.

In an attempt to understand this mechanism, *in vitro* studies of GSNO decomposition have been undertaken.

2.2 Synthesis of S-Nitrosoglutathione

Nitrosation of glutathione affords GSNO. GSH can be nitrosated by a variety of methods as previously described. GSNO was synthesised and isolated as a pink solid by Hart[7] in 72% yield, based on weight of product. Elemental analysis requires C; 35.2, H; 4.9, N; 16.4, and C; 35.0, H; 4.8, N; 15.7, were obtained. No melting point could be measured as the nitrosothiol decomposes before melting. The UV-Visible spectrum was characterised by a small peak at 546nm and one at 335nm, with an extinction coefficient of 889±7 mol^{-1} dm^3 cm^{-1} (c.f. 922 mol^{-1} dm^3 cm^{-1})[7].

The percentage of GSH present as impurity was established using Ellman's reagent (5,5'dithiobis(2-nitrobenzoic acid), DTNB)[8]. It is commonly used as a thiol assay for SH groups in proteins. DTNB reacts with the thiol to give the mixed disulphide and 2-nitro-5-thiobenzoic acid (TNB) (eqn. 2.1)

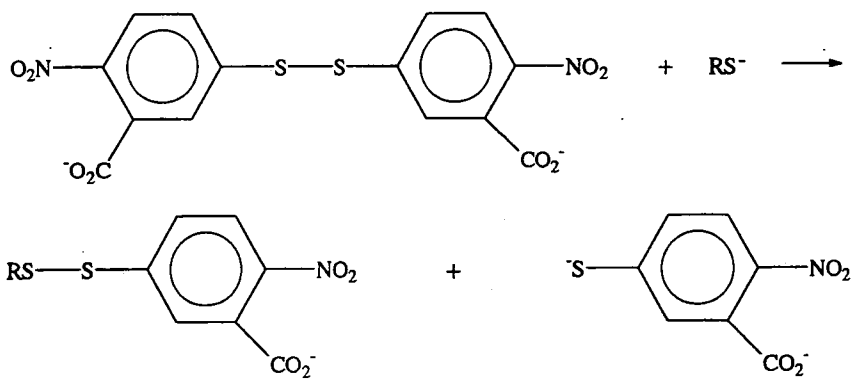

(eqn. 2.1)

The $[TNB^{2-}]$ can be quantified by its absorption peak at 412nm. ε_{412} varies from 11,000-14,000 $mol^{-1}dm^3cm^{-1}$ depending on the pH, temperature and aqueous medium. Therefore ε_{412} was measured in aqueous pH 7.4 phosphate buffer at 25^0C using authentic glutathione. ε_{412}= 14,100±900 $mol^{-1}dm^3cm^{-1}$ and 0.80±0.05% GSH was found in solid GSNO.

The NMR spectra of both GSNO and GSH were obtained in D_2O using a 200MHz ^1H NMR instrument (see fig. 2.1 and 2.2). Resonances of carbon protons only were observed as a result of 1) carboxylic protons being ionised and 2) labile NH and SH protons being replaced by deuterium[9]. Using (2.2) the proton resonances can be assigned as follows:

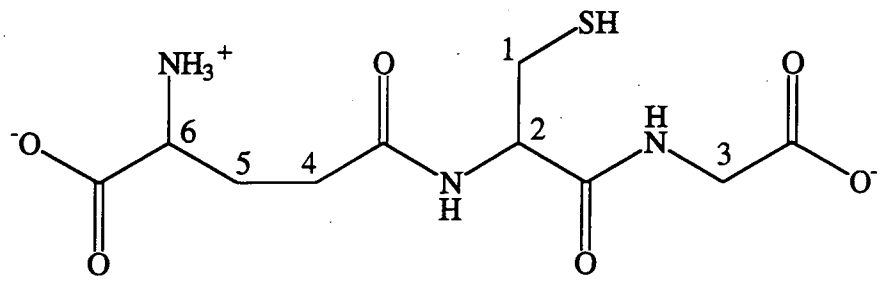

(2.2)

The main chain C-1 methylene protons gave a doublet at 2.8ppm, C-2 proton gave a triplet at 4.4ppm and the C-3 methylene protons gave a singlet at 3.8ppm. The C-4 protons of the glutamate side chain gave a triplet at 2.4ppm; C-5 protons, a quartet at 2.0ppm and the C-6 proton gave a triplet at 3.7ppm. The peak at 4.7ppm was due to residual H_2O in the solvent. An NMR of GSNO was somewhat less resolved. Nitrosation caused the chemical shift of the C-2 proton to shift downfield by 0.1ppm. More importantly, the chemical shift of C-1 protons shifted from 2.8ppm downfield by 1.0ppm causing a multiplet signal at 3.8ppm. This downfield shift of protons adjacent to the SH group upon nitrosation has previously been reported[10,11] and is expected due to the greater electron withdrawing ability of the SNO group.

Unless stated otherwise, GSNO was normally made *in situ* via the nitrosation of GSH using sodium nitrite in 0.1M perchloric acid and diluted with pH 7.4 buffer to the required concentration.

Figure 2.1

^1H NMR spectrum of GSH in D_2O.

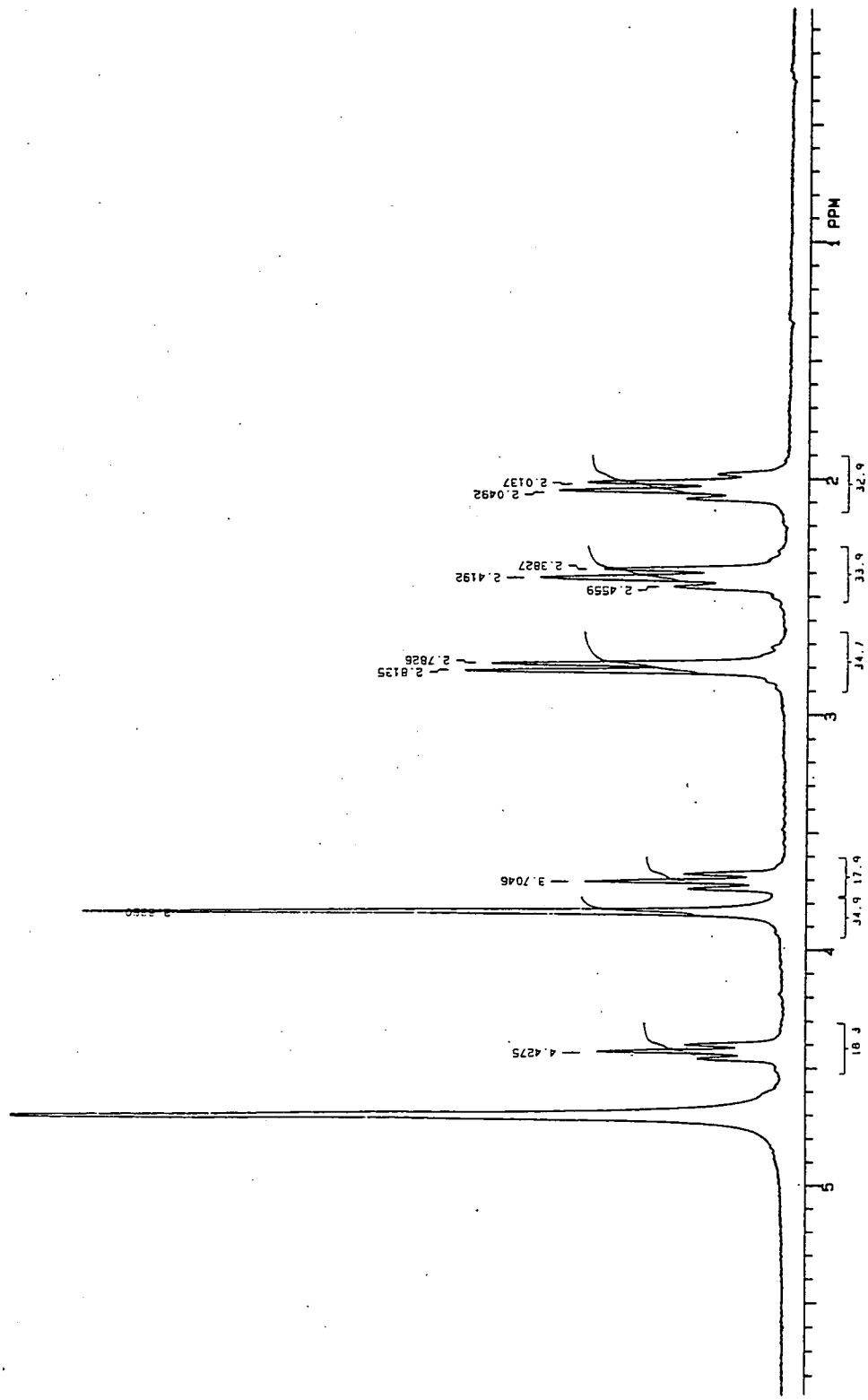

Figure 2.2

^1H NMR spectrum of GSNO in D_2O.

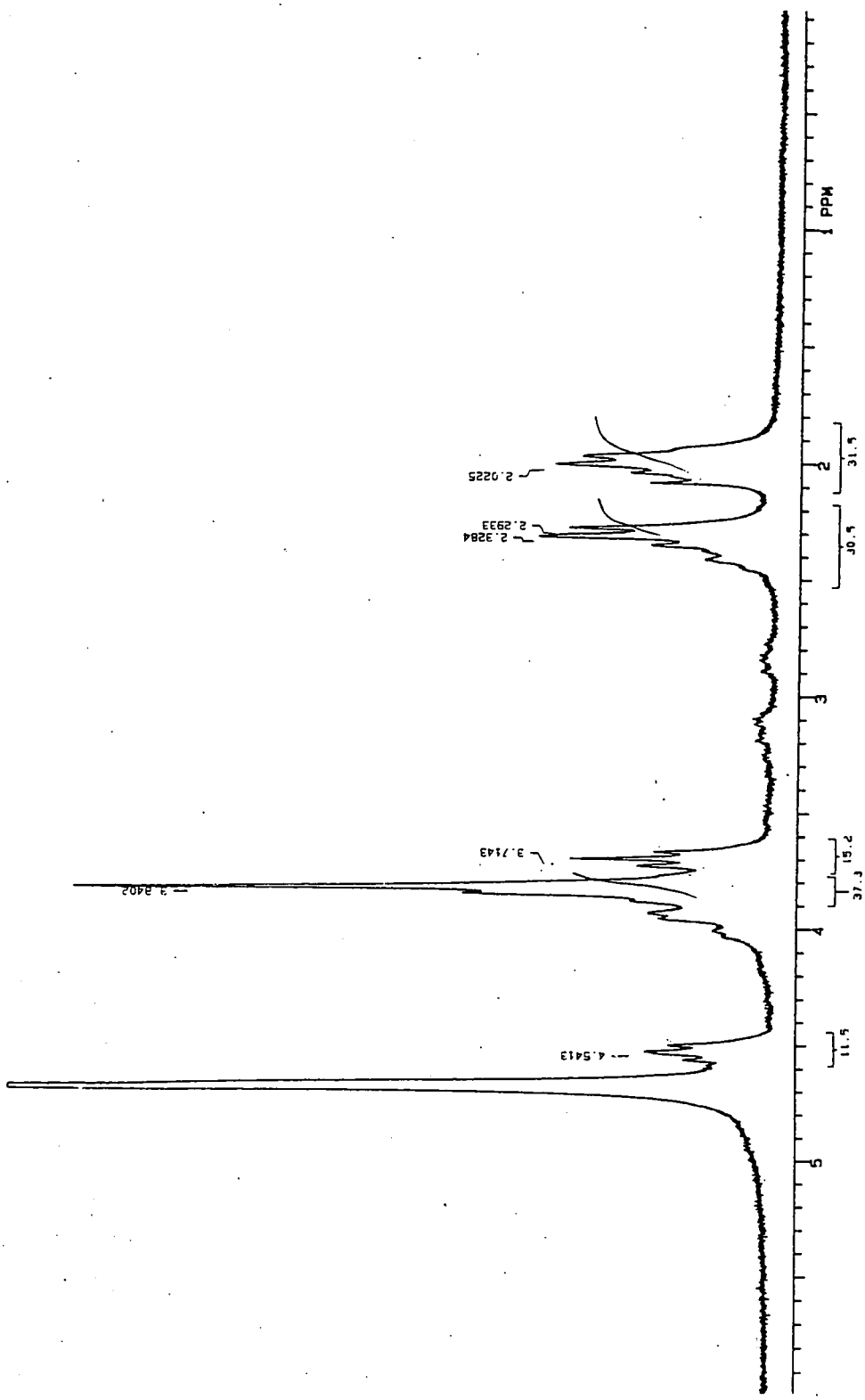

2.3 Identification of Decomposition Products

Being one of the most stable nitrosothiols (a solution of GSNO can be left for longer than 24 hours with minimal degradation) GSNO decomposition at physiological pH (pH 7.4) was brought about by the addition of Cu^{2+} and GSH. The products of GSNO decomposition were identified as being NO and GSSG observed as a Cu^{2+} complex.

2.3.1 NO Detection

In aqueous solution NO rapidly reacts with solvated O_2 producing the nitrite ion but not the nitrate ion[12] (scheme 2.1).

$$2NO + O_2 \longrightarrow 2NO_2$$

$$NO_2 + NO \xrightarrow{\text{fast}} N_2O_3$$

$$N_2O_3 + H_2O \xrightarrow{\text{fast}} 2NO_2^- + 2H^+$$

$$2NO_2 + H_2O \xrightarrow{\text{slow}} NO_2^- + NO_3^- + 2H^+$$

scheme 2.1

Nitrite ion production from NO, released from the decomposition of S-nitroso-N-acetylpenicillamine, has been quantitatively detected[13] using a diazotisation and azo coupling method known as the Griess test[14]. Sulfanilamide (2.3) is diazotised via the nitrite ion in an acidic medium (0.4M HCl) and coupled to N-(1-naphthyl)-ethylenediamine (2.4) to form a purple dye (2.5) which has an absorption maximum at 540nm (eqn 2.2).

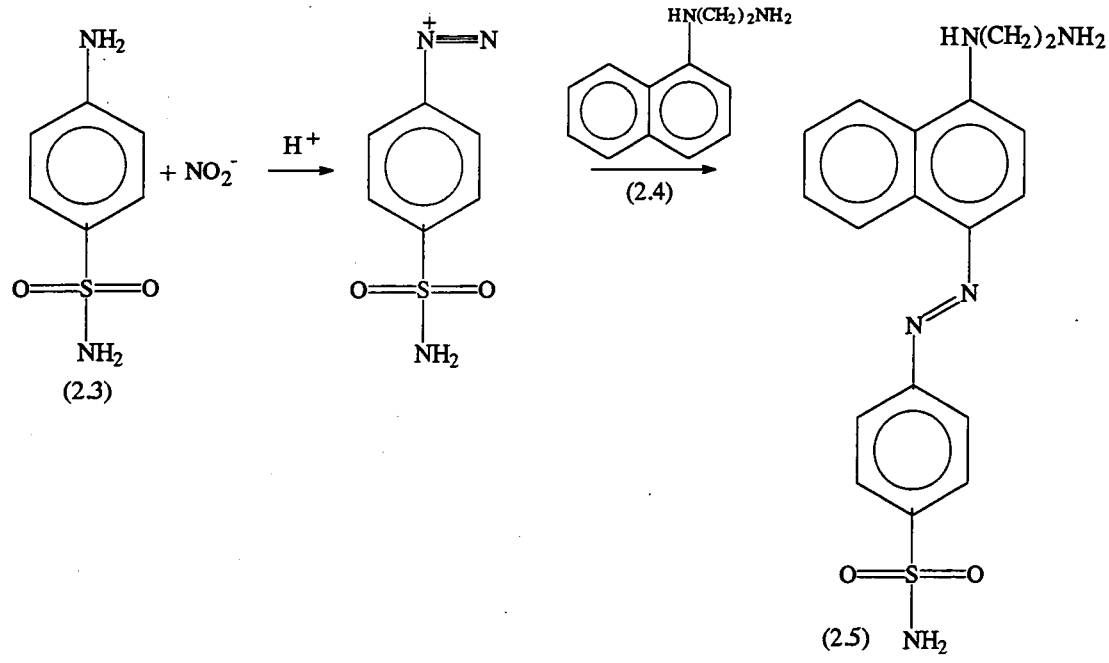

(eqn. 2.2)

Using authentic $NaNO_2$ the extinction coefficient at this wavelength was found to be 48,400±500 $mol^{-1}dm^3cm^{-1}$. ε_{540} was then used to quantify the [NO] released from GSNO. The decomposition of GSNO ($5x10^{-5}M$) in the presence of GSH ($1x10^{-4}M$) and Cu^{2+} ($5x10^{-5}M$) was measured spectrophotometrically at 340nm (ε= 895±7 $mol^{-1}dm^3cm^{-1}$)[15] and took ~1hr. to complete. The solution was then suitably diluted before the rapid addition of sulfanilamide (3.4%) and N-(1-napthyl)-ethylenediamine (0.1%). A peak at 540nm was immediately observed which remained constant for over an hour. 94% NO_2^- was detected corresponding to almost 100% production of NO from GSNO. As the [GSH] increased, the [NO_2^-] detected decreased. To ensure NO was the product and not NO_2^-, independent studies using an NO specific electrode were carried out. Due to the length of time of reaction and the subsequent loss of NO to headspace, NO could only be qualitatively identified but this study unequivocally showed that NO was indeed the product which agreed with Gorren *et al*[16].

2.3.2 Disulfide Detection

Typical spectral scans of GSNO at the start and end of the reaction are shown in fig. 2.3.

Figure 2.3

Spectral scan of GSNO ($5x10^{-4}M$) containing GSH ($1x10^{-4}M$) and Cu^{2+} ($5x10^{-5}M$) at A) t=0 and B) t=1hr.

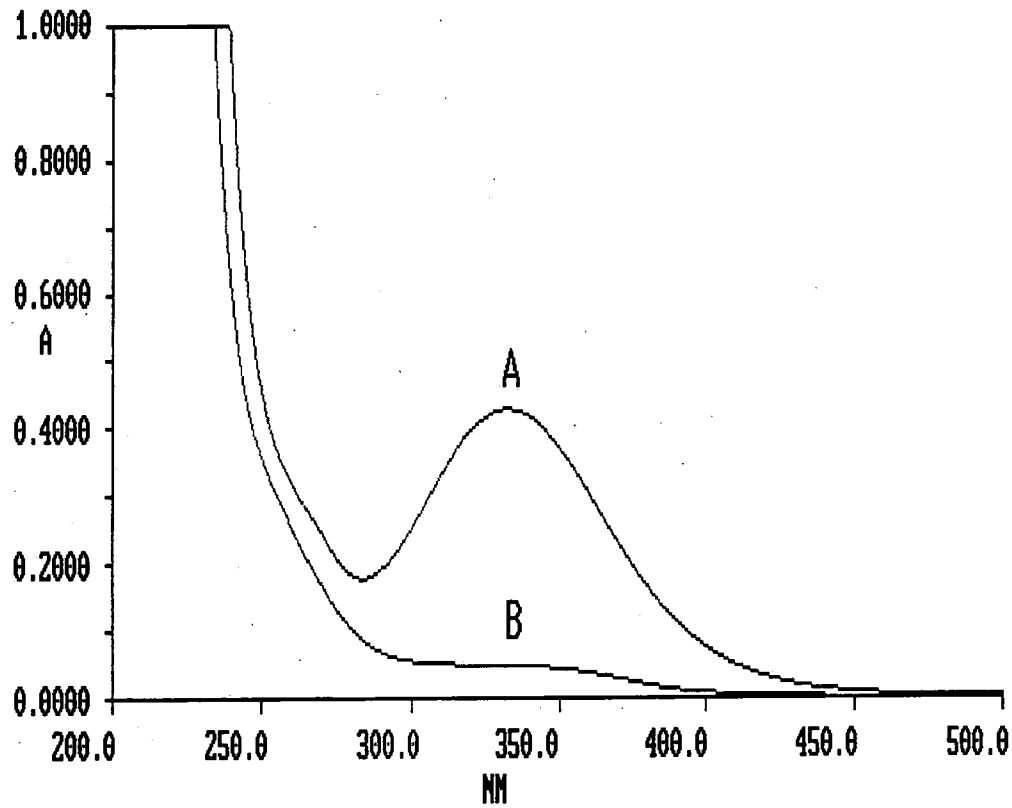

GSNO denitrosation was clearly evident by the decay of the peak at 340nm. A slight shoulder at 260nm was apparent in the initial spectrum and a less defined absorption in the same region at the end of the reaction. Qualitative studies using authentic GSH and GSSG were undertaken to identify the species absorbing in these regions.

2.3.2.1 Copper Ion Complexation By Oxidised Glutathione

GSSG showed no UV-Visible absorption. However in the presence of Cu^{2+} ions a shoulder at 250nm was observed which was stable for over 14hrs. Formation of a metal ion complex was presumed. In more concentrated solution a peak at 620nm was evident, see fig. 2.4. The extinction coefficient of the blue complex at 620nm was 58.4 ± 0.6 $mol^{-1}dm^3cm^{-1}$.

To determine the oxidation state of the metal ion, dithionite (which will reduce Cu^{2+} to Cu^{+} [17]) was added to a Cu^{2+} solution and then GSSG added. A black precipitate resulted presumed to be due to CuO formation[18]. This proved that the disulfide complexes Cu^{2+} only.

Figure 2.4

Spectral scan of GSSG:Cu^{2+} at A) [GSSG]= [Cu^{2+}]= $5x10^{-5}$M and B) [GSSG]= [Cu^{2+}]= $5x10^{-3}$M.

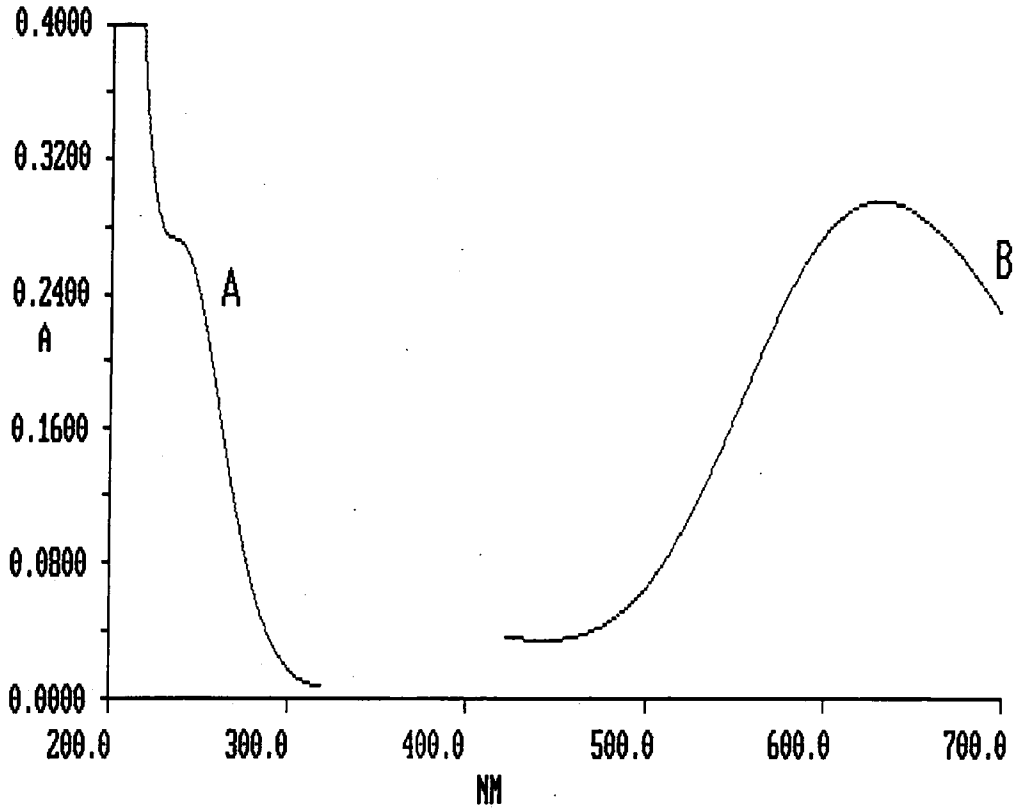

GSSG is a hexapeptide with numerous potential binding sites. A 1:1 complex was observed at acidic[19] and neutral[20] pH with a stability constant of $4x10^{14}$ $mol^{-1}dm^3$ and ε_{620}= 61 $mol^{-1}dm^3cm^{-1}$. Basic conditions afforded a 2:1 Cu^{2+}:GSSG complex[21,22] even in the presence of excess GSSG[23]. Given the spectrophotometric data and the pH of the solution it can be assumed that a 1:1 GSSG:Cu^{2+} complex was formed in this instance. Cu^{2+} complexes are normally tetragonally distorted octahedral complexes as a result of the Jahn Teller effect[24]. Axial ligands are the most weakly bonded and furthest away from the metal centre barely making Van der Waals contacts causing square planar and square pyramidal complexes. On the basis of this, Varnagy *et al*[20] proposed a structure for the GSSG:Cu^{2+} complex (2.6). The geometry surrounding the metal ion is square planar involving coordination of the glu-

NH_2 and glu-CO_2H groups. The coordination of Cu^{2+} in a 2:1 complex involves intervening NH groups and is described by Miyoshi *et al*[22].

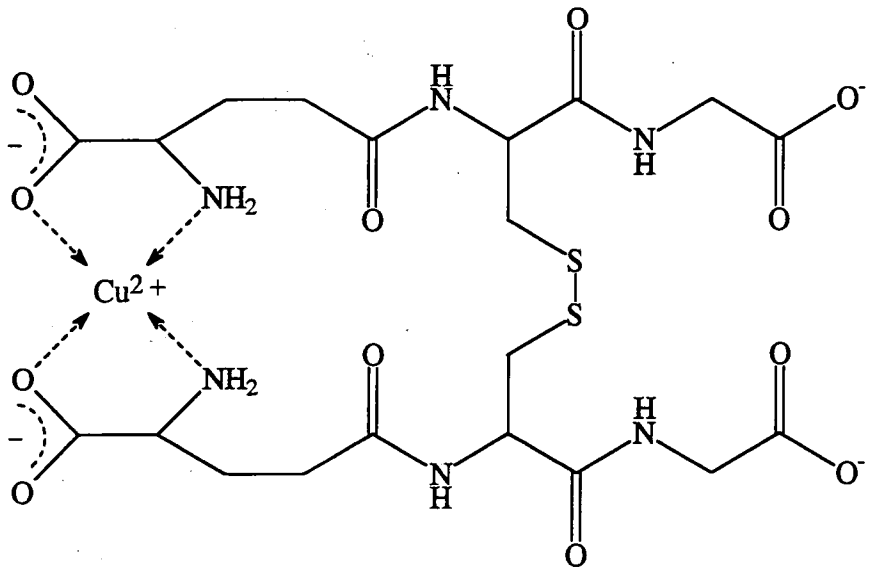

(2.6)

The broad absorption band at 620nm is due to Cu^{2+} d-d transitions and the 250nm shoulder can be tentatively assigned as the $N_\sigma \rightarrow Cu$ charge transfer transition[25].

2.3.2.2 Copper Ion Complexation By Reduced Glutathione

When Cu^{2+} ions were added to GSH a UV-Visible spectrum showed shoulders at 260nm and 300nm. However this spectrum disappeared over 14hrs. giving rise to a shoulder at 250nm, see fig. 2.5.

Figure 2.5

Spectral scan of GSH ($5x10^{-4}M$) and Cu^{2+} ($5x10^{-5}M$) at A) t=0 and B) t=14hrs.

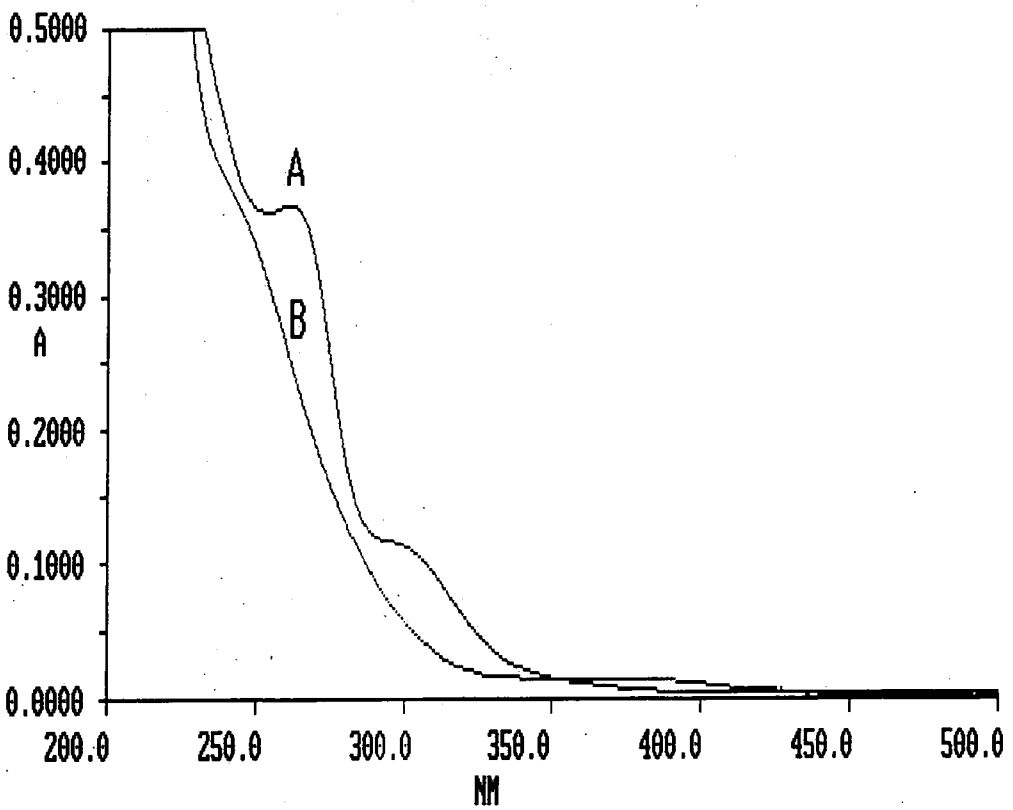

This suggests that a complex involving GSH and the copper ion was formed but was relatively unstable. GSH does not form a complex with Cu^{2+} but rather reduces it[26] (eqn. 2.3).

$$2Cu^{2+} + 2GSH \longrightarrow 2Cu^{+} + GSSG$$

(eqn. 2.3)

Cu^{+} is unstable to disproportionation in solution[18] (eqn 2.4) where K= (5.38 $\pm$0.37)$x10^{5}$ $mol^{-1}dm^{3}$ [27].

$$2Cu^{+} \underset{}{\overset{K}{\rightleftharpoons}} Cu^{2+} + Cu_{(s)}$$

(eqn. 2.4)

This is because the interactions of Cu^{2+} with water molecules are stronger and more favourable as it is smaller with a higher charge density. This is evident in the heats of hydration which are -2100 $kJmol^{-1}$ and -580 $kJmol^{-1}$ for Cu^{2+} and Cu^{+} respectively. The heat of hydration seems to outweigh the second ionisation energy and renders Cu^{2+} more stable in solution. Cu^{+} can be stabilised in acetonitrile or via complexation with ligands such as thiols. Indeed, Hemmerich[28] suggested eqn. 2.3 was an equilibrium reaction which would only go to completion if Cu^{+} was stabilised by the formation of a complex with the excess thiol. Therefore it seems that GSH reduced Cu^{2+} to Cu^{+} which complexed with excess thiol to form a GSH:Cu^{+} complex giving rise to the absorption spectrum shown (fig. 2.5). This is in agreement with work done by Gorren *et al*[16]. These 1:1 and 2:1 complexes have been prepared and used to reconstitute proteins such as ceruloplasmin[29] and Cu,Zn- superoxide dismutase[30] by effectively acting as copper ion donors. Cu^{+} is the softer of the two oxidation states and thus prefers to coordinate to the softer NH and SH moities. Bi- or ter-dentate coordination is preferred, thus on the basis of this the following structure for GSH:Cu^{+} complex involving the formation of favourable six membered ring can be proposed (2.7).

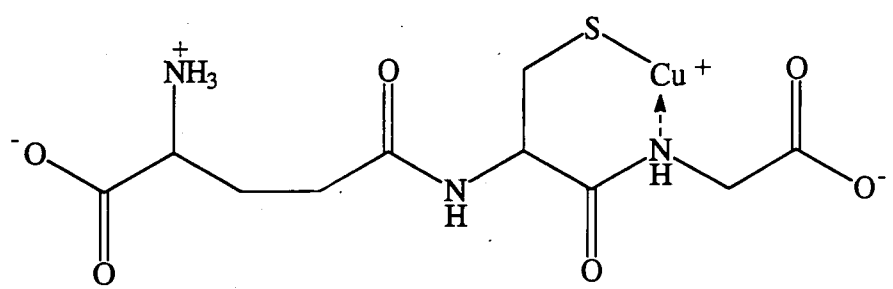

(2.7)

A 2:1 complex can be easily envisaged as coordination of a second GSH molecule in a similar fashion forming a tetrahedral geometry around the metal ion. Chelation via SH and the cys-NH group could also occur but the resulting five membered ring would be less favourable. However, Corazza *et al*[31] have recently reported evidence

to suggest that Cu^+ forms a 1:1 GSH:Cu^+ complex binding to the SH group only. The absorption peak at 300nm can be tentatively assigned to the $S_\sigma \rightarrow Cu$ charge transfer transition and the peak at 260nm assigned to the $N_\sigma \rightarrow Cu$ charge transfer transition[25]. Fig. 2.3 shows that this complex is not very stable and a GSSG:Cu^{2+} complex was formed with time. This is probably as a result of solvated oxygen causing the release and oxidation of the metal ion (see later) and subsequent chelation by the disulfide.

2.3.2.3 Determination of the Complexed Product

The absorption shoulder at 260nm observed at the start of GSNO decomposition was due to the rapid reduction of Cu^{2+} via GSH and complexation with excess thiol to form the GSH:Cu^+ complex. The absorption peak at 300nm was masked by the GSNO peak. The spectrum of the solution at the end of the reaction was matched with a spectrum of GSSG and Cu^{2+} (fig. 2.6). Many different spectral scans of GSSG and GSH with Cu^{2+} were tried but this gave the best match and corresponds to conversion of GSNO and GSH to GSSG.

Figure 2.6

Spectral scan of A) GSNO decomposition at end of reaction and B) GSSG ($3x10^{-4}M$) and Cu^{2+} ($5x10^{-5}M$)

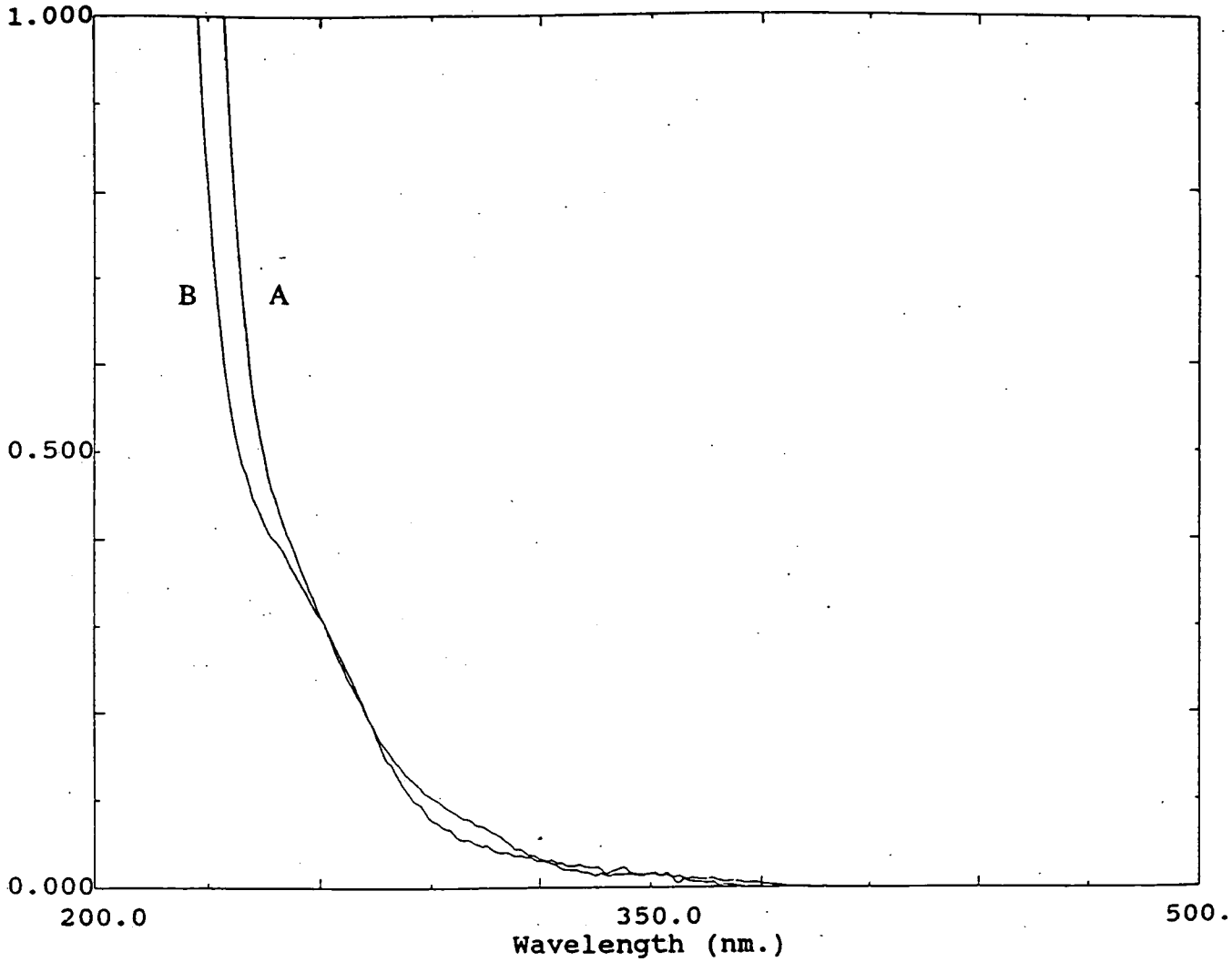

In summary, GSH/Cu^{2+} induced decomposition of GSNO involves the formation of a $GSH:Cu^{+}$ complex to produce NO and the $GSSG:Cu^{2+}$ complex.

2.4 Decomposition In The Presence of Various Chelating Agents

As previously discussed nitrosothiol denitrosation is catalysed by copper ions, more specifically by the Cu^+ ion (see section 1.2.5.4). The possibility of copper ion catalysis of GSNO denitrosation was investigated.

2.4.1 EDTA Chelation

Ethylenediaminetetraacetic acid, EDTA, is a non-specific metal ion chelator (2.8).

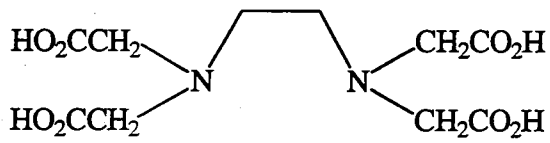

(2.8)

EDTA will chelate Cu^{2+} ions and disproportionate Cu^+ to form a 2:1 EDTA:Cu^{2+} complex involving coordination via the two N atoms[28]. S-nitrosocysteine (SNC), the nitroso derivative of cysteine is known to rapidly decompose via Cu^+ ion catalysis[32]. A typical pseudo first order decay (k_{obs}= 0.17±0.01 s^{-1}) is shown in fig. 2.7. However, decomposition stopped when EDTA was added.

Figure 2.7

Reaction profile of SNC ($5x10^{-4}M$) decomposition in the presence of Cu^{2+} ($5x10^{-5}M$) with of A) [EDTA]= 0 and B) [EDTA]= $1x10^{-4}M$.

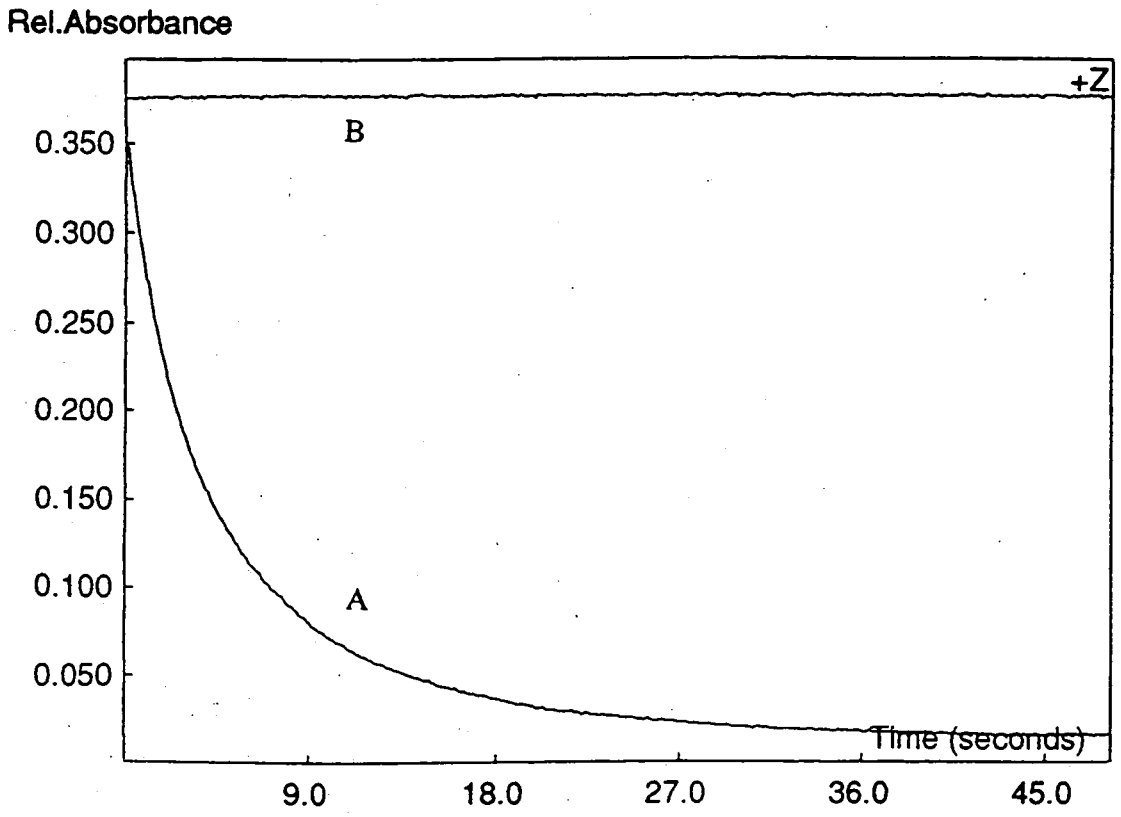

Similarly, GSNO decomposition was not observed in the presence of EDTA (fig. 2.8).

Figure 2.8

Reaction profile of GSNO ($5x10^{-4}M$) decomposition in the presence of Cu^{2+} ($5x10^{-5}M$) and GSH ($5x10^{-5}M$) with A) [EDTA]= 0 and B) [EDTA]= $1x10^{-4}M$.

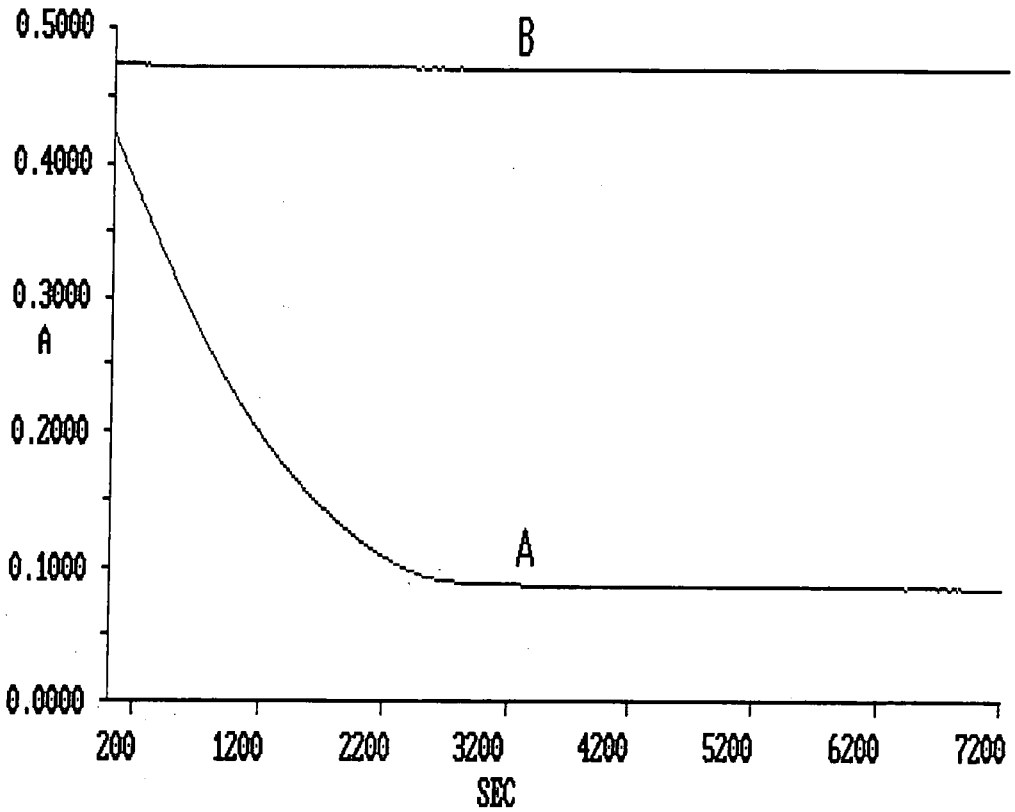

This experiment clearly showed that GSNO denitrosation was catalysed by copper ions.

2.4.2 Neocuproine Chelation

Neocuproine was employed to determine the oxidation state of the catalytic species. Neocuproine (2.9) is a known Cu^{+} specific chelator[33] which forms a 2:1 neocuproine:Cu^{+} complex easily identified by its absorption maximum at 453nm (ε_{453}=7950 $mol^{-1}dm^{3}cm^{-1}$).

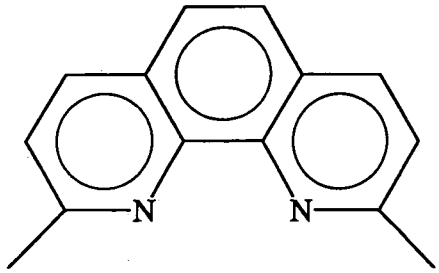

(2.9)

The structure of this complex is shown (2.10)[33].

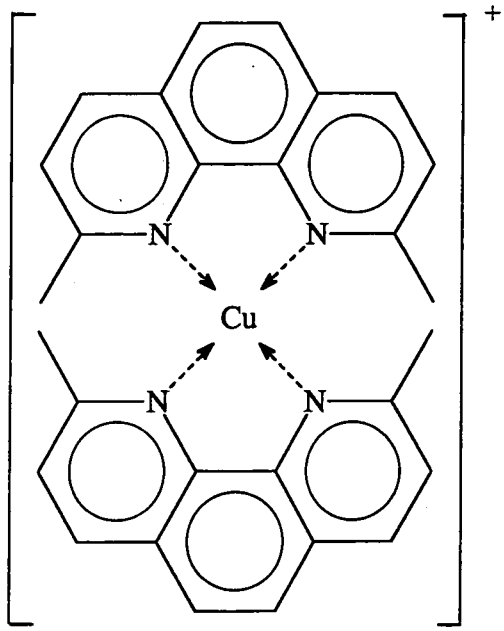

(2.10)

The specificity of the chelator towards Cu^+ has been tested by comparing the spectrum of Cu^{2+} and neocuproine, and Cu^+ (produced from the reduction of Cu^{2+} by dithionite) and neocuproine with authentic neocuproine[34]. A spectrum of the former was no different to authentic neocuproine whereas a peak at 453nm was observed for the latter. When neocuproine (5 fold excess) was added to a GSH/Cu^{2+} solution a peak at 453nm was immediately observed and was stable for over an hour. The [neocuproine:Cu^+] corresponded to 92% reduction of Cu^{2+} via the thiol. Halting GSNO denitrosation was then attempted by the addition of neocuproine but a precipitate resulted and no clear measurements could be made. However, experiments using a NO probe detected no NO in the presence of neocuproine[16]. These results collectively confirm that the catalytic species was Cu^+.

2.4.3 Cuprizone Chelation

It was unclear as to whether copper was a true catalyst i.e. whether decomposition involved a Cu^{+}/Cu^{2+} redox reaction or whether the copper ion remained in its +1 oxidation state. Two possible reactions can be proposed:

$$GSNO + Cu^{+} \longrightarrow GS^{-} + Cu^{2+} + NO$$

(eqn. 2.5)

$$GSNO + Cu^{+} \longrightarrow GS^{\cdot} + Cu^{+} + NO$$

(eqn. 2.6)

Cuprizone (2.11) is a Cu^{2+} specific chelator which forms a 2:1 cuprizone:Cu^{2+} complex with an absorption maximum at 620nm, $\varepsilon_{620}=16000$ $mol^{-1}dm^{3}cm^{-1}$ and thus can be easily detected[35].

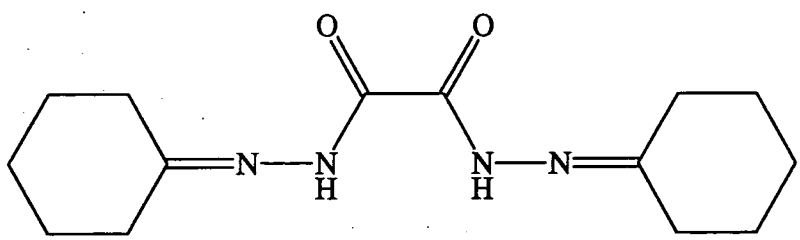

(2.11)

The structure of this complex is shown (2.12)[36].

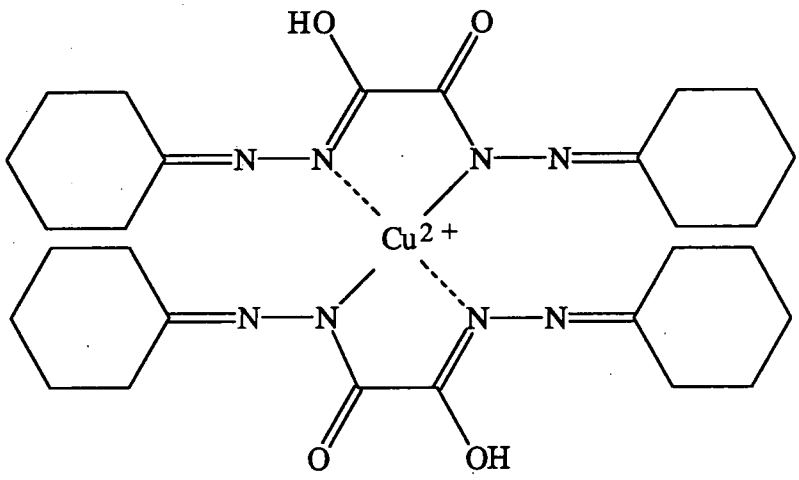

(2.12)

To test its specificity dithionite (50 fold excess) was added to a Cu^{2+} solution and cuprizone (4 fold excess) added. No absorption spectrum was observed clearly indicating that the chelator could not complex Cu^{+}. If reoxidation of Cu^{+} occurred (eqn. 2.5) then the addition of cuprizone would inhibit the reaction due to Cu^{2+} ion chelation. However cuprizone could not stop decomposition when added after the start of the reaction or when initially present. This was also observed by Gorren *et al*[16] who proposed eqn. 2.6 on this basis. What was not recognised was the complexing ability of the disulfide. At the start of the reaction copper ions are in the +1 oxidation state and complexed with GSH thus cuprizone was unable to chelate the metal ion at the start of reaction. As decomposition occurred the disulfide, which has a higher affinity for Cu^{2+}, preferentially complexed the metal ion and hence cuprizone had no effect on the reaction. To confirm this, cuprizone ($4x10^{-4}M$) was added to a solution of GSSG ($4x10^{-4}M$) and Cu^{2+} ($5x10^{-5}M$). No cuprizone complex was observed. Therefore eqn. 2.5 was not necessarily wrong. In fact it was presumed to be more likely considering the nature of the GSSG product and the instability of Cu^{+} in aqueous solution.

2.4.4 Disulfide Chelation

The apparent stability of the GSSG:Cu^{2+} complex poses a puzzling question. The disulfide effectively acts as a chelator of Cu^{2+} and stops GSH from reducing it. Therefore why did GSNO decomposition normally go to completion? In answer to this GSH ($2x10^{-3}M$) was added to a solution of GSSG:Cu^{2+} ($2x10^{-3}M$). A decrease in absorbance at 620nm resulted and showed that GSH could disrupt the disulfide

complex in some way. What is more, GSH ($2x10^{-4}M$) was added to a GSSG:Cu^{2+} ($2x10^{-4}M$) solution and a peak at 453nm was immediately observed upon the addition of neocuproine ($8x10^{-4}M$) and corresponded to 82% conversion of Cu^{2+} to Cu^{+}. Hence, GSH is capable of releasing and reducing Cu^{2+} from the GSSG:Cu^{2+} complex (eqn. 2.7).

$$GS^{-} + GSSG{:}Cu^{2+} \longrightarrow GS^{\cdot} + Cu^{+} + GSSG$$

(eqn. 2.7)

So not only does the thiol produce the catalytic species in the first instance, it also regenerates it from the product. This is probably the reason why such high concentrations of thiol are required, compared to other more fast reacting nitrosothiols, before reaction will go to completion.

In the presence of added disulfide, decomposition did not slow but was prevented from going to completion, see fig. 2.9. This was probably because [GSSG]>[GSH] and the copper ion could not be retrieved from the stable disulfide complex.

Figure 2.9

Reaction profile of GSNO ($5x10^{-4}M$) decomposition via GSH ($5x10^{-5}M$) and Cu^{2+} ($5x10^{-5}M$) in the presence of A) no added GSSG B) [GSSG]= $5x10^{-5}M$ C) [GSSG]= $5x10^{-4}M$ D) [GSSG]= $1.25x10^{-3}M$.

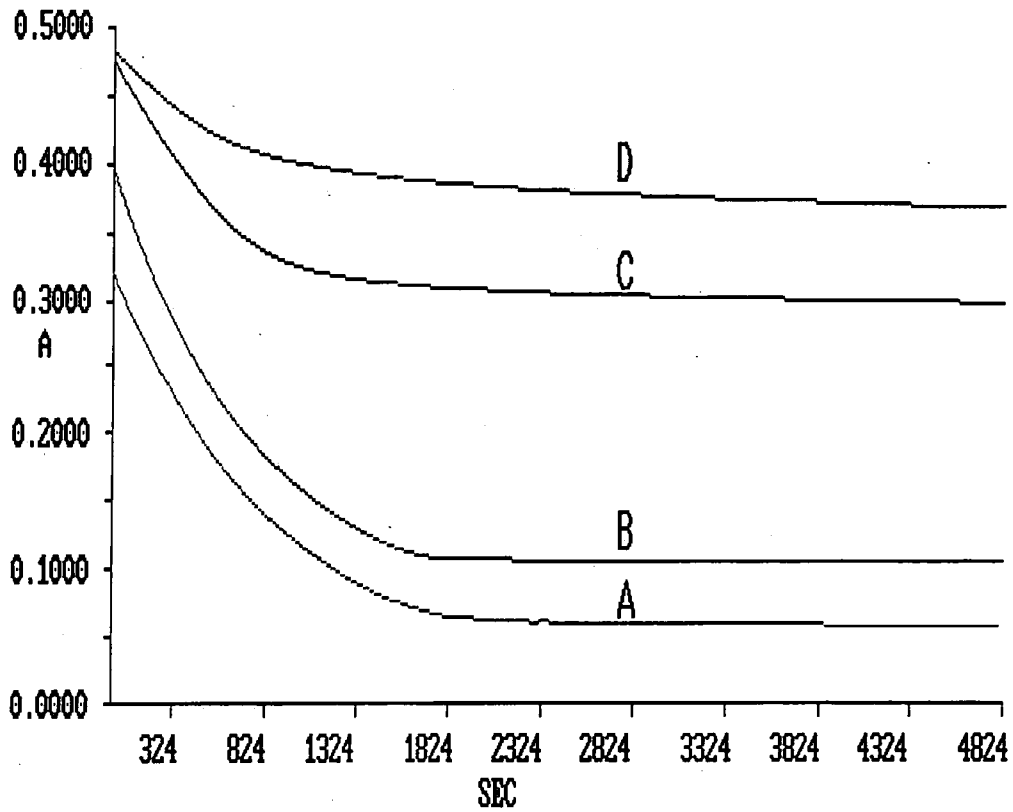

In summary, decomposition is a Cu^{2+}/Cu^{+} redox reaction. GSH produces the Cu^{+} catalytic species and can regenerate it from the GSSG:Cu^{2+} complex.

2.5 Kinetic Studies of Decomposition

Reaction profiles for GSNO decomposition were obtained at 340nm such that the effects of varying [GSH], [Cu^{2+}] and [O_2] on the reaction could be established.

2.5.1 Addition of GSH

The importance of thiol in decomposition reactions has previously been discussed (section 1.2.5.4). Generally only a small amount (~10^{-6}M) is required; the concentration of thiol naturally present due to the slight reversibility of the nitrosation reaction (see section 1.2.4.2) is often enough. However, because GSNO is so stable and because of the complexing ability of the disulfide (section 2.4.4) a comparatively high concentration of GSH was required before decomposition would go to completion. Similarly, [Cu^{2+}] naturally present in the buffer (at 10^{-6}M) is enough to cause decomposition but a higher concentration was required for GSNO. A typical reaction profile for 1:1 and 2:1 GSH:Cu^{2+} ratios is shown in fig. 2.8. The decay was neither clean zero nor first order but was reproducible and took about 1hr. to complete. This was a much slower reaction than that reported by Gorren *et al*[16]. They were observing GSNO($1x10^{-4}$M) decomposition in the presence of GSH($1x10^{-5}$M) and Cu^{2+}($2.5x10^{-4}$M) using stopped-flow techniques. Reaction profiles also showed no conventional order but took only ~200s to complete. This could have been because they were using a solid source of GSNO which may have contained thiol impurities thus causing the [GSH] to be greater than expected; they did report 5% GSH impurity in their sample. In an attempt to understand this difference in timescale, reactions were undertaken using solid GSNO (for synthesis see section 2.2) under the same experimental conditions. Decomposition still took 1hr. complete and there was no significant difference in the shape of the profile or the spectrum of the solution at the start and end of reaction. Therefore this difference in time was not due to the GSNO source but more probably due to the comparatively high [Cu^{2+}] they used.

The GSH:Cu^{2+} ratio was increased to 10:1 and an initial induction period of ~4hrs. was observed prior to decomposition which again took ~1hr. to complete. If the concentration of GSH was increased the induction time increased. However, the time interval in which decomposition occurred remained constant (see fig. 2.10).

Figure 2.10

Reaction profile of GSNO decomposition in the presence of Cu^{2+} ($5x10^{-5}M$) with A) [GSH]= $5x10^{-4}M$ B) [GSH]= $1x10^{-3}M$.

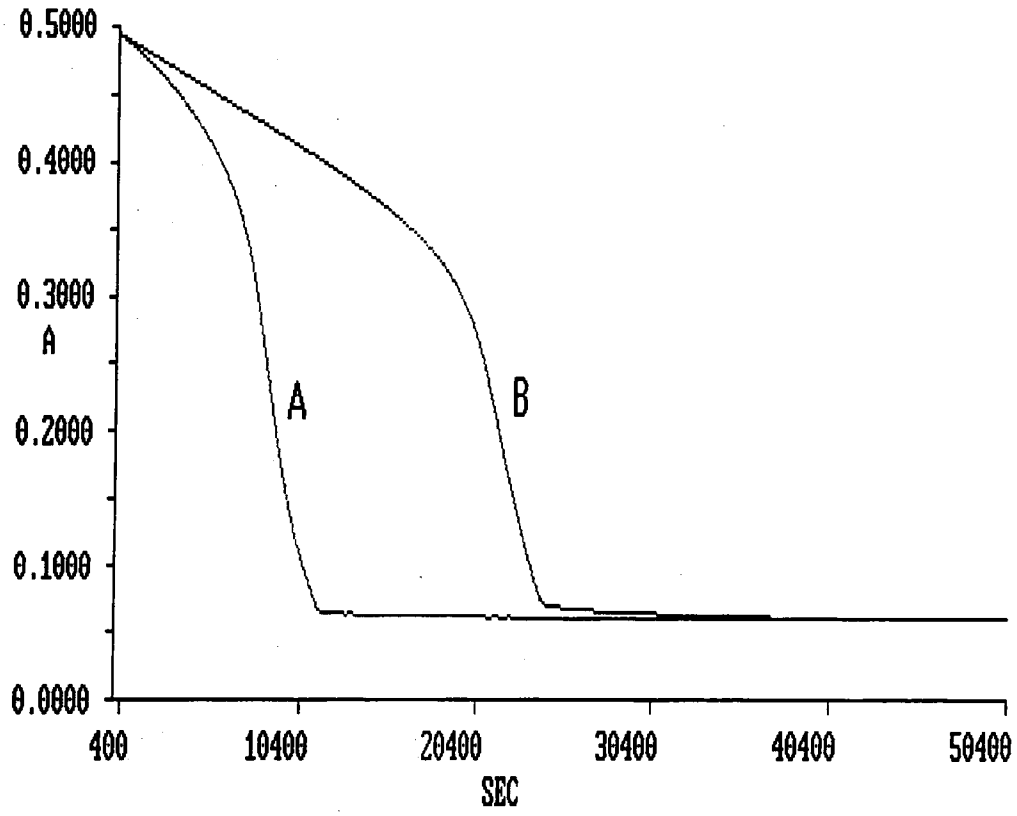

The increase in [GSH] also resulted in an increase in absorbance at 260nm and 340nm in the initial spectrum, see fig. 2.11.

Figure 2.11

Spectral scan at t= 0 of GSNO decomposition in the presence of Cu^{2+} ($5x10^{-5}M$) with A) [GSH]= $5x10^{-5}M$ B) [GSH]= $1x10^{-4}M$ C) [GSH]= $5x10^{-4}M$.

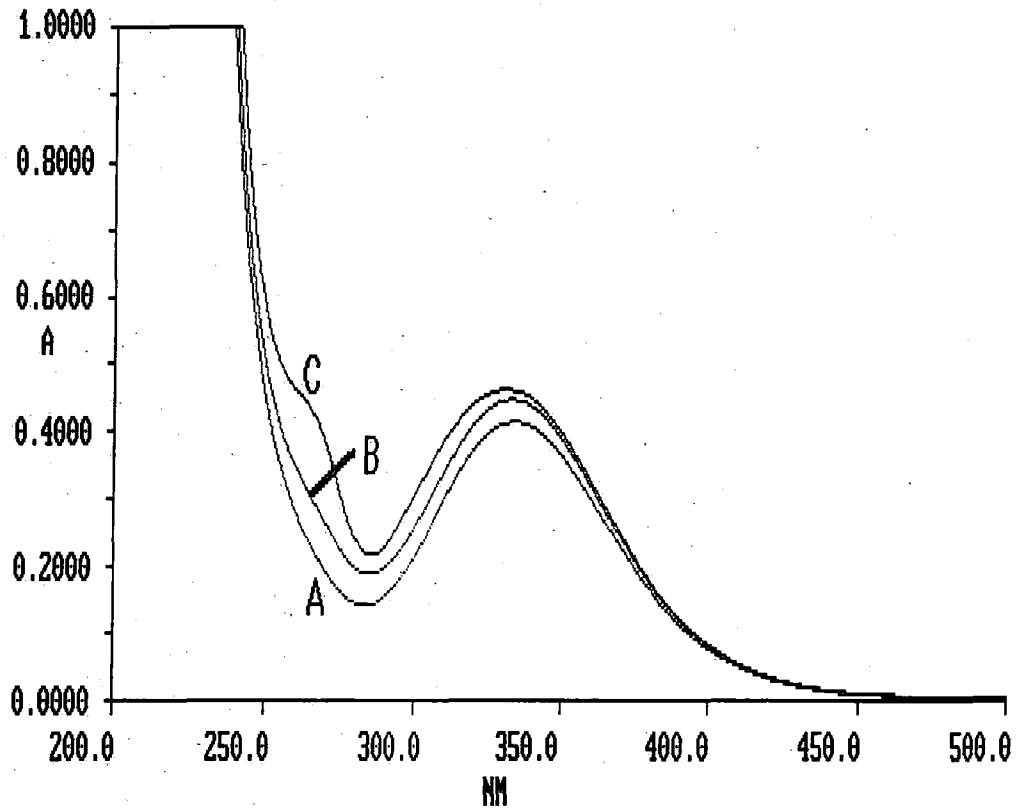

This showed that at a GSH/Cu^{2+} ratio of one there was very little GSH:Cu^{2+} complex formation whereas at a GSH/Cu^{2+} ratio of ten the thiol complex was prominent and the formation of higher order complexes possible[37]. Therefore the induction period could be as a result of GSH:Cu^{+} chelation inhibiting the ion from reacting with the nitrosothiol.

2.5.2 Addition of Cu^{2+}

A two fold increase in [Cu^{2+}] did not alter the decomposition time ([GSH]= $5x10^{-5}M$). However, the induction time was reduced by 30mins due to the GSH/Cu^{2+} ratio being lowered, see fig. 2.12.

Figure 2.12

Reaction profile of GSNO decomposition in the presence of GSH ($5x10^{-4}M$) with A) $[Cu^{2+}]= 5x10^{-5}M$ B) $[Cu^{2+}]= 1x10^{-4}M$.

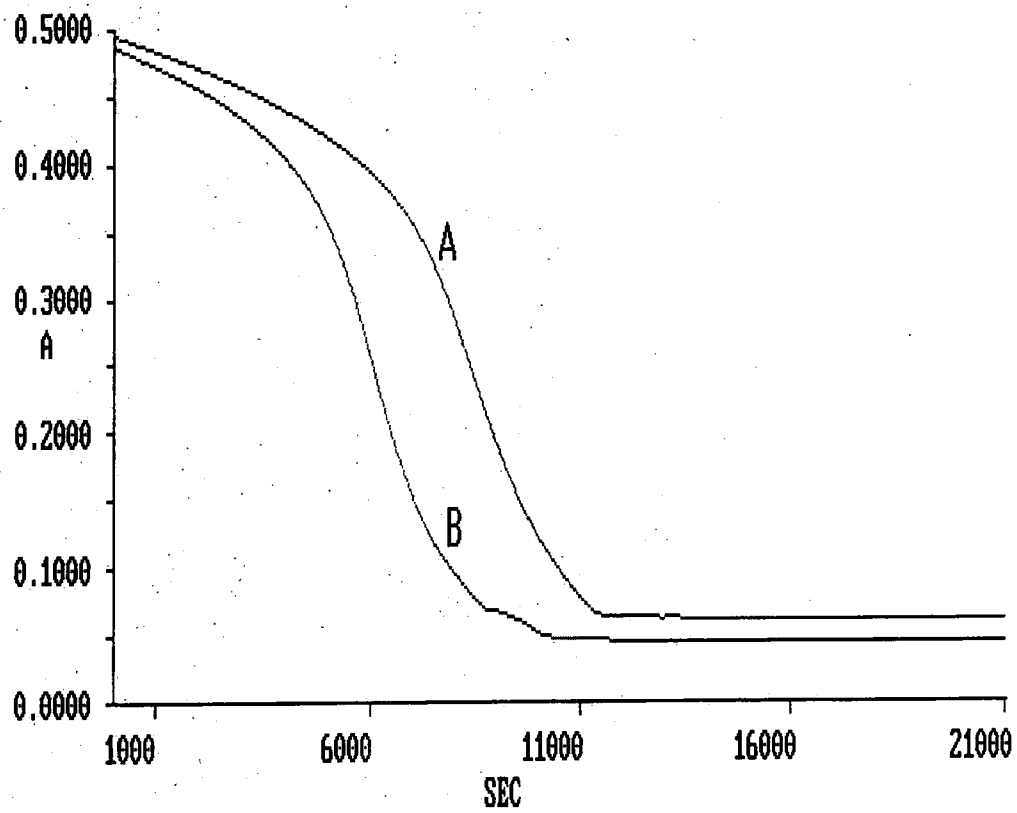

2.5.3 Effect of Oxygen

It soon became apparent that solvated oxygen had an effect on the reaction profile. The $[O_2]$ in water is ~$3x10^{-4}M$[38]. Solutions were purged with N_2, to eliminate the majority of solvated O_2, prior to reaction. In a separate set of experiments solutions were purged with O_2, to increase the concentration of solvated oxygen. The effect on decomposition and induction times is shown in fig. 2.13 and 2.14 respectively.

Figure 2.13

Reaction profile of GSNO decomposition in the presence of GSH ($5x10^{-5}M$) and Cu^{2+} ($5x10^{-5}M$) in A) deaerated B) aerated C) O_2 rich solution.

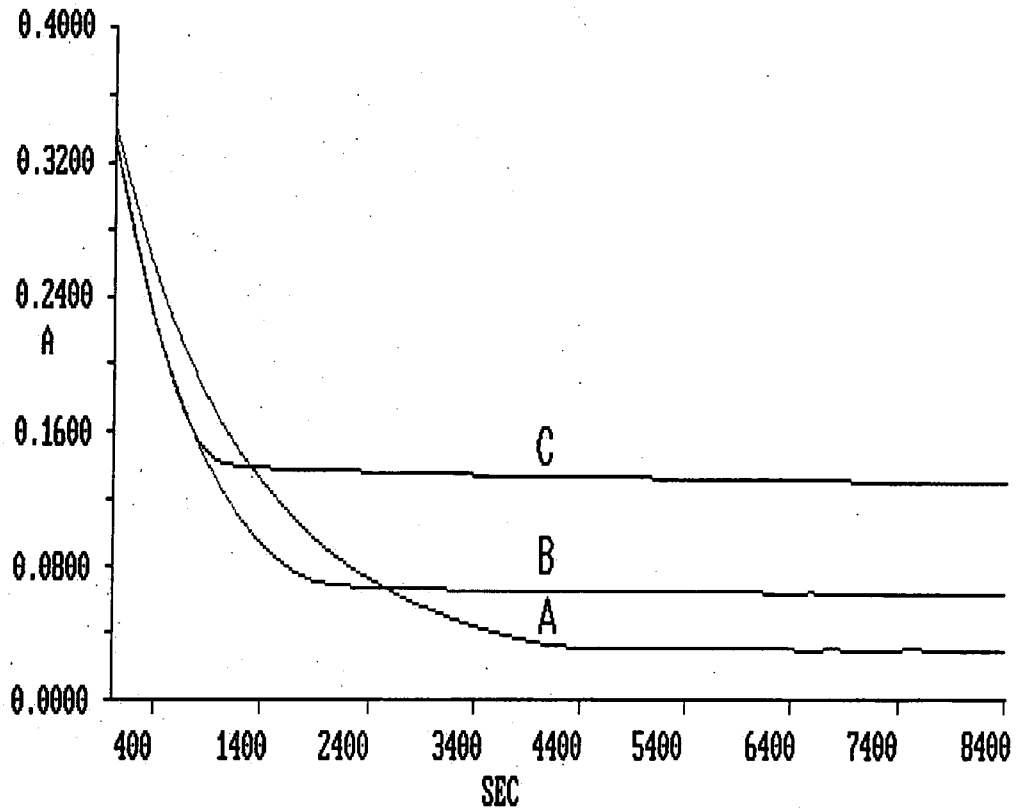

Figure 2.14

Reaction profile of GSNO decomposition in the presence of GSH ($5x10^{-4}M$) and Cu^{2+} ($5x10^{-5}M$) in A) deaerated B) aerated C) O_2 rich solution.

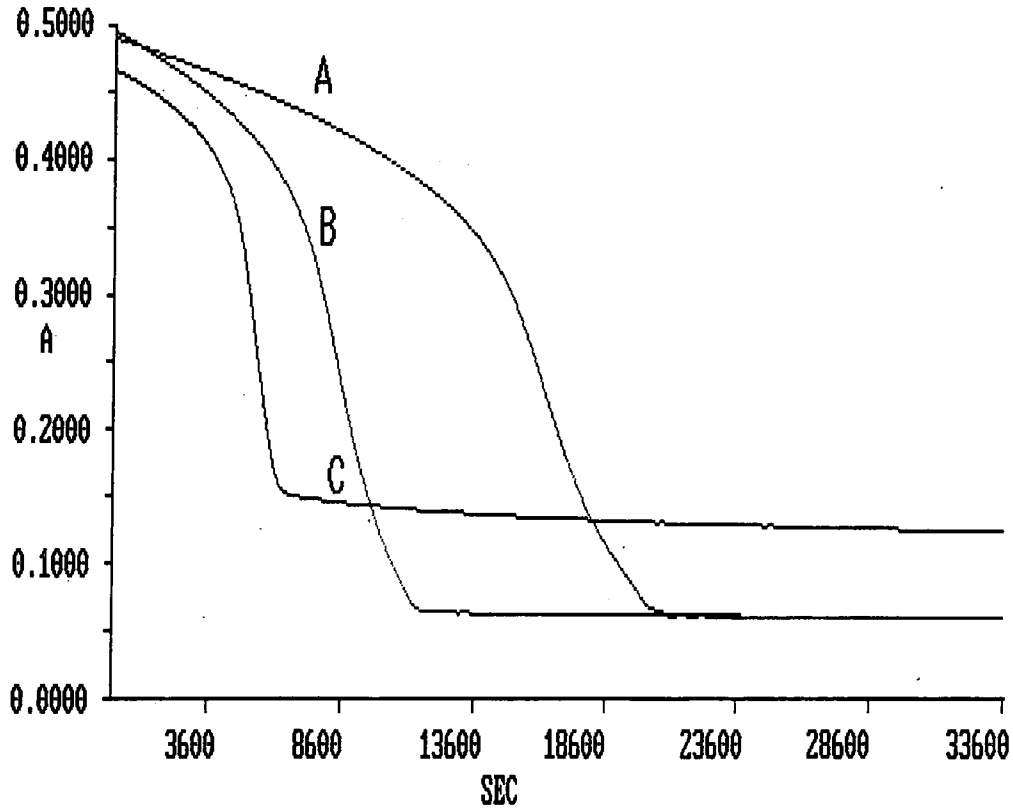

Anaerobic conditions were also obtained in a separate set of reactions using the glucose/ glucose oxidase method[16]. Glucose (10mM) was added to a 100ml phosphate buffer containing 2mg glucose oxidase and 1mg catalase. The solution was incubated at 37°C for 1hr. 100ml 0.1M perchloric acid was deaerated likewise and solutions used to make up GSH, GSNO and Cu^{2+} stock solutions. Under these conditions, decomposition was no different to when anaerobiosis was attained using N_2 gas. As the $[O_2]_{dis}$ increased the decomposition and induction times decreased. The appearance of the induction period and the depleted $[NO_2^-]$ detected at higher concentrations of GSH (see section 2.3.1) would suggest that the catalytic species was the free Cu^+ ion and not the GSH:Cu^+ complex. To account for its effect, Gorren *et al*[16] proposed that O_2 could release Cu^+ from this complex (eqn. 2.8).

$$O_2 \quad + \quad GSCu \quad \longrightarrow \quad O_2^{-\cdot} \quad + \quad Cu^+ \quad + \quad GS^{\cdot}$$

(eqn. 2.8)

Thus the induction period could be described as being the time taken for solvated oxygen to release Cu^+ from the thiol complex and would explain why it was reduced when the GSH/Cu^{2+} ratio was lowered (see section 2.5.2). The superoxide ion can be spectrophotometrically detected in solution using tetranitromethane[39]. $O_2^{-\cdot}$ reacts with $C(NO_2)_4$ to form the nitroform ion which absorbs at 350nm, ε_{350}= 14,800mol^{-1}dm^{3}cm^{-1} [40] (eqn. 2.9).

$$O_2^{-\cdot} \quad + \quad C(NO_2)_4 \quad \longrightarrow \quad O_2 \quad + \quad C(NO_2)_3^- \quad + \quad NO_2^{\cdot}$$

(eqn. 2.9)

$NO_2^{\cdot}$ subsequently reacts with another $O_2^{-\cdot}$ molecule to give the nitrite ion (eqn. 2.10).

$$O_2^{-\cdot} \quad + \quad NO_2^{\cdot} \quad \longrightarrow \quad O_2 \quad + \quad NO_2^-$$

(eqn. 2.10)

Therefore, one molecule of $C(NO_2)_3^-$ corresponds to two molecules of $O_2^{-\cdot}$. $C(NO_2)_4$ was added to an equimolar solution of GSH and Cu^{2+} ($3x10^{-5}$M) and an absorption peak at 350nm was immediately observed. The absorbance remained constant for over an hour and corresponded to 60% $O_2^{-\cdot}$ detected thus demonstrating the validity of eqn. 2.8.

The superoxide ion is in equilibrium with its protonated form (pK_a= 4.8) (eqn. 2.11).

$$H^+ + O_2^{-\cdot} \rightleftharpoons HO_2^{\cdot}$$

(eqn. 2.11)

At pH 7.4 therefore 0.25% $O_2^{-\cdot}$ is protonated. Both forms have reducing and oxidising properties although the unprotonated form is the most reactive. $O_2^{-\cdot}$ disproportionates in aqueous solution via the following reactions:

$$O_2^{-\cdot} + HO_2^{\cdot} \xrightarrow{H^+} H_2O_2 + O_2$$

($k = 8.5 \times 10^7$ mol^{-1}dm^{3}s^{-1}) (eqn. 2.12)

$$HO_2^{\cdot} + HO_2^{\cdot} \longrightarrow H_2O_2 + O_2$$

($k = 8.3 \times 10^5$ mol^{-1}dm^{3}s^{-1})(eqn. 2.13)

$$O_2^{-\cdot} + O_2^{-\cdot} \xrightarrow{2H^+} H_2O_2 + O_2$$

($k < 0.3$ mol^{-1}dm^{3}s^{-1})(eqn. 2.14)

Dismutation is also catalysed by metal ions especially copper[41]. Rate constants for the following reactions have been determined in aqueous solution:

$$Cu^{2+} + O_2^{-\cdot} \longrightarrow Cu^+ + O_2$$

($k = 8.0 \times 10^9$ mol^{-1}dm^{3}s^{-1})(eqn. 2.15)

$$Cu^{2+} + HO_2^{\cdot} \longrightarrow Cu^{+} + O_2 + H^{+}$$

($k = 1.0 \times 10^8$ mol^{-1}dm^{3}s^{-1})(eqn. 2.16)

$$Cu^{+} + O_2^{-\cdot} \xrightarrow{2H_2O} Cu^{2+} + H_2O_2 + 2OH^{-}$$

($k \sim 10^{10}$ mol^{-1}dm^{3}s^{-1})(eqn. 2.17)

$$Cu^{+} + HO_2^{\cdot} \xrightarrow{H_2O} Cu^{2+} + H_2O_2 + OH^{-}$$

($k > 10^9$ mol^{-1}dm^{3}s^{-1})(eqn. 2.18)

The rates of $O_2^{-\cdot}$ disproportionation via Cu^{2+} and Cu^{+} are equal and greater than that of the uncatalysed reaction therefore the depleted concentration of $O_2^{-\cdot}$ detected was probably due to eqns. 2.15 and 2.17. During denitrosation it is presumed that these two reactions counterbalance each other such that a net increase in Cu^{+} results.

When the $[O_2]_{dis}$ was increased the extent of decomposition decreased. No reasonable explanation for this can be given. If [GSH] was depleted and the $[Cu^{2+}]$ increased more disulfide complex would be formed, the Cu^{+} ion would not be regenerated (eqn. 2.7) and the reaction would be prematurely stopped. Further studies must be done before incomplete denitrosation under these conditions is understood.

In summary, kinetics of decomposition proved difficult due to the formation of the GSH:Cu^{+} complex which caused non-exponential reaction profiles and induction periods. The first experimental evidence for O_2 induced release of Cu^{+} from the complex has been reported.

2.6 Mechanism of GSNO Decomposition

The mechanism of simple first order nitrosothiol decomposition induced by added thiol and Cu^{2+} is given in scheme 2.2:

$$RS^- + Cu^{2+} \xrightarrow{fast} RS^{\cdot} + Cu^+$$

$$RSNO + Cu^+ \xrightarrow{slow} RS^- + Cu^{2+} + NO$$

scheme 2.2

This occurs when reduction of Cu^{2+} is rapid and the rate determining step is denitrosation. The result is a first order decay described by eqn. 2.19.

$$-\frac{d[RSNO]}{dt} = k_{obs}[RSNO]$$

(eqn. 2.19)

As $[Cu^{2+}]<[RS^-]$ then

$$k_{obs} = k[Cu^{2+}]$$

(eqn. 2.20)

NO release from GSNO has been shown to be very slow but is stimulated by GSH and Cu^{2+}. Products were identified as NO and a GSSG:Cu^{2+} complex corresponding to quantitative conversion of GSH and GSNO to GSSG and NO. Experiments with neocuproine showed that the free Cu^+ ion is the catalyst produced by rapid reduction of Cu^{2+} by GSH (scheme 2.3)

$$GS^- + Cu^{2+} \xrightarrow{fast} GS^{\cdot} + Cu^+$$

$$GSNO + Cu^+ \xrightarrow{slow} GS^- + Cu^{2+} + NO$$

scheme 2.3

However decomposition is not cleanly first order as it is complicated by the complexing abilities of GSH for Cu^+ and GSSG for Cu^{2+}. GSH forms a 1:1 and 2:1 complex with Cu^+ (λ_{max} = 260 and 300nm) (eqns. 2.21 and 2.22).

$$GSH + Cu^+ \longrightarrow GSCu + H^+$$

(eqn. 2.21)

$$GSH + GSCu \longrightarrow [(GS)_2Cu]^- + H^+$$

(eqn. 2.22)

GSSG forms a 1:1 complex with Cu^{2+} (λ_{max} = 250 and 620nm) (eqn. 2.23).

$$GSSG + Cu^{2+} \longrightarrow GSSG{:}Cu^{2+}$$

(eqn. 2.23)

Nitrosation of the SH group causes a decrease in the electron density on S due to the electron withdrawing properties of -NO therefore Cu^+ chelation via GSNO is likely to be much less favourable than via GSH. Most fast reacting nitrosothiols can easily complex Cu^+ due to the "gem-dimethyl effect" previously described in section 1.2.5.4. GSNO has no geminal methyl group thus the "gem-dimethyl effect" does not apply.

For homolytic cleavage of the S-NO bond it is unknown as to whether coordination of Cu^+ is via S or N (see 2.13 and 2.14). Both possibilities have been discussed[13]. However, coordination via S would more likely cause heterolytic fission of the S-NO bond producing NO^+ as described for Hg^{2+} decomposition (see section

4.4). If coordination is via N then an unfavourable seven membered ring will result which may contribute to the reluctance for GSNO to denitrosate but a six membered ring involving cys-NH could still be possible.

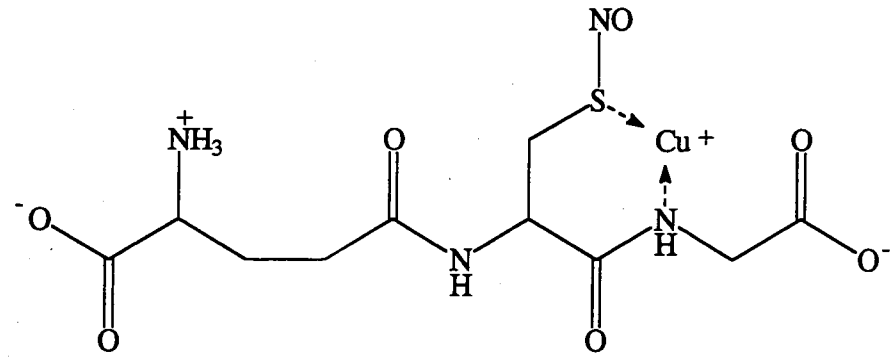

(2.13)

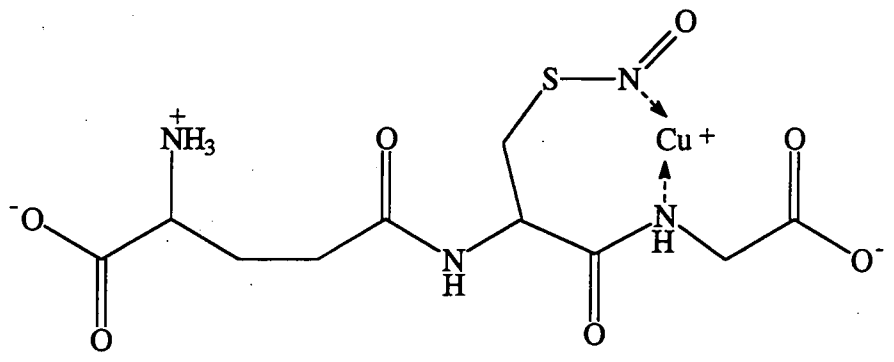

(2.14)

Therefore it seems that GSNO decomposition is relatively slow due to ineffective binding of Cu^+. This is because of the reduced electron density around S of the SNO group and there being no constraints on the tripeptide comformation. The stability of the GSH:Cu^+ complex can be attributed to coordination to the ion via SH and gly-NH groups (see (2.7)) forming a favourable six membered ring.

As the decomposition reaction is so slow GSH has the opportunity to complex Cu^+ ions. The catalyst is thus inhibited from stimulating decomposition but the action of O_2 on the GSH:Cu^+ complex will free the catalyst and rectify this (eqn. 2.8). Superoxide ion detection gave experimental evidence for this reaction. Towards the end of the reaction the concentration of Cu^{2+} is reduced due to GSSG

chelation which can only be released via the reaction with GSH (eqn. 2.7). Therefore complexation of GS^- with Cu^+ and GSSG with Cu^{2+} effectively reduces the concentration of "free" copper. Thus the total concentration of available copper does not remain constant and decomposition deviates from pseudo first order.

At higher concentrations of GSH the complexation of Cu^+ with excess thiol will immediately occur. An induction period results where rapid formation of Cu^+ via GSH and release of Cu^+ via O_2 occurs until excess GSH has been oxidised. Decomposition time and the shape of the profile however are unchanged. Hence after such time GSNO decomposition occurs as described previously.

Gorren *et al*[16] also described GSH/Cu^{2+} induced decomposition as being Cu^+ catalysed producing NO and GSSG:Cu^{2+}. They used much smaller GSH/Cu^{2+} concentration ratios ranging from 1/25 up to 2/1 and saw stimulation of decomposition when the [GSH] was increased at low GSH/Cu^{2+} ratios but inhibition at higher ratios. The ratio was not taken high enough to observe induction periods. They suggested no net oxidation of Cu^+ occurred during reaction on the basis that cuprizone had no effect on the reaction. However they failed to recognise the superior chelating properties of the disulfide. Also, the relatively small amplitude in decomposition at low GSH/Cu^{2+} ratios could not be explained. Such low [GSH] suggest that Cu^+ could not be regenerated from the disulfide complex (eqn. 2.7) thus resulting in a premature end to decomposition.

2.7 Conclusion

In vitro GSNO decomposition is brought about by the addition of GSH and Cu^{2+}. It is a far from simple first order mechanism, characteristic of nitrosothiols, as a result of the slow reaction between Cu^{+} and GSNO, and the chelating abilities of GSH and GSSG for the metal ions. It has been shown to be a comparatively stable nitrosothiol supporting its potential use as an endogenous carrier of NO.

NO released via degradation of this compound, accounts for its vasodilatory properties and its ability to inhibit platelet aggregation. Mayer *et al*[42] observed that in the presence of EDTA, GSNO induced vascular smooth muscle relaxation was attenuated. Askew *et al*[43] explained this in terms of NO transfer from GSNO to free thiol (transnitrosation), and enzymatic cleavage of the glutamyl-cystyl peptide bond (via glutamyl transpeptidase). In each case a nitrosothiol was formed which was more susceptible to metal ion catalysed NO release. Similarly, bathocuproine sulfonate (a Cu^{+} specific chelator) was found to reduce the inhibition of platelet aggregation by GSNO[44] which was also explained in terms of the formation of a more unstable derivative by transnitrosation[45]. However, Gordge *et al*[46] showed that transnitrosation reactions could not explain the biological potency of GSNO nor could the enzymatic cleavage of this compound. What these observations do show is that *in vivo* release of NO from GSNO is mediated by a copper dependent mechanism. Whether NO release occurs *in vivo* in a similar manner to that described in this chapter remains to be established.

References

1. R.Osterberg, *Biological Roles of Copper*, D.Evered, G.Lawerson, Eds., Excerta Medica, Amsterdam, 1980, p.p. 283.

2. L.Stryer, *Boichemistry*, Third Ed., W.H.Freeman and Co., New York, 1988.

3. E.A.Kowaluk, H.Fung, *J. Pharmacol. Exp. Ther.*, 1990, **255**, 1256.

4. M.W.Radomski, D.D.Rees, A.Dutra, S.Moncada, *Br. J. Pharmacol.*,1992,**107**, 745.

5. E.J.Langford, A.S.Brown, R.J.Wainwright, A.J.deBelder, M.R.Thomas, R.E.A.Smith, M.W.Radomski, J.F.Martin, S.Moncada, *Lancet*, 1994, **344**, 1459.

6. A.deBelder, C.Lees, J.Martin, S.Moncada, S.Campbell, *Lancet*, 1995, **345**, 124.

7. T.W.Hart, *Tet. Lett.*, 1985, **26**, 2013.

8. P.W.Riddles, R.L.Blakeley, B.Zerner, *Anal. Biochem.*, 1979, **94**, 75.

9. D.L.Rabenstein, D.A.Keine, *Coenzymes Cofactors*, 1989, **3**, 67.

10. G.Bannenberg, J.Xue, L.Engman, I.Cotgreave, P.Moldeus, A.Ryrfeldt, *J. Pharmacol. Exp. Ther.*, 1995, **272**, 1238.

11. B.Roy, A.duMoulinet d'Hardemare, M.Fontecave, *J. Org. Chem.*, 1994, **59**, 7019.

12. D.A.Wink, J.F.Darbyshire, R.W.Nims, J.E.Saavedra, P.C.Ford, *Chem. Res. Toxicol.*, 1993, **6**, 23.

13. S.C.Askew, D.J.Barnett, J.McAninly, D.L.H.Williams, *J. Chem. Soc. Perkin Trans. 2*, 1995, 741.

14. *Vogel's Textbook of Quantitative Inorganic Analysis*, Fourth Ed., Longman, New York, 1978, p.p. 755.

15. D.J.Barnett, Ph.D. Thesis, University of Durham, 1994.

16. A.C.F.Gorren, A.Schrammel, K.Schmidt, B.Mayer, *Arch. Biochem. Biophys.*, 1996, **330**, 219.

17. A.G.Sharpe, *Inorganic Chemistry*, Longman, 1986, p.p. 611.

18. N.N.Greenwood, A.Earnshaw, *Chemistry of the Elements*, Pergamon Press, Oxford, 1989, Chap. 28, p.p. 1364.

19. J.M.White, R.A.Manning, N.C.Li, *J. Am. Chem. Soc.*, 1956, **78**, 2367.

20. K.Varnagy, I.Sovago, H.Kozlowski, *Inorg. Chim. Acta.*, 1988, **151**, 117.

21. P.Kroneck, *J. Am. Chem. Soc.*, 1975, **97**, 3839.

22. K.Miyoshi, Y.Sugiura, K.Ishizu, Y.Iitaka, H.Nakamura, *J. Am. Chem. Soc.*, 1980, **102**, 6130.

23. P.Piu, G.Sanna, M.A.Zoroddu, R. Seeber, R. Basosi, R. Pogni, *J. Chem. Soc. Dalton Trans.*, 1995, 1267.

24. R.W.Hay, *Bio-Inorganic Chemistry*, Ellis Horwood Ltd., 1987.

25. A.R.Amundsen, J.Whelan, B.Bosnich, *J. Am. Chem. Soc.*, 1977, **99**, 6730.

26. P.C.Jocelyn, *Biochemistry of the SH Group*, Academic Press, London, 1972, Chap. 4, p.p. 94.

27. L.Cravatta, D.Ferri, R.Palombari, *J. Inorg. Nucl. Chem.*, 1980, **42**, 593.

28. P.Hemmerich, *The Biochemistry of Copper*, J.Peisach, P.Aisen, W.E.Blumberg, Eds., Academic Press, New York, 1966, p.p. 15.

29. G.Musci, S.D.Marco, G.C.Bellenchi, L.Calabrese, *J. Biol. Chem.*, 1996, **271**, 1972.

30. M.R.Ciriolo, A.Desideri, M.Paci, G.Rotilio, *J. Biol. Chem.*, 1990, **265**, 11030.

31. A.Corazza, I.Harvey, P.J.Sadler, *Eur. J. Biochem.*, 1996, **236**, 697.

32. A.P.Dicks, Thesis, to be submitted.

33. G.F.Smith, W.H.McCurdy, *Anal. Chem.*, 1952, **24**, 371.

34. A.P.Dicks, H.R.Swift, D.L.H.Williams, A.R.Butler, H.H.Al Sa'doni, B.G.Cox, *J. Chem. Soc. Perkin Trans. 2*, 1996, 481.

35. R.E.Peterson, M.E.Bollier, *Anal. Chem.*, 1955, **27**, 1195.

36. E.Jacobsen, F.J.Langmyhr, A.R.Selmer-Olsen, *Anal. Chim. Acta.*, 1961, **24**, 579.

37. R.Osterberg, R.Ligaarden, D.Persson, *J. Inorg. Biochem.*, 1979, **10**, 341.

38. *International Critical Tables vol III*, E.W.Washurn ed., McGraw-Hill, New York, 1928.

39. R.V.Bensasson, E.J.Land, T.G.Truscott, *Excited States and Free Radicals in Biology and Medicine*, Oxford University Press, 1993, Chap. 4, p.p. 101.

40. J.Rabini, W.A.Mulac, M.S.Matheson, *J. Phys. Chem.*, 1965, **69**, 53.

41. J.Rabini, D.Klug-Roth, J.Lilie, *J. Phys. Chem.*, 1973, **77**, 1169.

42. B.Mayer, A.Schrammel, P.Klatt, D.Koesling, K.Schmidt, *J. Biol. Chem.*, 1995, **270**, 17355.

43. S.Askew, A.R.Butler, F.W.Flitney, G.D.Kemp, I.L.Megson, *Bioorg. Med. Chem.*, 1995, **3**, 1.

44. M.P.Gordge, D.J.Meyer, J.Hothersall, G.H.Neild, N.N.Payne, A.Noronha-Dutra, *Br. J. Pharmacol.*, 1995, **114**, 1083.

45. J.E.Freedman, B.Frei, G.N.Welch, J.Loscalzo, *J. Clin. Invest.*, 1995, **96**, 394.

46. M.P.Gordge, J.S.Hothersall, G.H.Neild, A.A.N.Dutra, *Br. J. Pharmacol.*, 1996, 119, 533.

Chapter 3:

Other Aspects of S-Nitrosothiol Decomposition

Chapter 3: Other Aspects of S-Nitrosothiol Decomposition

3.1 Introduction

In vitro, copper ion catalysed nitrosothiol decomposition has been previously discussed (see section 1.2.5.4). The reaction requires only small concentrations of thiol and copper ions. Generally the amount of thiol present due to the slight reversibility of the nitrosation reaction and the concentration of copper present naturally in the aqueous medium are sufficient to cause decomposition. However, there are some nitrosothiols which show negligible reaction (k_2~0 $mol^{-1}dm^3s^{-1}$) under these conditions[1]. S-nitroso-N-acetylcysteine ((SNAC)(3.1)), S-nitrosocaptopril ((SNOCAP)(3.2)) and S-nitrosoglutathione ((GSNO)(3.3)) are just three such nitrosothiols.

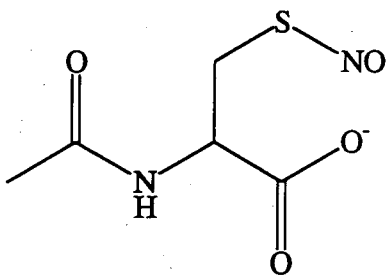

(3.1)

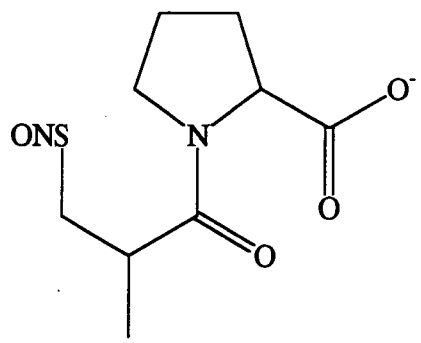

(3.2)

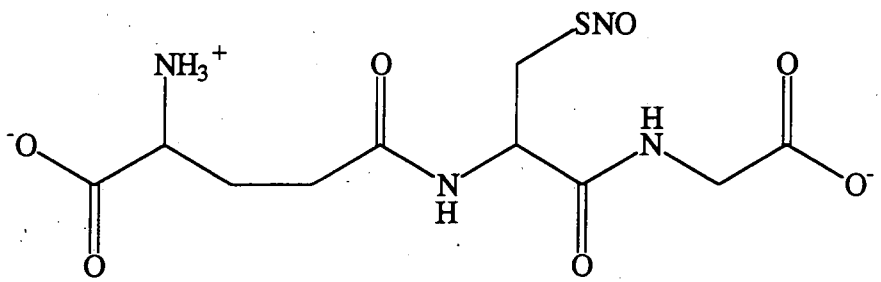

(3.3)

Generally, it is thought that the catalytic copper ion coordinates to the N atom of the nitroso group. However, coordination to a second functional group (most commonly an amino group) seems also to be required for decomposition to occur. In the case of

SNAC, N-acetylation of the $-NH_2$ group leaves the N atom lone pair less available for coordination, and GSNO and SNOCAP do not possess a second appropriate functional group in the vicinity of the nitroso group. Hence their inability to effectively bind copper ions render these compounds relatively stable to copper catalysed decomposition.

An investigation into the conditions required to cause decomposition of such nitrosothiols was undertaken.

3.2 Thiol Induced Decomposition

In the previous chapter, GSNO decomposition was shown to occur upon the addition of glutathione (GSH) and Cu^{2+}. The reaction took about 1hr. to complete although profiles were neither clean zero nor first order due to the complexing capabilities of the thiol and disulfide for the copper ion. However, good first order behaviour was observed when GSH *only* was added to a GSNO solution ([GSH]>>[GSNO]) and took around 16hrs. to complete.

3.2.1 Kinetic Studies

The decomposition of GSNO (made in solution via the nitrosation of GSH by acidic sodium nitrite) was observed in the presence of GSH in pH 7.4 phosphate buffer at 25^0C by noting the disappearance of the nitrosothiol at 340nm as a function of time. Experiments were carried out with $[GSH]_0>>[GSNO]_0$ and good first order behaviour was found in each individual kinetic run. The reaction was studied over a range of thiol concentrations and the quoted rate constants (k_{obs}), obtained from the integrated first order rate equation, were mean values of five determinations; the standard error was generally less than 5%. A plot of k_{obs} against [GSH] was linear (see fig. 3.1), showing the reaction to be first order in GSH, with a small intercept, k'.

Figure 3.1

Plot of k_{obs} against [GSH] for the decomposition of S-nitrosoglutathione ($5x10^{-4}M$).

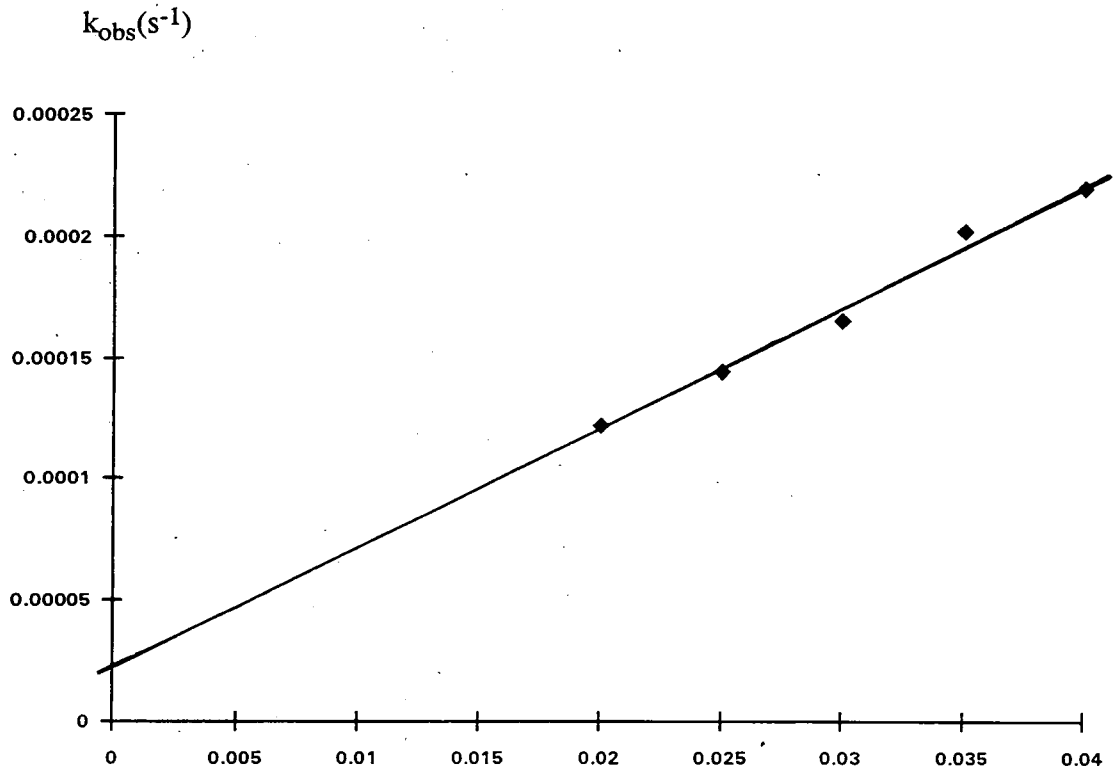

Therefore,

$$\frac{-d[RSNO]}{dt} = k_2[RSNO][RSH] + k'[RSNO]$$

(eqn. 3.1)

As [RSH]>>[RSNO], [RSH] is effectively constant hence,

$$\frac{-d[RSNO]}{dt} = k_{obs}[RSNO]$$

where

$$k_{obs} = k_2[RSH] + k'$$

(eqn. 3.2)

A value for k_2, the second order rate constant could be obtained from the slope of fig. 3.1. For the reaction of GSNO, $k_2 = (5.09\pm0.32)\times10^{-3}$ $mol^{-1}dm^3s^{-1}$ with intercept $k' = (1.82\pm0.98)\times10^{-5}$ s^{-1}. In a similar fashion, k_2 values were obtained for the decomposition of SNAC and SNOCAP induced by N-acetylcysteine (NAC) and captopril (CAP) respectively (see tables 3.1 and 3.2).

Table 3.1

Rate data for the reaction of S-nitroso-N-acetylcysteine (5×10^{-4}M) with N-acetylcysteine at pH 7.4.

10^2[NAC] ($moldm^{-3}$)	10^4k_{obs} (s^{-1})
1.0	1.37±0.04
1.25	1.50±0.05
1.5	1.69±0.05
1.75	1.81±0.06
2.0	2.21±0.08
2.25	2.48±0.03
2.5	2.67±0.09
2.75	2.92±0.07
3.0	3.16±0.05

$k_2 = (9.37\pm0.39)\times10^{-3}$ $mol^{-1}dm^3s^{-1}$.

$k' = (3.28\pm0.82)\times10^{-5}$ s^{-1}.

Table 3.2

Rate data for the reaction of S-nitrosocaptopril ($5x10^{-4}M$) with captopril at pH 7.4.

10^3[CAP] ($moldm^{-3}$)	10^4k_{obs} (s^{-1})
1.0	0.31±0.01
2.5	0.79±0.02
5.0	1.38±0.04
7.5	1.89±0.06
10.0	2.39±0.08

$$k_2 = (2.27\pm0.11)x10^{-2}\ mol^{-1}dm^3s^{-1}.$$

$$k' = (1.69\pm0.07)x10^{-5}\ s^{-1}.$$

The results are summarised in table 3.3.

Table 3.3

Second order rate constants for the thiol induced decomposition of the nitrosothiols studied.

RSH/RSNO	10^3k_2 ($moldm^{-3}$)	$10^5k'$ (s^{-1})
GSH/GSNO	5.09±0.32	1.82±0.98
NAC/SNAC	9.37±0.39	3.28±0.82
CAP/SNOCAP	22.7±1.10	1.69±0.07

The intercept, k', probably represents thermal and possible photochemical decomposition of the nitrosothiol. This is not normally observed experimentally but due to the length of time of reaction, become significant under these conditions.

3.2.1.1 Addition of Cu^{2+}

An NO specific electrode was used to detect NO release from the GSH ($2x10^{-2}M$) induced decomposition of GSNO ($5x10^{-4}M$), and 64% NO_2^- (produced from the reaction of NO with solvated O_2) was detected using the Griess test (see section 2.3.1). Due to the length of time of reaction and the subsequent loss of NO to headspace, 100% production of NO from GSNO could not be obtained by either method. The other product was presumed to be oxidised glutathione (GSSG). Unfortunately due to the low [Cu^{2+}] (determined by atomic absorption spectroscopy to be typically $1x10^{-6}M$) a UV-Vis absorption band at 250nm characteristic of a GSSG:Cu^{2+} complex (see section 2.3.2.1) was not observed. The disulfide could have been more easily detected by the glutathione reductase- 5,5'-dithiobis-(2-nitrobenzoic acid)(DTNB) recycling method described by Griffith[2] or by capilliary zone electrophoresis[3].

In order to establish whether the release of NO from RSNO under these conditions was copper ion catalysed, the reaction of NAC with SNAC and GSH with GSNO were studied in the presence of *added* Cu^{2+}. First order rate constants were obtained over a range of Cu^{2+} concentrations (see tables 3.4 and 3.5).

Table 3.4

Rate data for the reaction of S-nitroso-N-acetylcysteine ($5x10^{-4}M$) with N-acetylcysteine ($1.5x10^{-2}M$) in the presence of added Cu^{2+} at pH 7.4.

$10^5[Cu^{2+}]_{added}$ ($moldm^{-3}$)	10^4k_{obs} (s^{-1})
0	1.84±0.07
1.25	1.89±0.06
2.5	1.65±0.05
12.5	1.56±0.05
25.0	1.54±0.05

Table 3.5

Rate data for the reaction of S-nitrosoglutathione ($5x10^{-4}M$) with glutathione ($1.5x10^{-2}M$) in the presence of added Cu^{2+} at pH 7.4.

$10^5[Cu^{2+}]_{added}$ ($moldm^{-3}$)	10^4k_{obs} (s^{-1})
0	2.47±0.02
0.75	2.38±0.02
1.5	2.37±0.03
7.5	2.27±0.04
15.0	2.41±0.06

Tables 3.4 and 3.5 show that k_{obs} was hardly changed by the addition of Cu^{2+}. This implies that decomposition under these conditions was not copper ion catalysed. However, both reactions were studied at only one thiol concentration. To obtain a better reflection of the independence of $[Cu^{2+}]$ on this reaction the same procedure should be carried out at various [RSH], k_2 calculated as shown in the previous section, and compared to that obtained in the absence of added Cu^{2+}.

3.2.1.2 Addition of EDTA

EDTA is a non-specific metal ion chelator[4] (see section 2.4.1) and has already been shown to stop decomposition of RSNO due to chelation of the Cu^{2+} ion catalyst[1,5]. Hence k_{obs} for the NAC induced decomposition of SNAC was obtained in the presence of EDTA in order to determine whether this reaction was Cu^{2+} catalysed (see table 3.6).

Table 3.6

Rate data for N-acetylcysteine ($2x10^{-2}M$) induced decomposition of S-nitroso-N-acetylcysteine ($5x10^{-4}M$) with $[Cu^{2+}]_{added} = 2x10^{-5}M$ in the presence of EDTA at pH 7.4.

10^4[EDTA] ($moldm^{-3}$)	10^4k_{obs} (s^{-1})
0	2.31±0.12
0.4	2.37±0.12
2.0	2.37±0.1.0
5.0	2.35±0.07
10.0	2.25±0.05

Table 3.6 shows that k_{obs} was also hardly affected by the presence of EDTA which is in stark contrast to all other observed RSNO decompositions studied, *in vitro*, to date. Again, k_{obs} for only one thiol concentration was measured but both these experiments demonstrate the unimportance of the copper ion on this reaction, and infer a very different mechanism of decomposition to those encountered so far.

3.2.2 Mechanism of Thiol Induced Nitrosothiol Decomposition

GSNO, SNAC and SNOCAP are relatively stable to copper ion catalysed decomposition due to their ineffective binding of the metal ion. However, decomposition was stimulated by addition of a large quantity of their respective thiol, and NO released. These reactions took around 16hrs. to complete, were first order with respect to RSH and RSNO, and were not Cu^{2+} ion catalysed. On the basis of these observations, the mechanism shown in scheme 3.1 has been proposed.

$$RSH + 1/2O_2 \xrightarrow{k} RS^{\cdot} + 1/2H_2O_2$$

$$RS^{\cdot} + RSNO \xrightarrow{k_3} RSSR + NO$$

$$RS^{\cdot} \xrightarrow{k_4} 1/2RSSR$$

scheme 3.1

where,

$$\frac{-d[RSNO]}{dt} = \frac{kk_3[O_2]^{1/2}[RSH][RSNO]}{k_4 + k_3[RSNO]}$$

(eqn. 3.3)

Dimerisation of two radical species is expected to be very fast hence, $k_4 >> k_3[RSNO]$ and

$$\frac{-d[RSNO]}{dt} = \frac{kk_3}{k_4}[O_2]^{1/2}[RSH][RSNO]$$

(eqn. 3.4)

Therefore, the second order rate constant, k_2, is defined by eqn. 3.5.

$$k_2 = \frac{kk_3}{k_4}[O_2]^{1/2}$$

(eqn. 3.5)

Oxidation of thiols via molecular oxygen is a slow process but can be catalysed by metal ions such as Cu^{2+} and Fe^{2+} [6]. A mechanistic investigation of the copper ion catalysed oxidation of cysteine[7] revealed that the metal ion acted as electron carrier from cysteine to oxygen and involved the formation of a 2:1 cysteine:Cu^{2+} complex where the $-NH_2$ and -SH groups of both cysteine molecules coordinate to

Cu^{2+}. However, it seems unlikely that oxidation of the thiols studied here, which are unable to bind Cu^{2+} effectively, were catalysed by trace copper ions in solution. If this was the case decomposition would have slowed in the presence of EDTA and quickened upon the addition of Cu^{2+}. Peroxide ions have also been reported to oxidise thiols[6]. Therefore, in this instance, most RSH was oxidised by solvated oxygen to form the thiyl radical and H_2O_2. HO_2^- in turn may have also oxidised RSH, but Cu^{2+} catalysed oxidation was minimal. The non-catalytic oxidation of the thiol could explain the abnormal length of time the reaction took to complete.

Transnitrosation occurs via attack of the thiolate anion at the nitroso nitrogen atom and can be very rapid (k_2= 20-400 $mol^{-1}dm^3s^{-1}$)[8] depending on the pH of the solution and the nature of the thiol and nitrosothiol involved (see section 1.2.5.5). However, transnitrosation cannot be detected here as the same thiol as its nitroso derivative was used to cause decomposition. The action of the thiyl radical on the nitrosothiol causing homolytic fission of the S-NO bond seems more probable in this instance. Observed k_2 values were much smaller than those typically observed for transnitrosation reactions (c.f. k_2= 24 $mol^{-1}dm^3s^{-1}$ for the reaction between S-nitrosocysteine and the thiolate ion derived from thiomalic acid at pH 7.75[9]) reflecting the lower nucleophilicity of the thiyl radical. Thiyl radical attack on RSNO has been reported in a mechanism proposed for the oxidation of thiophenol via NO_2 gas which involves a RSNO intermediate[10]. More recently, laser flash photolysis experiments have observed the reaction of the glutathione radical with S-nitrosoglutathione[11].

It is interesting to note that k_2 values increase in the order; CAP/SNOCAP> NAC/SNAC>GSH/GSNO. This could be a reflection of the relative stability of the disulfide or the ease of oxidation of the thiol.

In order to support the mechanism given in scheme 3.1, RSH induced decomposition should be carried out in anaerobic conditions. If the above mechanism is correct the reaction should be stopped in the absence of O_2. Other nitrosothiols, such as S-nitroso-N-acetylcysteamine, which also show negligible Cu^{2+} catalysed decomposition should be studied in order to obtain a structural reactivity pattern and compared to that of Cu^{2+} induced decomposition. It would also be interesting to investigate the possibility of RSH induced decomposition of the more reactive nitrosothiols such as S-nitrosocysteine.

3.3 S-Nitroso-N-acetylcysteine

In the previous section, S-nitroso-N-acetylcysteine was shown to decompose in the presence of high concentrations of N-acetylcysteine. The reaction took over 16hrs. to complete, was first order with respect to SNAC and NAC, and occurred via a radical mechanism as opposed to a Cu^{2+} catalysed reaction. However, at much *lower* concentrations of thiol a reaction profile, at 340nm, similar to that observed for the Cu^{2+} catalysed decomposition of GSNO when [GSH]>[Cu^{2+}] (see section 2.5.1) was obtained. A typical profile acquired in pH 7.4 phosphate buffer at 25^0C, is shown in fig. 3.2. Profiles were reproducible.

Figure 3.2

Reaction profiles of the decomposition of SNAC ($5x10^{-4}$M) in the presence of NAC ($1x10^{-4}$M) in A) aerated solution and B) deaerated solution at pH 7.4.

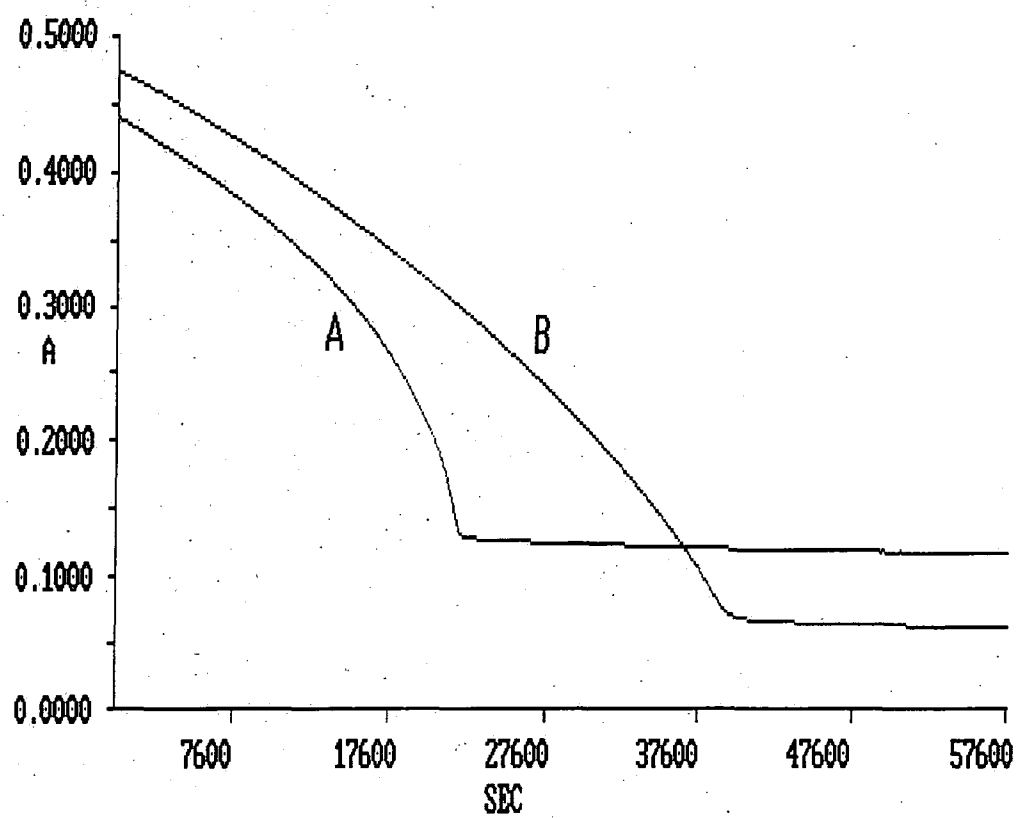

A reaction time of ~5hrs. was observed and was increased in the absence of oxygen. The addition of Cu^{2+} proved to decrease the time of reaction (see fig. 3.3).

Figure 3.3

Reaction profiles of the decomposition of SNAC ($5x10^{-4}M$) in the presence of NAC ($1x10^{-4}M$) with A) $[Cu^{2+}]= 1x10^{-6}M$, B) $[Cu^{2+}]= 5x10^{-6}M$ and C) $[Cu^{2+}]= 1x10^{-5}M$ at pH 7.4.

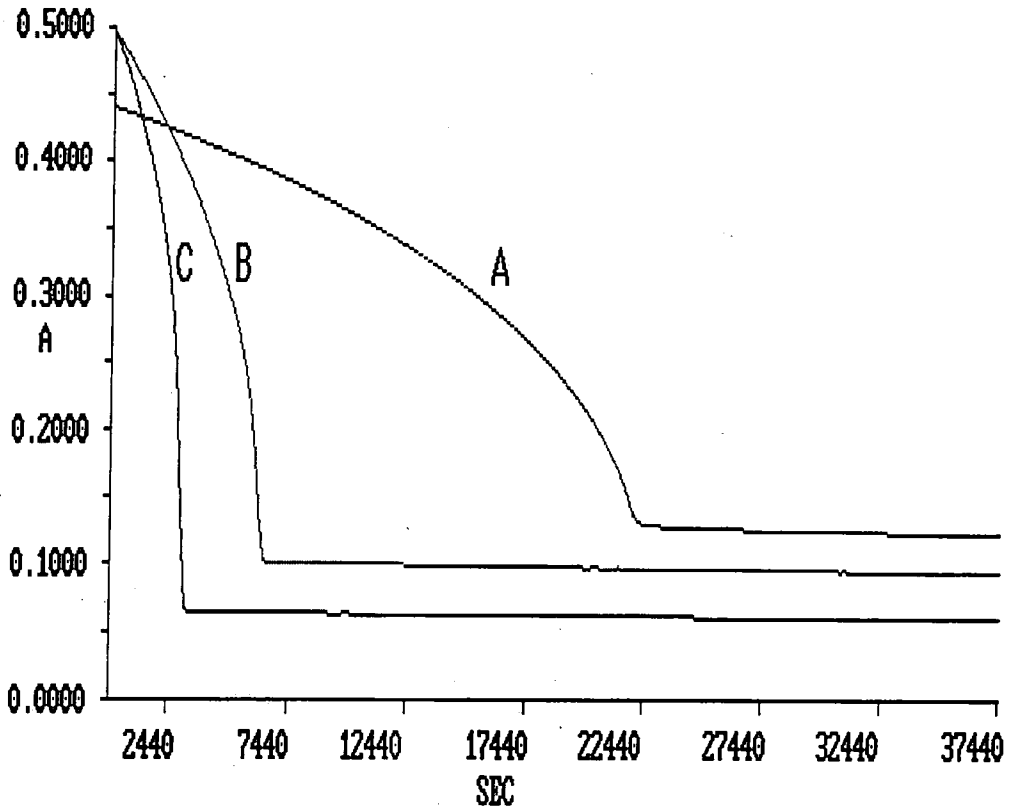

Again, profiles were reproducible. Note that the $[Cu^{2+}]$ in profile A) is the $[Cu^{2+}]$ naturally present in the aqueous medium, determined by atomic absorption spectroscopy. GSH/Cu^{2+} induced decomposition of GSNO showed a similar reaction profile. However, the induction period and time of decay were more clearly defined. The induction period was caused by the immediate formation of a GSH:Cu^{+} complex with excess thiol. Cu^{+} was released from the complex via solvated oxygen and in doing so, oxidised the thiol. This cycle of reactions occurred until all excess thiol had been oxidised. The Cu^{+} catalytic species was then free to react with GSNO and decomposition commenced. Hence, in deaerated solution, the induction period increased in length and as the $[Cu^{2+}]$ increased the induction time decreased.

Therefore, it seems that like GSNO, SNAC decomposition can be stimulated by the addition of NAC and Cu^{2+}. The evidence suggests that, as in the case of GSNO, the mechanism is far from simple. That is to say that the slow reaction

between Cu^{2+} and SNAC is complicated by the copper ion chelating abilities of NAC and its disulfide derivative. However, much work must be done to prove this hypothesis.

The reaction must be recognised as being copper ion catalysed via the use of EDTA, and the oxidation state of the catalytic metal ion determined by the use of neocuproine and cuprizone (see section 2.4). Also, the products of the reaction need to be positively identified as being NO and the disulfide derivative of N-acetylcysteine. NO can be detected and the amount released, quantified with the use of the NO specific electrode and the Griess test (see section 2.3.1). The disulfide can be identified either by UV-Vis spectrophotometry (see section 2.3.2), if the disulfide does indeed absorb in this region, or either by glutathione reductase- DTNB recycling method[2], or via capillary zone electrophoresis[3]. Only then can the hypothesis be proved.

3.4 The Effect of Oxygen on GSNO and SNAC

GSNO and SNAC are two of the most stable nitrosothiols. However, degradation of a solution of GSNO can be brought about by the exclusion of oxygen from solution[12]. Figure 3.4 shows the reaction profiles, at 340nm, of a GSNO solution (made *in situ* in the usual way and diluted to the correct concentration by the addition of pH 7.4 phosphate buffer) in aerobic and anaerobic conditions, at 25^{0}C.

Figure 3.4

Reaction profiles of GSNO ($5x10^{-4}$M) in A) aerobic and B) anaerobic conditions at pH 7.4.

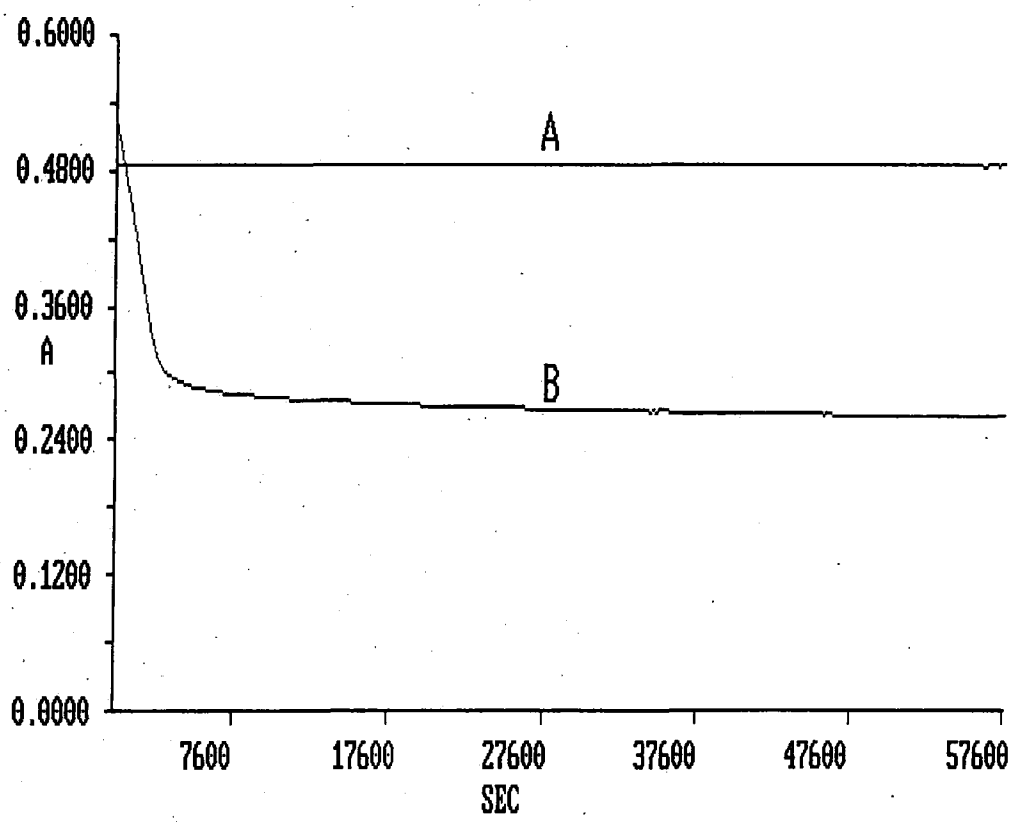

In the absence of O_2, 45% of the solution decomposed in the first 90mins but was stable after this time. Degradation of a SNAC solution was similarly observed (see fig. 3.5).

Figure 3.5

Reaction profiles of SNAC ($5x10^{-4}M$) in A) aerobic and B) anaerobic conditions at pH 7.4.

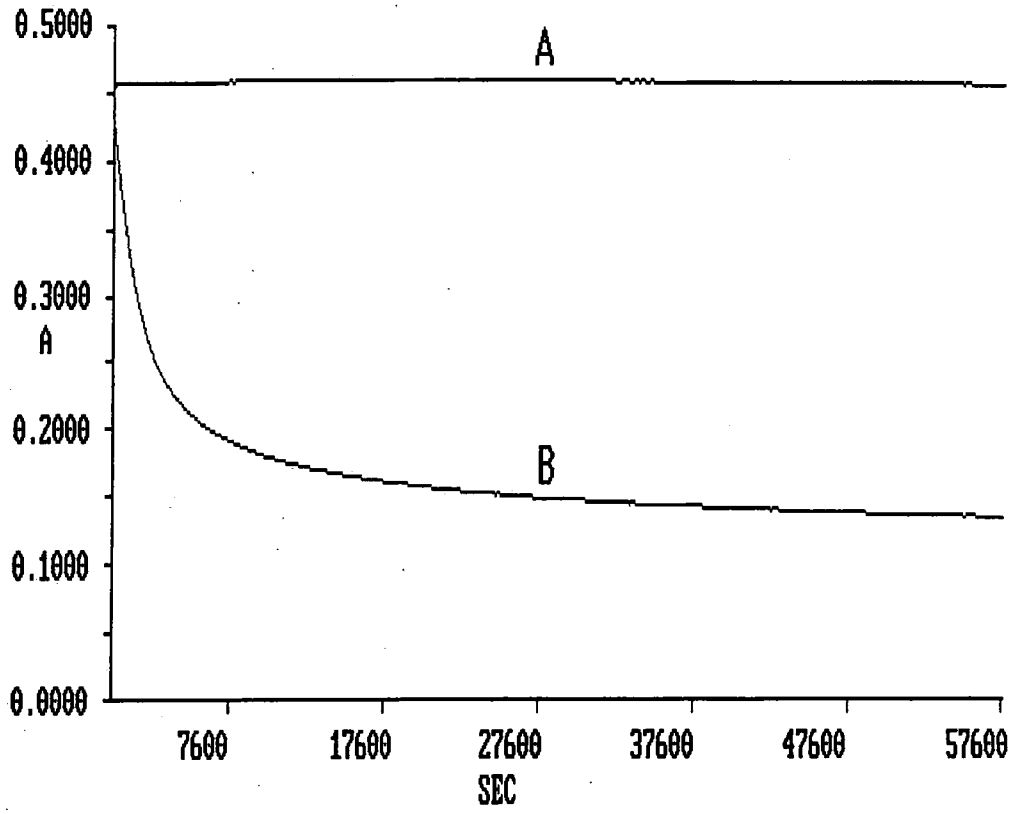

42% of the solution decomposed in the first 50mins, in the absence of O_2, but showed very little degradation after this time.

These observations could not be satisfactorily explained but may be due to the oxidation of Cu^+ by solvated oxygen in aqueous solution[13]. If it is presumed that there is enough thiol present in the GSNO solution to reduce Cu^{2+} ions naturally present in the aqueous medium, then in anaerobic conditions, the reaction of Cu^+ with GSNO would occur causing decomposition (see scheme 3.2).

$$GS^-_{res} + Cu^{2+} \xrightarrow{fast} GS^{\cdot} + Cu^{+}$$

(eqn. 3.6)

$$GSNO + Cu^{+} \xrightarrow{slow} GS^{-} + Cu^{2+} + NO$$

(eqn. 3.7)

scheme 3.2

Presumably, decomposition finished prematurely because the copper ions were complexed by the disulfide and thiol products (see eqns. 3.8 and 3.9), and the metal ions could not be released (eqns. 3.10 and 3.11) due to the absence of GSH and O_2 (see chapter 2 for the experimental evidence for these reactions).

$$GSSG + Cu^{2+} \longrightarrow GSSG{:}Cu^{2+}$$

(eqn. 3.8)

$$GSH + Cu^{+} \longrightarrow GSCu + H^{+}$$

(eqn. 3.9)

$$GS^{-} + GSSG{:}Cu^{2+} \longrightarrow GSSG + Cu^{+} + GS^{\cdot}$$

(eqn. 3.10)

$$O_2 + GSCu \longrightarrow O_2^{-\cdot} + Cu^{+} + GS^{\cdot}$$

(eqn. 3.11)

Cu^{+} can be oxidised back to Cu^{2+} in aqueous solution (eqn. 3.12).

$$O_2 + Cu^+ \longrightarrow O_2^{-\cdot} + Cu^{2+}$$

(eqn. 3.12)

In the case of GSH/Cu^{2+} induced decomposition (chapter 2), oxidation of Cu^+ by O_2 does not normally occur due to the immediate complexation of Cu^+ by excess GSH.

Hence, in aerobic conditions, O_2 and GSNO compete for Cu^+ (eqns. 3.7 and 3.12) and because eqn. 3.7 was so slow, Cu^+ was oxidised back to Cu^{2+} before it could react with GSNO. Therefore, in aerobic conditions, decomposition was not observed. Presumably the same arguments apply for the observed SNAC decomposition under anaerobiosis.

3.5 Conclusion

In this chapter, preliminary observations have been presented which indicate a mechanism of nitrosothiol degradation very different to that observed, *in vitro*, to date. The thiol induced decomposition of some of the more stable nitrosothiols has been explained by a radical mechanism involving attack of the thiyl radical on the RS-NO bond. However, further work is required to prove this mechanism which may be implicated in the vasodilatory action of these nitrosothiols, *in vivo*.

Initial experiments suggest that decomposition of S-nitroso-N-acetylcysteine, another relatively stable nitrosothiol, can be induced by the addition of Cu^{2+} and its respective thiol and may react in a similar fashion to that of GSNO. Again, much work is required to prove this hypothesis which may result in a further understanding of the mechanism of decomposition under these conditions.

GSNO and SNAC have been shown to decompose in the absence of oxygen. Further work is required to explain satisfactorily this observation.

References

1. S.C.Askew, D.J.Barnett, J.McAninly, D.L.H.Williams, *J. Chem. Soc. Perkin Trans. 2*, 1995, 741.

2. O.W.Griffith, *Anal. Biochem.*,1980, **106**, 207.

3. J.S.Stamler, J.Loscalzo, *Anal. Chem.*, 1992, **64**, 779.

4. P.Hemmerich, *The Biochemistry of Copper*, J.Peisach, P.Aisen, W.E.Blumberg, Eds., Academic Press, New York, 1966, p.p. 15.

5. J.McAninly, D.L.H.Williams, S.C.Askew, A.R.Butler, C.Russell, *J. Chem. Soc. Chem. Commun.*, 1993, 1758.

6. P.C.Jocelyn, *Biochemistry of the SH Group*, Academic Press, London, 1972, Chap. 4, p.p. 94.

7. D.Cavallini, C.deMarco, S.Dupre, G.Rotilio, *Arch. Biochem. Biophys.*, 1969, **130**, 354.

8. D.J.Barnett, A.Rios, D.L.H.Williams, *J. Chem. Soc. Perkin Trans. 2*, 1995, 1279.

9. D.J.Barnett, J.McAninly, D.L.H.Williams, *J. Chem. Soc. Perkin Trans. 2*, 1994, 1131.

10. W.A.Pryor, D.F.Church, C.K.Govindan, G.Crank, *J. Org. Chem.*, 1982, **47**, 156.

11. P.D.Wood, B.Mutus, R.W.Redmond, *Photochem. Photobiol.*, 1996, **64**, 518.

12. A.P.Dicks, H.R.Swift, D.L.H.Williams, A.R.Butler, H.H.Al Sa'doni, B.G.Cox, *J. Chem. Soc. Perkin Trans. 2*, 1996, 481.

13. L.Mi, A.D.Zuberbuhler, *Helv. Chim. Acta.*, 1991, **74**, 1679.

Chapter 4:

Mercuric Ion Induced Denitrosation of S-Nitrosothiols

Chapter 4: Mercuric Ion Induced Denitrosation of S-Nitrosothiols

4.1 Introduction

Nitrosothiols are susceptible to thermal and photolytic decomposition and thus are generally less stable than their alkyl nitrite counterparts. However, the equilibrium shown in eqn. 4.1 lies well over to the right whereas alkyl nitrite formation is generally less favourable, probably as a result of the greater basicity of the oxygen atom.

$$RSH + HNO_2 \overset{H^+}{\rightleftharpoons} RSNO$$

(eqn. 4.1)

As the equilibrium lies so far over to the side of the nitrosothiol the reaction cannot be kinetically treated as an equilibrium situation, as in the case of alcohols (see section 1.2.4). Instead, the two reactions are treated separately. Nitrosation in mildly acidic conditions and denitrosation at high acidity in the presence of a nitrous acid trap have previously been discussed.

In 1958 Saville[1] reported the use of mercury (II) salts to denitrosate nitrosothiols. Conditions were much less forcing and the reaction used as part of an analytical procedure for the detection of thiols. McAninly[2] observed that the denitrosation of two thiols, S-nitroso-N-acetylpenicillamine and S-nitrosoglutathione via mercury (II) nitrate was extremely fast. Total denitrosation was accomplished with stoichiometric ratios of 2:1 RSNO:Hg^{2+} but virtually no reaction was observed with ratios of 50:1, indicating a non-catalytic reaction.

Product identification and kinetic studies were undertaken to determine the mechanism of mercuric ion induced denitrosation of nitrosothiols and compared with Cu^{2+} induced decomposition.

4.2 Identification of Denitrosation Products

The products of reaction of Hg^{2+} with several nitrosothiols were identified as being nitrous acid and a RSH: Hg^{2+} complex. Unless stated otherwise all reactions were carried out at pH 1.0 (0.1M perchloric acid) to avoid hydrolysis of the mercuric ion and the subsequent formation of basic salts such as $Hg_2(OH)(OH_2)_3^{3+}$, $Hg_3O(OH_2)_3^{4+}$ and $Hg_4O(OH)(OH_2)_3^{5+}$ [3]. Nitrosothiols were made in solution via nitrosation of the corresponding thiol using acidic sodium nitrite.

4.2.1 Nitrous Acid Detection

The possibility of nitric oxide (NO) release from this reaction has already been investigated. An NO specific electrode detected no NO from Hg^{2+} induced decomposition of S-nitroso-N-acetylpenicillamine in aqueous solution[4]. However, HNO_2 (NO^+ in aqueous acid) has been quantitatively detected from S-nitrosocysteine denitrosation using the Griess test[1] (section 2.2.1). Using ε_{540}=48,400±500 $mol^{-1}dm^3cm^{-1}$ the [HNO_2] released from S-nitroso-N-acetylpenicillamine ((SNAP (4.1)) and S-nitrosothiomalic acid ((SNTMA (4.2)) was measured. The NO probe experiment showed that nitrous acid was formed as a result of the reaction of NO^+ with H_2O in acidic medium and not as a result of the reaction of NO with O_2 in aqueous solution (see section 2.3.1).

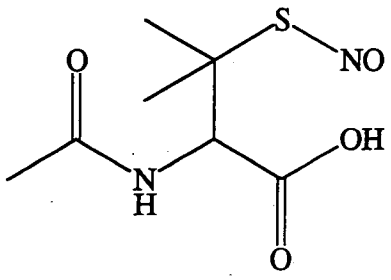

(4.1)

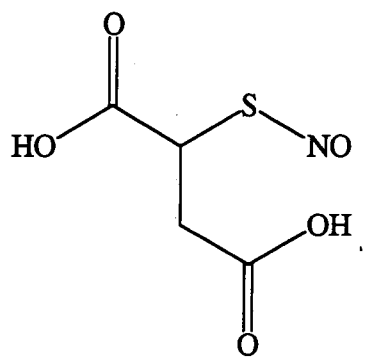

(4.2)

SNAP ($2x10^{-5}M$) was reacted with $Hg(NO_3)_2$ ($4x10^{-4}M$). After 2 minutes sulfanilamide (3.4%) was rapidly added followed by the addition of N-(1-naphthyl)-ethylenediamine (0.1%). A peak at 540nm was immediately observed which remained constant for over an hour. The same procedure was repeated using SNTMA. The results are shown in table 4.1.

Table 4.1

Concentration of HNO_2 detected from the reaction of RSNO ($2x10^{-5}M$) and $Hg(NO_3)_2$ ($4x10^{-4}M$).

RSNO	Average Abs. at 340nm	$10^5[HNO_2]$ ($moldm^{-3}$)	% HNO_2 detected
SNAP	0.9432±0.0062	1.95±0.02	97.5±1.0
SNTMA	0.9342±0.0048	1.93±0.02	96.5±1.0

HNO_2 could be easily identified by a characteristic five fingered absorbance centred around 350nm. A typical absorption spectrum is shown in fig. 4.1.

Figure 4.1

Absorption spectrum of nitrous acid ($1x10^{-2}M$) at pH 1.0.

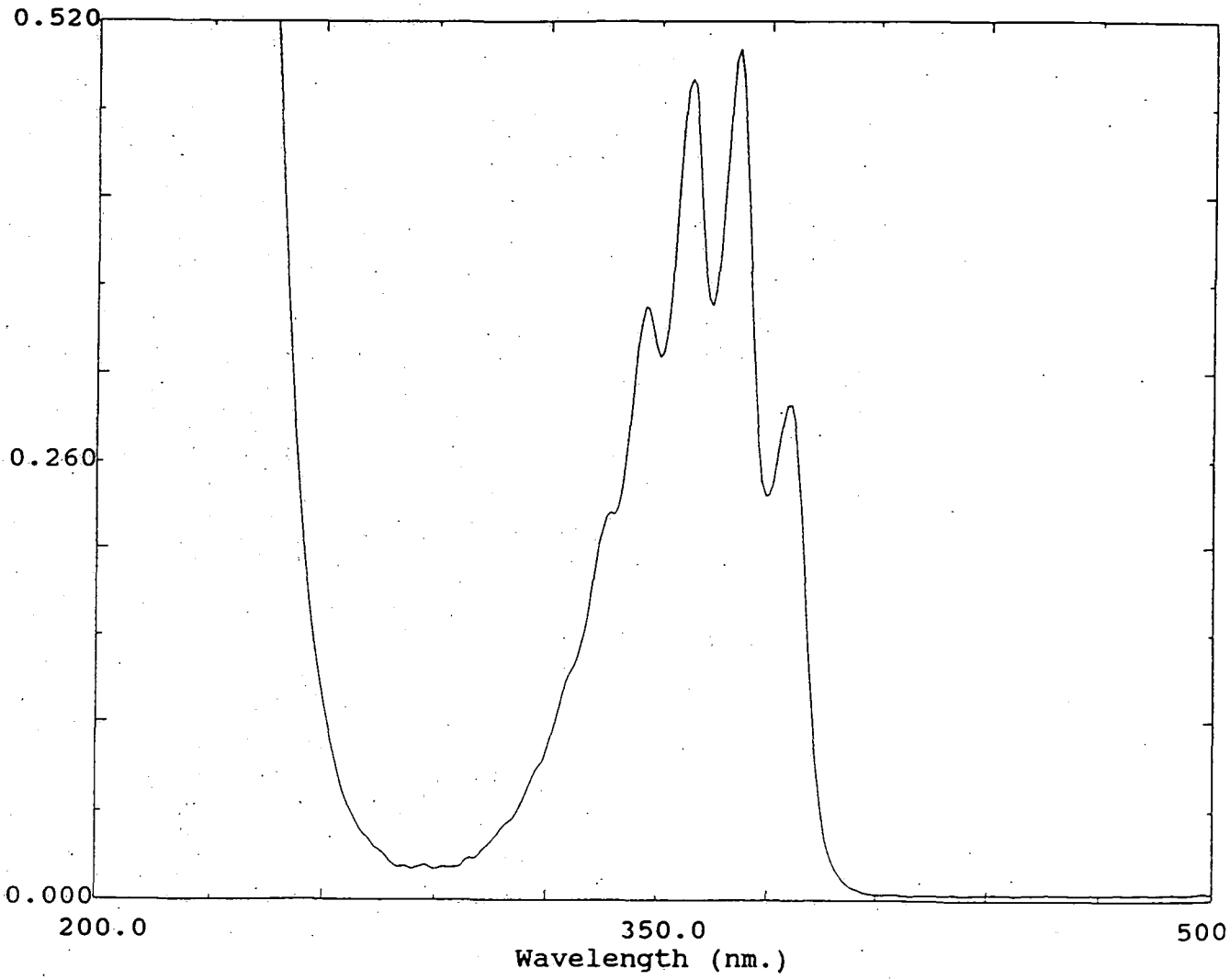

4.2.2 Thiol Detection

Denitrosation via Hg^{2+} was a very rapid process taking only seconds to complete therefore a spectrum of reactants at the start of reaction could not be obtained. Fig. 4.2 shows a spectrum of the products of the reaction of $HgCl_2$ with S-nitroso-N-acetylcysteine ((SNAC)(4.3)) and a typical spectrum of SNAC for comparison.

Figure 4.2

Spectrum of A) SNAC ($5x10^{-4}M$)and B) the products from the reaction of SNAC ($5x10^{-4}M$)and $HgCl_2$($1.5x10^{-3}M$).

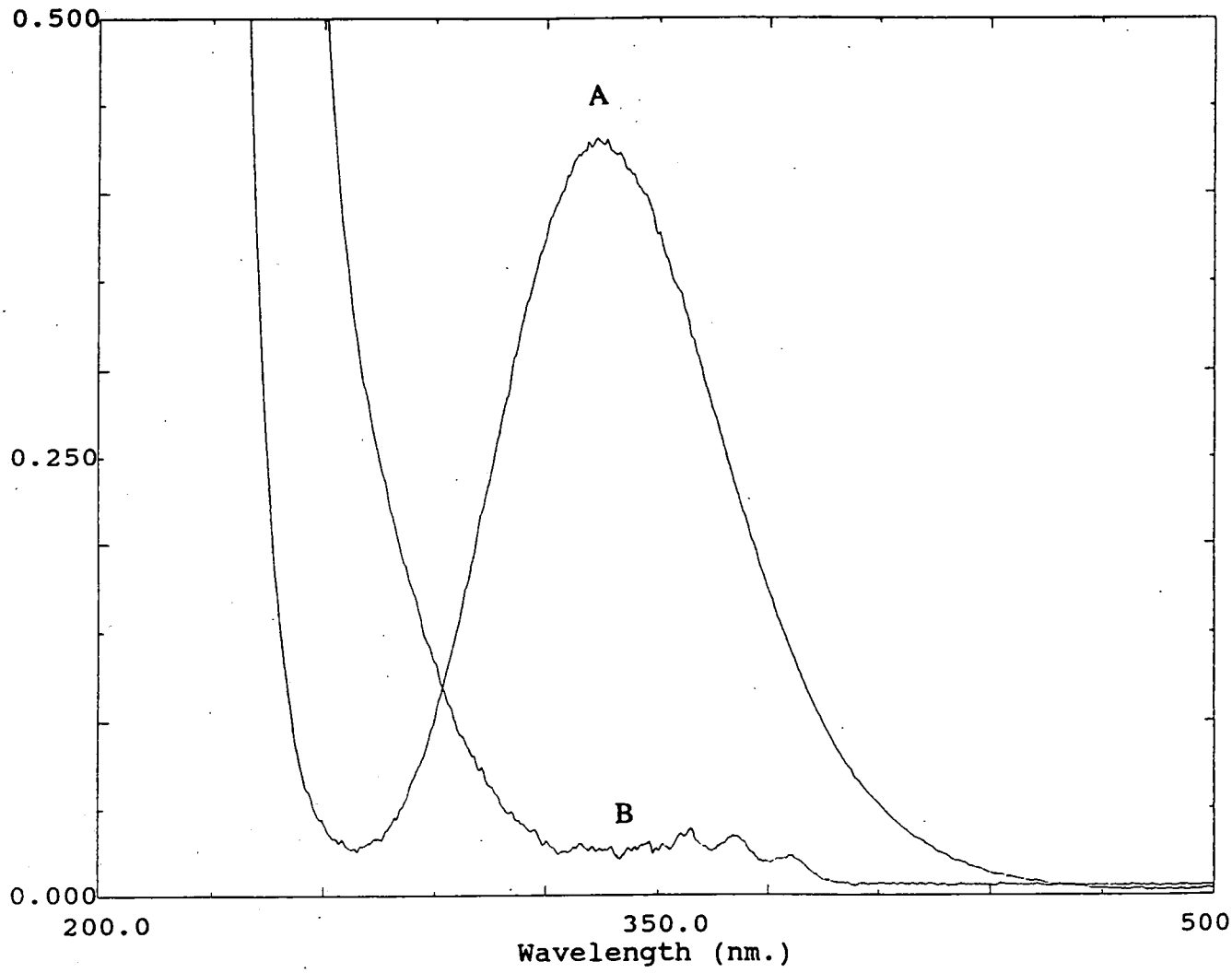

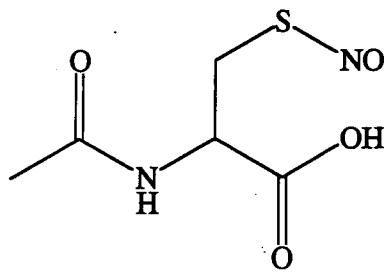

(4.3)

The reduced absorbance at 340nm clearly indicated that denitrosation had taken place and the characteristic five fingered absorption peak at c.a. 350nm affirmed the production of HNO_2. Hg^{2+} electrophilically cleaves disulfides[5] (eqn. 4.2). Therefore it seemed unlikely that the final product was the disulfide of N-acetylcysteine.

$$2Hg^{2+} + 2RSSR \longrightarrow 2RSHg^{+} + 2RS^{+}$$

(eqn. 4.2)

A spectrum of a solution containing N-acetylcysteine ((NAC) $5x10^{-4}M$), $HgCl_2$ ($1.5x10^{-3}M$) and HNO_2 ($5x10^{-4}M$) closely matched the product spectrum (see fig. 4.3) indicating that the other product was in fact NAC observed as a NAC:Hg^{2+} complex. There remains the possibility that the disulfide was formed but subsequently decomposed.

Figure 4.3

Spectrum of A) products of Hg^{2+} induced SNAC denitrosation and B) NAC ($5x10^{-4}M$), $HgCl_2$ ($1.5x10^{-3}M$) and HNO_2 ($5x10^{-4}M$).

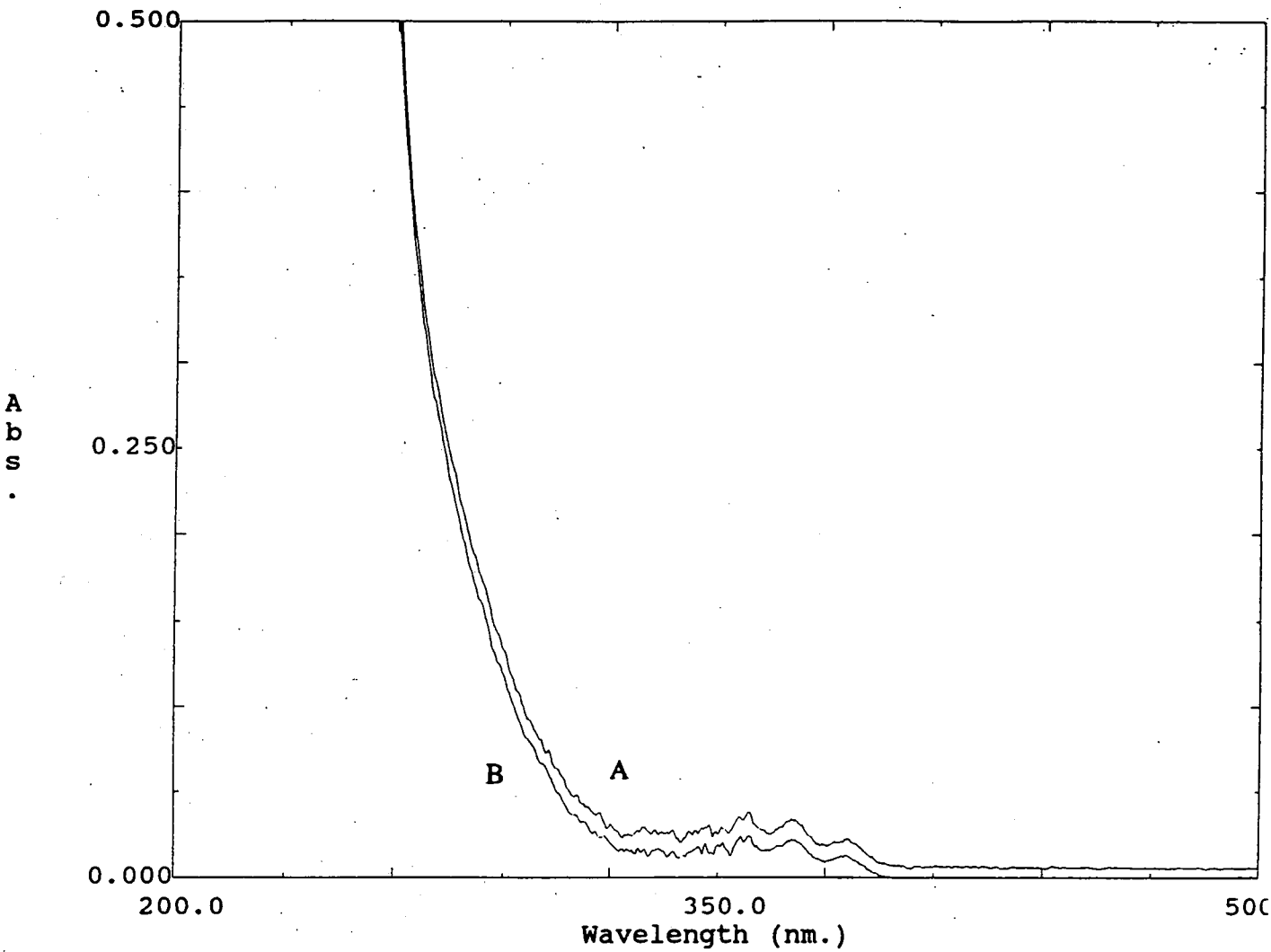

4.3 Kinetic Studies of Denitrosation

Denitrosation of several nitrosothiols were observed using a stopped-flow spectrophotometer in aqueous acidic solution at 25^0C. Reactions typically took 0.05-5 seconds. The decomposition of RSNO via Cu^{2+} naturally present in the acid was negligible on this timescale. The effects of mercury (II) salt and substrate structure on the reaction were investigated. The reaction was also carried out at physiological pH.

4.3.1 Mercury (II) Counter-ion Effect

The reaction of S-nitrosohomocysteine (4.4) with $HgCl_2$ was followed by noting the disappearance of the nitrosothiol at 340nm as a function of time. Experiments were carried out with $[HgCl_2]_0 >> [RSNO]_0$, and good first order behaviour was found in each individual kinetic run. The reaction was studied for a range of Hg^{2+} concentrations ($2\text{-}6 \times 10^{-3}$M) and rate constants ($k_{obs}$) obtained from the integrated first order rate equation. The quoted values of the rate constants are the means of at least five determinations; the standard error was generally less than 5%.

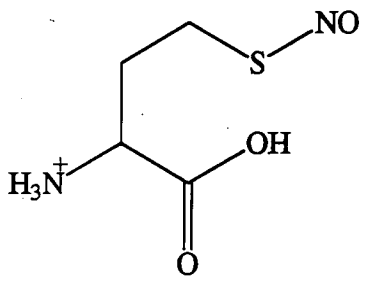

(4.4)

A plot of k_{obs} against $[Hg^{2+}]$ was linear (see fig. 4.4) hence showing the reaction to be first order in Hg^{2+}.

Figure 4.4

Plot of k_{obs} against $[Hg^{2+}]$ for the denitrosation of S-nitrosohomocysteine ($2x10^{-4}M$).

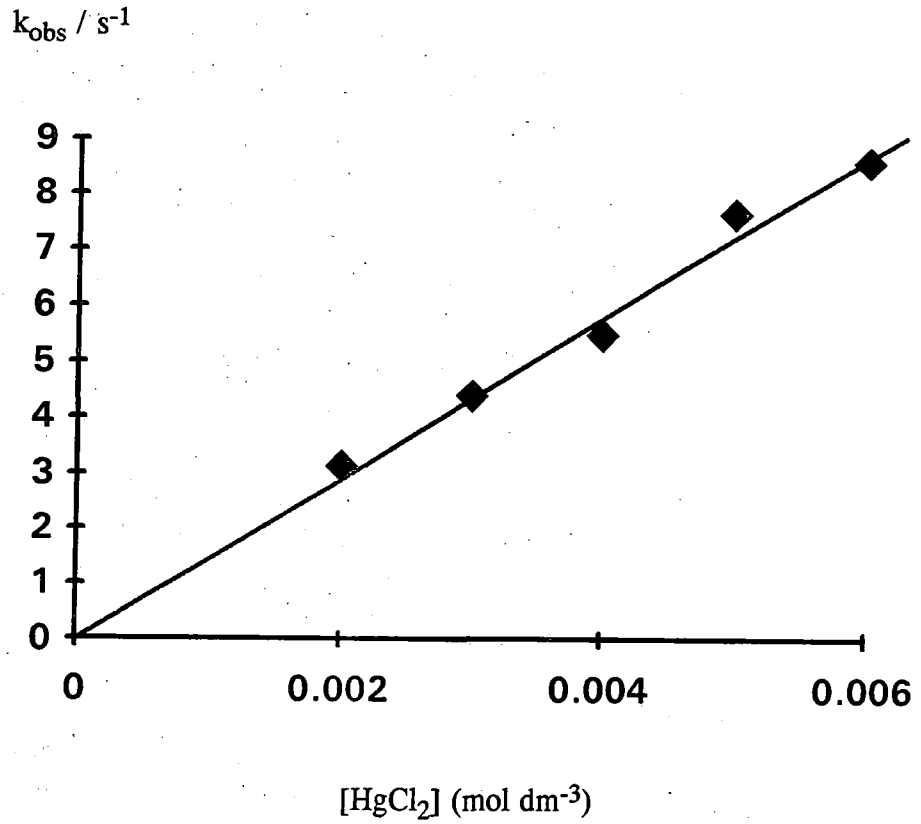

Therefore,

$$\frac{-d[RSNO]}{dt} = k_2[RSNO][Hg^{2+}]$$

(eqn. 4.3)

As $[Hg^{2+}]>>[RSNO]$, $[Hg^{2+}]$ is constant hence,

$$\frac{-d[RSNO]}{dt} = k_{obs}[RSNO]$$

where

$$k_{obs} = k_2[Hg^{2+}]$$

(eqn. 4.4)

A value for k_2, the second order rate constant can be obtained from the slope of fig. 4.4. For the reaction with S-nitrosohomocysteine $k_2 = (1.46\pm0.01)x10^3$ $mol^{-1}dm^3s^{-1}$.

k_2 for the denitrosation of S-nitrosocysteamine (4.5) was obtained in a similar fashion (see table 4.2).

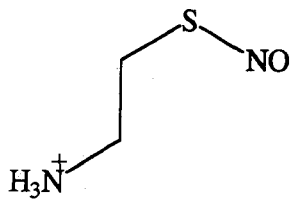

(4.5)

Table 4.2

Rate data for the reaction of S-nitrosocysteamine ($2x10^{-4}M$) with $HgCl_2$.

$10^3[Hg^{2+}]$ ($moldm^{-3}$)	k_{obs} (s^{-1})
2	2.87±0.04
3	4.39±0.06
4	5.84±0.08
5	7.48±0.05
6	9.26±0.06

$k_2 = (1.50\pm0.02)x10^3\ mol^{-1}dm^3s^{-1}$.

The reactions of $Hg(NO_3)_2$ with these nitrosothiols were carried out. However, under first order conditions the reactions were too fast to observe on a stopped-flow timescale. To overcome this problem the reaction was carried out in 1:1 RSNO:Hg^{2+} conditions and the second order rate constant obtained from the integrated second order rate equation.

$$k_2t = \frac{1}{[RSNO]_t} - \frac{1}{[RSNO]_0}$$

where $[RSNO]_0$ is the initial concentration of RSNO and $[RSNO]_t$, the concentration of RSNO at time t.

Using the Beer-Lambert Law, $A = \varepsilon cl$,

$$k_2 t = \frac{\varepsilon l}{A_t} - \frac{\varepsilon l}{A_0}$$

hence,

$$\frac{k_2}{\varepsilon l} t = \frac{1}{A_t} - \frac{1}{A_0}$$

(eqn. 4.5)

k_{2nd}, the rate constant obtained from the second order fit analysis, has units of $A^{-1}s^{-1}$ and is defined by eqn. 4.6.

$$k_{2nd} t = \frac{1}{A_t} - \frac{1}{A_0}$$

(eqn. 4.6)

Therefore comparing eqns. 4.5 and 4.6:

$$k_{2nd} = \frac{k_2}{\varepsilon l}$$

(eqn. 4.7)

The second order rate constants were calculated using eqn. 4.7 (see table 4.3).

Table 4.3

Rate data for the reaction of S-nitrosohomocysteine and S-nitrosocysteamine with $Hg(NO_3)_2$ ($[Hg^{2+}]$= [RSNO]= $2x10^{-4}$M) at pH 1.0.

RSNO	k_{2nd} (s^{-1})	ε_{340}* ($mol^{-1}dm^3cm^{-1}$)	$10^{-6}k_2$ ($mol^{-1}dm^3s^{-1}$)
S-nitroso homocysteine	1474±62	840±25	1.24±0.06
S-nitroso cysteamine	4400±79	553±7	2.43±0.05

*- results from work carried out by D.J.Barnett[4].

The results are summarised in tables 4.4 and 4.5.

Table 4.4

Second order rate constants for the reaction of S-nitrosohomocysteine with $HgCl_2$ and $Hg(NO_3)_2$.

Hg(II) salt	$10^{-3}k_2$ ($mol^{-1}dm^3s^{-1}$)
$HgCl_2$	1.46±0.01
$Hg(NO_3)_2$	1240±60

Table 4.5

Second order rate constants for the reaction of S-nitrosocysteamine with $HgCl_2$ and $Hg(NO_3)_2$.

Hg(II) salt	$10^{-3}k_2$ ($mol^{-1}dm^3s^{-1}$)
$HgCl_2$	1.50±0.02
$Hg(NO_3)_2$	2430±50

These results show that the mercury (II) salt counter-ion has a pronounced effect on the rate of the reaction and is clearly not due to nucleophilic catalysis. Second order rate constants for the reactions with $HgCl_2$ are ~10^3 *less* than the corresponding reaction with $Hg(NO_3)_2$. This reduced reactivity in the presence of chloride ions has also been observed for the Hg^{2+} induced hydrolysis of *p*-nitrophenyl isothiocyanate[6]. Throughout this work, reactions were carried out at acidic pH to avoid hydrolysis of the mercury(II) ion. However, nitrates, sulfates and perchlorates are the only mercuric salts which fully ionise in aqueous solution[7]. The mercury (II) halides form anionic complexes where, as well as water, coordination of the parent ion to the metal sphere occurs. Thus $HgCl_2$ in acidic aqueous solution can be represented as an equilibrium of the complexes shown in scheme 4.1[8].

$$HgCl^+ \rightleftharpoons HgCl_2 \rightleftharpoons HgCl_3^- \rightleftharpoons HgCl_4^{2-}$$

scheme 4.1

The equilibrium balance depends on the relative concentrations of mercuric and chloride ions. Up to 2:1 Cl^-:Hg^{2+}, $HgCl^+$ and $HgCl_2$ are the major species present in solution. As the chloride ion concentration increases $HgCl_3^-$ and $HgCl_4^{2-}$ feature more predominantly in solution[9]. The coordinated chloride anions cannot be as easily displaced from the metal ion as the more labile water ligands. This may account for the relatively small k_2 value for the reactions of $HgCl_2$ compared to that of $Hg(NO_3)_2$. The chloride ions effectively hinder the reaction of Hg^{2+} with RSNO by successfully complexing the metal ion.

4.3.2 Denitrosation at Physiological pH

The denitrosation of S-nitrosoglutathione (4.6) via $HgCl_2$ was carried out in pH 7.4 phosphate buffer (0.12M) under first order conditions. The rate constants obtained were compared to the same reaction at pH 1.0. The rate data are shown in tables 4.6 and 4.7 respectively.

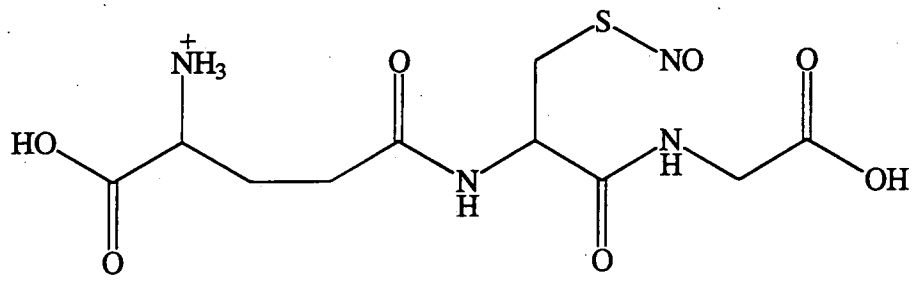

(4.6)

Table 4.6

Rate data for the reaction of S-nitrosoglutathione ($2x10^{-4}M$) with $HgCl_2$ at pH 7.4.

$10^3[Hg^{2+}]$ ($moldm^{-3}$)	k_{obs} (s^{-1})
2	395.1±3.4
3	379.9±3.3
4	357.4±3.2
5	375.1±6.3

Table 4.7

Rate data for the reaction of S-nitrosoglutathione ($2x10^{-4}M$) with $HgCl_2$ at pH 1.0.

$10^3[Hg^{2+}]$ ($moldm^{-3}$)	k_{obs} (s^{-1})
2	8.46±0.11
3	11.67±0.09
4	16.54±0.15
5	19.57±0.20
6	21.91±0.16

$k_2 = (3.86\pm0.10)x10^3\ mol^{-1}dm^3s^{-1}$.

k_{obs} showed a linear dependency on $[Hg^{2+}]$ at pH 1.0. However at pH 7.4 k_{obs} became independent of $[Hg^{2+}]$. Eqn. 4.4 was no longer true at this pH. The formation of basic salts, previously described in section 4.2, complicated the situation. Eqn. 4.3 could not adequately describe the reaction as the identity of the reacting mercuric ion was unknown. Further investigation into the mechanism at this pH is required.

4.3.3 Substrate Structure Independency of Denitrosation

The second order rate constant, k_2, was obtained as described in section 4.3.1 for the reactions of $HgCl_2$ and $Hg(NO_3)_2$ with a variety of nitrosothiols. Rate data for reactions of $HgCl_2$ are shown in tables 4.8-4.13. Similarly, rate data for reactions of $Hg(NO_3)_2$ are shown in table 4.14.

Table 4.8

Rate data for the reaction of S-nitroso-N-acetylpenicillamine ($2x10^{-4}M$) with $HgCl_2$ at pH 1.0.

$10^3[Hg^{2+}]$ ($moldm^{-3}$)	k_{obs} (s^{-1})
2	113.7±1.6
3	168.7±4.3
4	217.1±5.4
5	293.4±2.5
6	355.4±12.0

$k_2 = (60.8\pm2.7)x10^3\ mol^{-1}dm^3s^{-1}$.

Table 4.9

Rate data for the reaction of S-nitrosocysteine ($2x10^{-4}M$) with $HgCl_2$ at pH 1.0.

$10^3[Hg^{2+}]$ ($moldm^{-3}$)	k_{obs} (s^{-1})
2	11.48±0.07
3	18.88±0.17
4	22.56±0.18
5	27.31±0.27
6	31.49±0.29

$k_2 = (5.50\pm0.15)x10^3\ mol^{-1}dm^3s^{-1}$.

Table 4.10

Rate data for the reaction of S-nitroso-N-acetylcysteine ($2x10^{-4}M$) with $HgCl_2$ at pH 1.0.

$10^3[Hg^{2+}]$ ($moldm^{-3}$)	k_{obs} (s^{-1})
2	7.54±0.02
3	10.36±0.06
4	14.95±0.13
5	18.00±0.09
6	20.75±0.14

$k_2 = (3.56\pm0.06)x10^3\ mol^{-1}dm^3s^{-1}$.

Table 4.11

Rate data for the reaction of S-nitroso-N-acetylcysteamine ($2x10^{-4}M$) with $HgCl_2$ at pH 1.0.

$10^3[Hg^{2+}]$ ($moldm^{-3}$)	k_{obs} (s^{-1})
2	6.75±0.12
3	8.32±0.11
4	11.68±0.17
5	13.46±0.26
6	15.33±0.29

$k_2 = (2.72\pm0.1.0)x10^3\ mol^{-1}dm^3s^{-1}$.

Table 4.12

Rate data for the reaction of S-nitrosocysteine ethyl ester ($2x10^{-4}M$) with $HgCl_2$ at pH 1.0.

$10^3[Hg^{2+}]$ ($moldm^{-3}$)	k_{obs} (s^{-1})
2	3.60±0.06
3	5.06±0.02
4	7.21±0.04
5	8.75±0.03
6	10.44±0.07

$k_2 = (1.75\pm0.05)x10^3\ mol^{-1}dm^3s^{-1}$.

Table 4.13

Rate data for the reaction of S-nitrosocaptopril ($2x10^{-4}M$) with $HgCl_2$ at pH 1.0.

$10^3[Hg^{2+}]$ ($moldm^{-3}$)	k_{obs} (s^{-1})
2	3.10±0.01
3	4.03±0.01
4	5.41±0.02
5	6.35±0.05
6	7.38±0.10

$k_2 = (1.29\pm0.04)x10^3\ mol^{-1}dm^3s^{-1}$.

Table 4.14

Rate data for the reaction of $Hg(NO_3)_2$ with various nitrosothiols at pH 1.0 ($[Hg^{2+}] = [RSNO] = 2x10^{-4}M$).

RSNO	k_{2nd} (s^{-1})	ε_{340}* ($mol^{-1}dm^3cm^{-1}$)	$10^{-6}k_2$ ($mol^{-1}dm^3s^{-1}$)
S-nitrosocysteine	5654±96	855±47	4.83±0.28
s-nitroso-N-acetylcysteine	3098±72	920±29	2.85±0.11
S-nitroso glutathione	2956±61	895±7	2.65±0.06
S-nitrosocaptopril	1695±27	1108±24	1.88±0.05
S-nitroso-N-acetyl-cysteamine	1648±25	816±27	1.34±0.04
S-nitrosocysteine ethyl ester	746±19	772±21	0.58±0.02

*- results from work carried out by D.J.Barnett[4].

The reaction of S-nitroso-N-acetylpenicillamine was too fast to measure on a stopped-flow timescale. k_2 values are summarised in tables 4.15 and 4.16.

Table 4.15

Second order rate constants, k_2, for $HgCl_2$ denitrosation of nitrosothiols at pH 1.0, 25^0C.

RSNO	Structure	$10^{-3}k_2$ ($mol^{-1}dm^3$ s^{-1})
S-nitroso-N-acetyl penicill amine	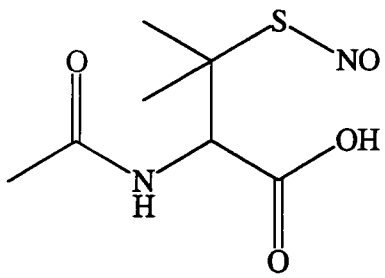	60.8±2.7
S-nitroso cysteine	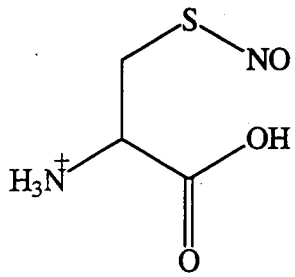	5.50±0.15
S-nitroso glutathione	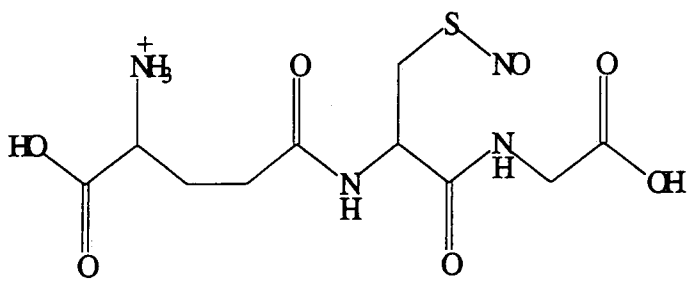	3.86±0.10
S-nitroso-N-acetyl cysteine	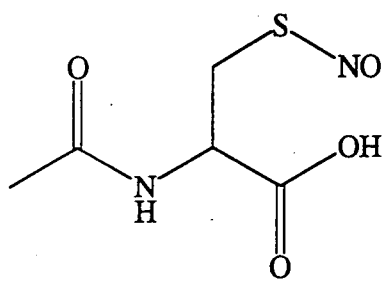	3.56±0.06

S-nitroso-N-acetyl cysteamine	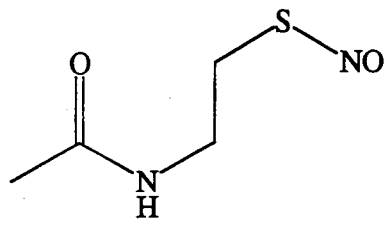	2.72±0.10
S-nitroso cysteine ethyl ester	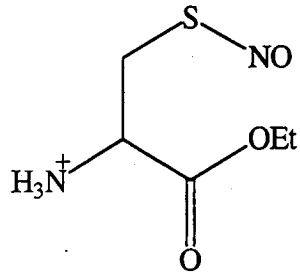	1.75±0.05
S-nitroso cysteamine	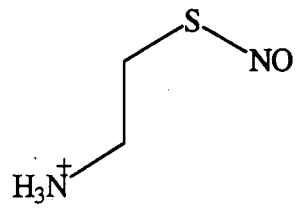	1.50±0.02
S-nitroso homo cysteine	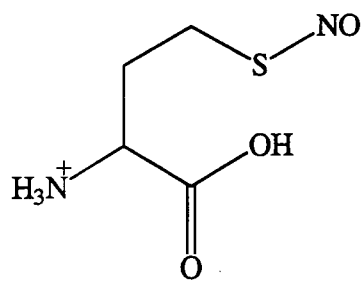	1.46±0.01
S-nitroso captopril	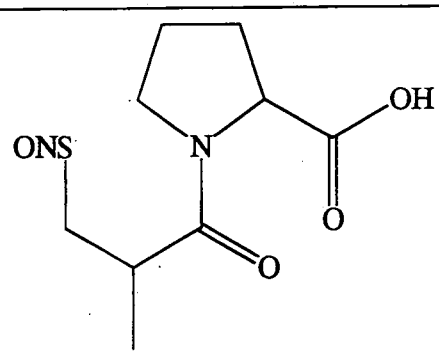	1.29±0.04

Table 4.16

Second order rate constants, k_2, for $Hg(NO_3)_2$ denitrosation of nitrosothiols at pH 1.0, 25^{0}C.

RSNO	Structure	$10^{-6}k_2$ ($mol^{-1}dm^3$ s^{-1})
S-nitroso cysteine	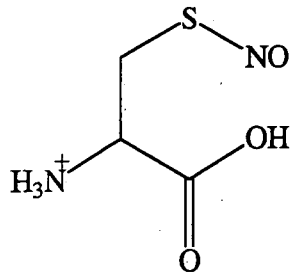	4.83±0.28
S-nitroso-N-acetyl cysteine	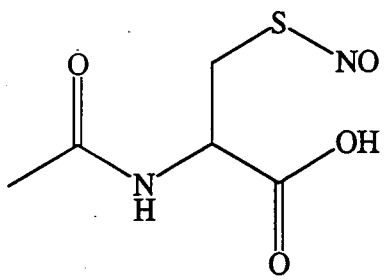	2.85±0.11
S-nitroso glutathione	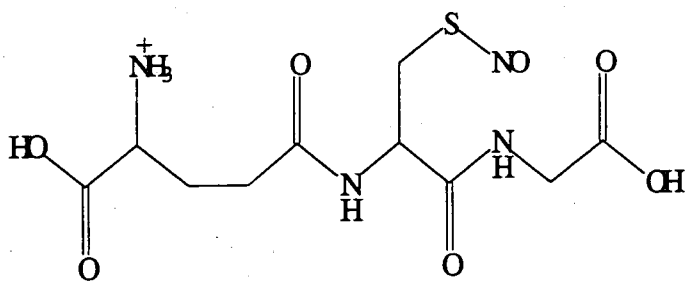	2.65±0.06
S-nitroso cysteamine	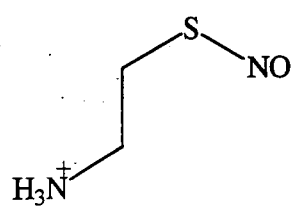	2.43±0.05

S-nitroso captopril	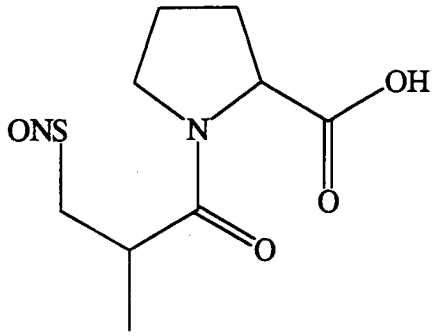	1.88±0.05
S-nitroso-N-acetyl cysteamine	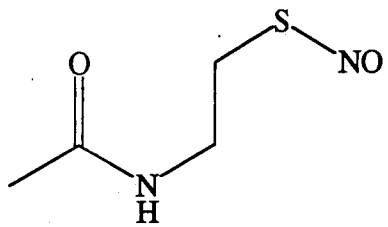	1.34±0.04
S-nitroso homo cysteine	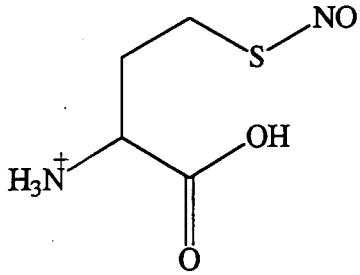	1.24±0.06
S-nitroso cysteine ethyl ester	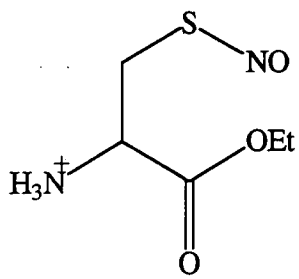	0.58±0.02

For every nitrosothiol studied, k_2 for the reaction with $Hg(NO_3)_2$ was ~10^3 greater than with $HgCl_2$ due to the counter-ion effect mentioned in section 4.3.1. k_2 values also show little variation with substrate structure. That is to say the reaction was unaffected by the environment surrounding the nitroso group. In contrast, the rate of Cu^{2+} induced decomposition which leads to NO formation at pH 7.4 is greatly dependent on the substrate structure as previously discussed in section 1.2.5.4. Rate constants of Hg^{2+} and Cu^{2+} [10] induced decomposition reactions are compared, although k_2 values could not be directly correlated due to the difference in pH, in order to comment on the mechanism.

N-acetylation of the amino group did not cause a reduction in reactivity to a virtually unmeasurable rate. This immediately implied that the amino group had little effect on the reaction which is unsurprising when one considers that at this pH the free amino group is protonated and unable to coordinate to the metal ion. The addition of a carboxylic acid group did not cause a reduction in k_2. In fact k_2 actually *increased* 2-5 fold (c.f. S-nitrosocysteamine and S-nitrosocysteine). This suggested that there was no competitive complexation of Hg^{2+} by the acid group as in the case of Cu^{2+}. The addition of an extra methylene group did cause a 4 fold reduction in the rate but this is insignificant compared to the 10^3 fold reduction in rate observed for Cu^{2+} decomposition. The biggest surprise is that S-nitrosoglutathione and S-nitrosocaptopril *did* react with Hg^{2+} and at a comparable rate with the rest of the nitrosothiols. S-nitroso-N-acetylpenicillamine did show the greatest reactivity towards the metal ion. However, this is probably more a reflection of the enhanced electron density around sulfur due to the inductive effect of the methyl groups than the conformational constraints they impose on the amino acid.

The experimental evidence suggests that the mechanism involves the coordination of Hg^{2+} to the -SNO group only.

4.4 Mechanism of RSNO Denitrosation

The products of the reaction were identified as HNO_2 and a $RSH:Hg^{2+}$ complex corresponding to quantitative conversion of RSNO to NO^+ and RSH. NO was not released by this reaction. The rate was first order in RSNO and Hg^{2+}, and was independent of the substrate structure. These observations support the mechanism initially proposed by Saville[1]. Hg^{2+} coordinates to the sulfur atom and causes heterolytic fission of the S-N bond to give $RSHg^+$ and NO^+ (scheme 4.2).

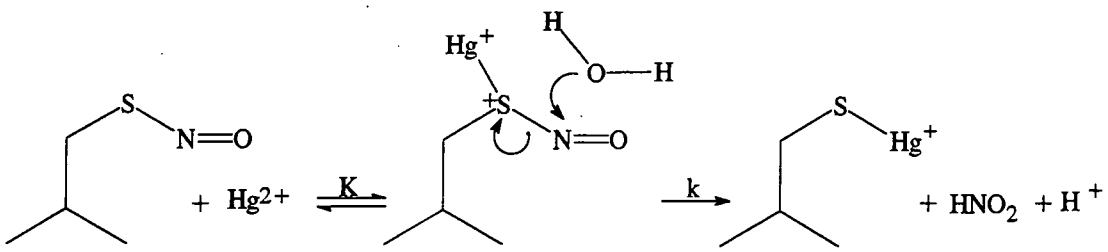

scheme 4.2

The general rate equation for scheme 4.2 is given by eqn. 4.8.

$$\frac{-d[RSNO]}{dt} = \frac{kK[Hg^{2+}][RSNO]}{1+K[Hg^{2+}]}$$

(eqn. 4.8)

The initial equilibrium is expected to lie to the side of RSNO as the formation of a doubly charged species is unfavourable. Therefore, $1 >> K[Hg^{2+}]$ and hence;

$$\frac{-d[RSNO]}{dt} = kK[Hg^{2+}][RSNO]$$

(eqn. 4.9)

The rate equation for the reaction is described by eqn. 4.9 where $k_2=kK$. A similar mechanism was proposed for the Hg^{2+} promoted hydrolysis of *p*-nitrophenyl isothiocyanate[6]. Coordination of Hg^{2+} to the sulfur atom, rather than the nitrogen atom of the nitroso group seems more probable due to the size and polarising power of the metal ion, and the greater polarisability of the S atom. Direct attack at sulfur resulting in loss of NO^+ is analogous to denitrosation in strongly acidic conditions where protonation of the S atom is followed by the release of NO^+ [11]. In contrast, Cu^{2+} catalysed RSNO decomposition releases NO and is believed to occur via coordination of Cu^{2+} to the N-atom of the -SNO group and a second available functional group.

The affinity of Hg^{2+} for the -SH group is greater than for any other ligand. The term "mercapto" to describe the -SH group emphasises this. Although it seems unlikely that the initial product of the reaction is RSH which subsequently chelates Hg^{2+}, the complex produced by denitrosation has been identified as the same complex formed from the interaction of Hg^{2+} with RSH (see fig. 4.3) and is most probably $RSHg^+$. Heterolytic cleavage of the S-NO bond rules out the formation of $RS\cdot$, dimerisation and subsequent cleavage of the S-S bond via Hg^{2+} to give $RSHg^+$ (eqn. 4.2). Complexes of the type $Hg(SR)_2$ and $Hg(SR)_3$ have been observed but usually in the presence of excess ligand and at pH >5[12]. The relative ratio of $RSH:Hg^{2+}$ and the first order dependency of RSNO argue against two molecules of RSH coordinating to one Hg^{2+} atom. The complexes are thermodynamically very stable. For example, the stability constants for the 1:1 Hg^{2+} complexes with cysteine, N-acetylcysteine and N-acetylpenicillamine have been reported to be $6x10^{37}$ $mol^{-1}dm^3$, $3x10^{38}$ $mol^{-1}dm^3$ and $3x10^{35}$ $mol^{-1}dm^3$ respectively[13], and $9x10^{40}$ $mol^{-1}dm^3$ for S-nitrosoglutathione[14]. The formation of such stable complexes is probably the reason why the reaction did not need the forcing conditions required for acid denitrosation. Coordination of the metal ion in each case is via the sulfhydryl group only although a much less important second interaction with a free amino group has been reported[13]. However, considering the pH of the solution this type of secondary coordination is unlikely in this case.

4.5 Conclusion

Mercuric ion induced denitrosation of nitrosothiols at pH 1.0 is a very different reaction to that of decomposition via copper ions. The reaction occurs at a much greater rate, is non-catalytic and produces NO^+ as opposed to NO. However, the mechanism of denitrosation is typical of mercuric ion promoted reactions.

References

1. B. Saville, *Analyst*, 1958, **83**, 670.

2. J. McAninly, Ph.D. Thesis, University of Durham, 1994.

3. G. Wilkinson, *Comprehensive Coordination Chemistry*, Vol. 5, Pergamon Books Ltd., 1987, Chap. 56.2, p.p. 1068.

4. D.J. Barnett, Ph.D. Thesis, University of Durham, 1994.

5. P.C.Jocelyn, *Biochemistry of the SH Group*, Academic Press Inc. Ltd., 1972, Chap. 5, p.p. 118.

6. D.P.N. Satchell, R.S. Satchell, *J. Chem. Soc. Perkin Trans. 2*, 1991, 303.

7. A.G.Sharpe, *Inorganic Chemistry*, Second Ed., Longman, 1986, p.p. 654.

8. G. Wilkinson, F.A. Cotton, *Advanced Inorganic Chemistry*, Fourth Ed., John Wiley & Sons Inc., 1980, Chap. 19, p.p. 605.

9. T.R. Griffiths, R.A. Anderson, *J. Chem. Soc. Chem. Commun.*, 1979, 61.

10. S.C.Askew, D.J. Barnett, J. McAninly, D.L.H. Williams, *J. Chem. Soc. Perkin Trans. 2*, 1995, 741.

11. S.S. Al-Kaabi, D.L.H. Williams, R. Bonnett, S.L. Ooi, *J. Chem. Soc. Perkin Trans. 2*, 1982, 227.

12. B.V. Chessman, A.P. Arnold, D.L. Rabenstein, *J. Am. Chem. Soc.*, 1988, **110**, 6359.

13. M.A. Basinger, J.S. Casas, M.M. Jones, A.D. Weaver, *J. Inorg. Nucl. Chem.*, 1981, **43**, 1419.

14. W. Stricks, I.M. Kolthoff, *J. Am. Chem. Soc.*, 1953, **75**, 5673.

Chapter 5:

Silver Ion Induced Denitrosation of S-Nitrosothiols

Chapter 5: Silver Ion Induced Denitrosation of S-Nitrosothiols

5.1 Introduction

Like mercury (II), silver (I) shows a high affinity for sulfur[1]. Thiol-silver complexes are easily formed upon the addition of thiol to aqueous silver ions, are very stable with stability constants of around 10^{20} $mol^{-1}dm^3$ [2] but are generally insoluble. Ag^+ has also been noted for causing slight decomposition of the nitrosothiol, S-nitroso-N-acetylpenicillamine[3].

An investigation into the denitrosation of two nitrosothiols via Ag^+ was carried out and compared with Hg^{2+} and Cu^{2+} induced decompositions.

5.2 Identification of Denitrosation Products

The products of the reaction of Ag^+ with S-nitrosoglutathione ((GSNO)(5.1)) were identified as nitrous acid and thiol, observed as a Ag^+ complex.

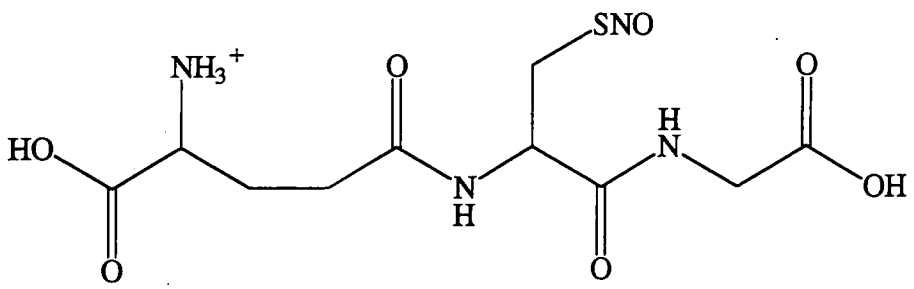

(5.1)

All reactions were carried out at pH 1.0 (0.1M perchloric acid) to enable direct comparison between Ag^+ and Hg^{2+} induced reactions. The nitrate salt of silver was used, being one of the few salts soluble in water[4], and nitrosothiols were made in solution via nitrosation of the corresponding thiol using acidic sodium nitrite.

5.2.1 Nitrous Acid Detection

An attempt was made to quantify the [HNO_2] produced from the reaction of Ag^+ with GSNO using the Griess Test (see section 2.3.1). However, the formation of a precipitate interfered with the absorbance of the purple azo dye at 540nm. When sulfanilamide was added to aqueous Ag^+ ions a similar residue resulted. Therefore, this precipitate was presumed to be a complex between excess Ag^+ ions and sulfanilamide. Hence using this method, HNO_2 could be only qualitatively detected. A nitric oxide specific electrode detected no NO released from this reaction. This confirmed that nitrous acid formation was as a result of the reaction of NO^+ with H_2O and not due to the reaction of NO with O_2 in aqueous solution (see section 2.3.1).

5.2.2 Thiol Detection

Typical spectral scans of Ag^+ induced GSNO denitrosation at the start and end of reaction are shown in fig. 5.1.

Figure 5.1

Spectra of GSNO($4x10^{-4}$M) and Ag^+($1.2x10^{-2}$M) at A) t=0 and B) t=45mins.

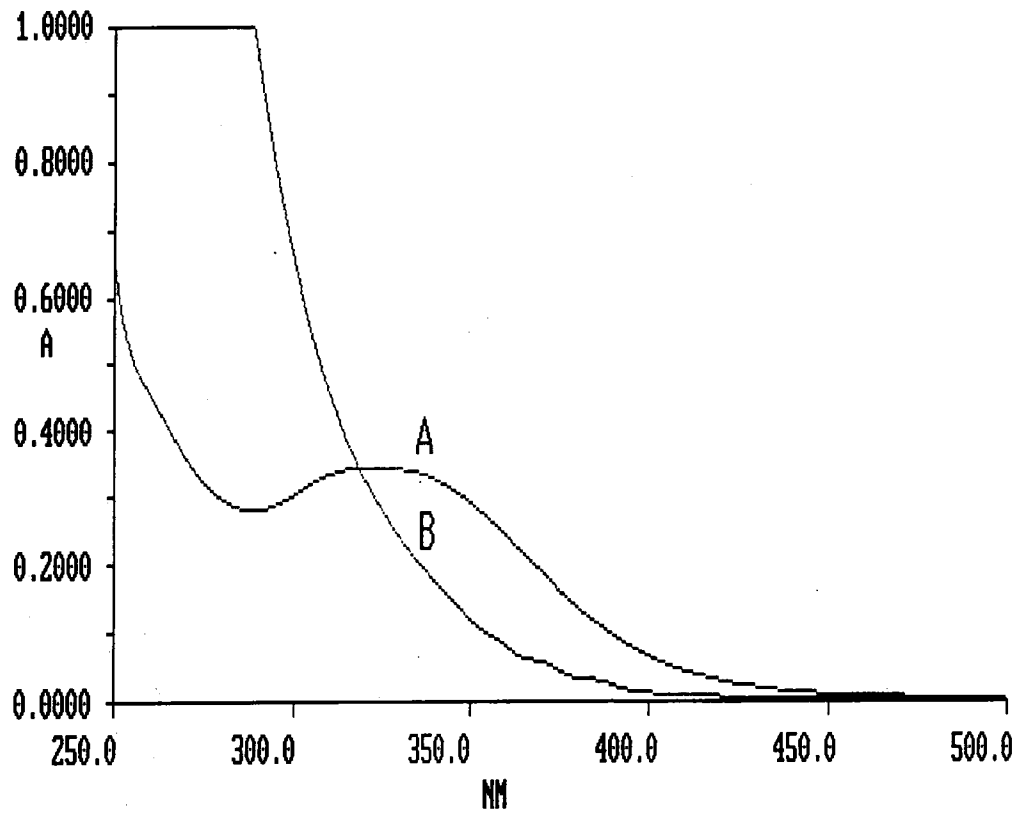

GSNO denitrosation was clearly evident from the decay of the peak at 340nm. Close inspection of spectrum B revealed signs of a five fingered absorbance peak centred around 350nm characteristic of nitrous acid (see section 4.2.1) and confirmed its presence at the end of the reaction. A spectrum of reduced glutathione ((GSH) ($4x10^{-4}M$)), $AgNO_3$($1.2x10^{-2}M$) and HNO_2($4x10^{-4}M$) was found to closely match the product spectrum (see fig. 5.2). This indicated that the other product was a GSH:Ag^+ complex.

Figure 5.2

Spectra of A) products of Ag^+ induced denitrosation of GSNO and B) GSH ($4x10^{-4}M$), $AgNO_3$($1.2x10^{-2}M$) and HNO_2($4x10^{-4}M$).

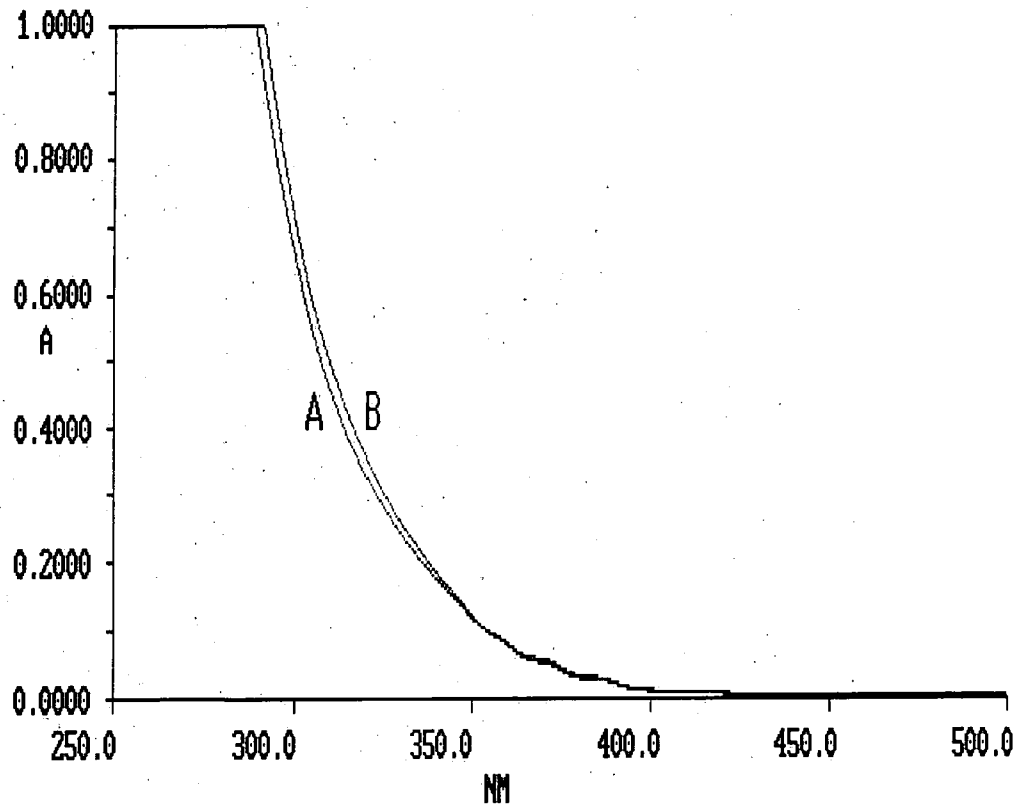

5.3 Kinetic Studies of Denitrosation

Denitrosation of S-nitrosocaptopril ((SNOCAP)(5.2)) by Ag^+ was observed using a UV-Vis spectrophotometer in aqueous acid solution at 25^0C. As k_2~0 $mol^{-1}dm^3s^{-1}$ [5] for the reaction of SNOCAP with Cu^{2+}, any decomposition due to copper ions naturally present in solution was negligible. The reaction was followed by noting the disappearance of SNOCAP at *360nm* as a function of time; it was more convenient to follow the reaction at this wavelength. The initial concentration of $AgNO_3$ was in excess of SNOCAP and reaction profiles were clean first order. The reaction was studied over a range of Ag^+ concentrations ($0.8\text{-}3.6x10^{-2}M$) and rate constants (k_{obs}) obtained from the integrated first order rate equation. The standard error of the means of five determinations of k_{obs} was less than 5%. A plot of k_{obs} against $[Ag^+]$ was not linear (see fig. 5.3) showing that the rate equation was not first order in Ag^+.

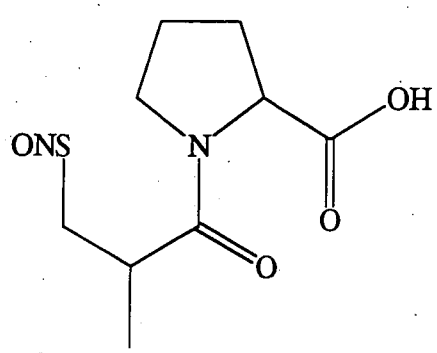

(5.2)

Figure 5.3

Plot of k_{obs} against $[Ag^+]$ for the denitrosation of S-nitrosocaptopril ($4x10^{-4}M$).

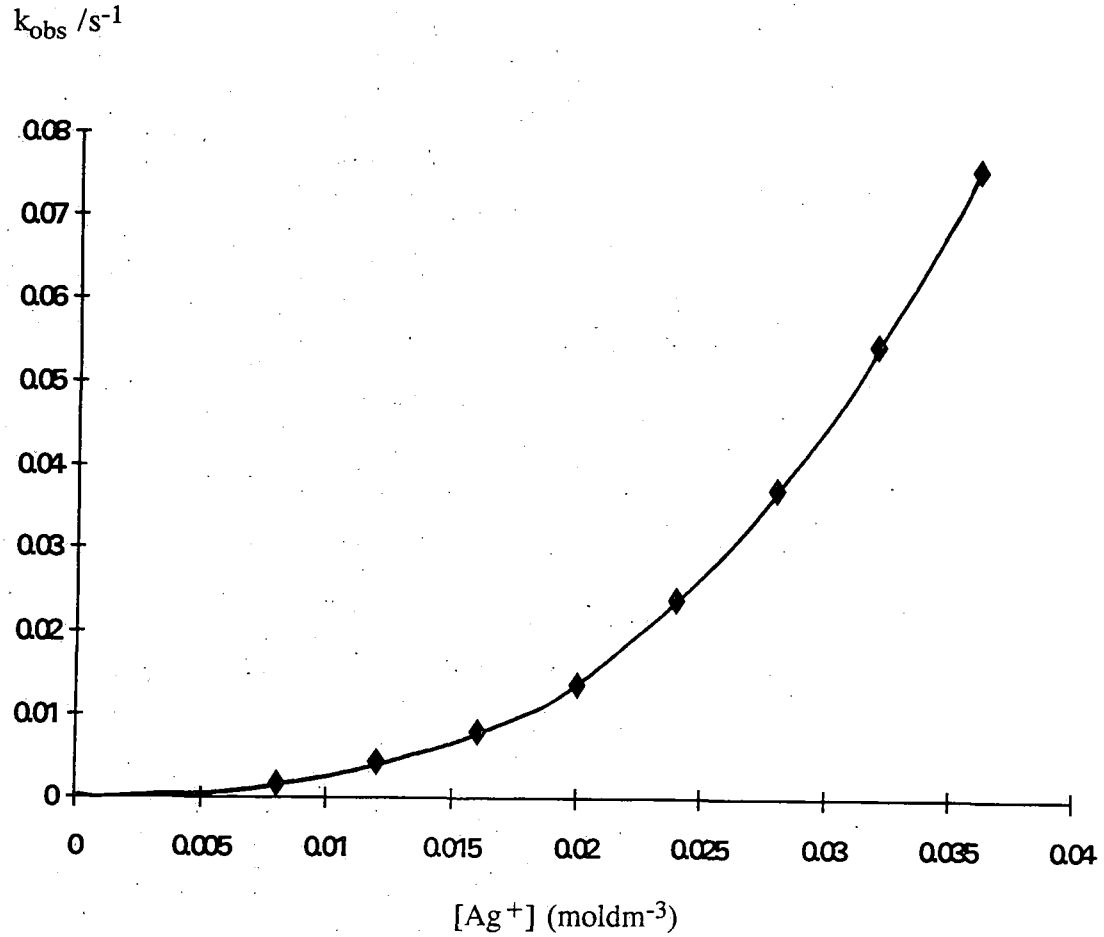

Hence,

$$k_{obs} = k[Ag^+]^n$$

(eqn. 5.1)

and

$$-\ln k_{obs} = -\ln k + n(-\ln[Ag^+])$$

(eqn. 5.2)

Therefore a plot of $-\ln k_{obs}$ against $-\ln[Ag^+]$ would be linear with gradient, n and intercept, -lnk (see fig. 5.4).

Figure 5.4

Plot of $-\ln k_{obs}$ against $-\ln[Ag^+]$ for the denitrosation of S-nitrosocaptopril ($4x10^{-4}M$).

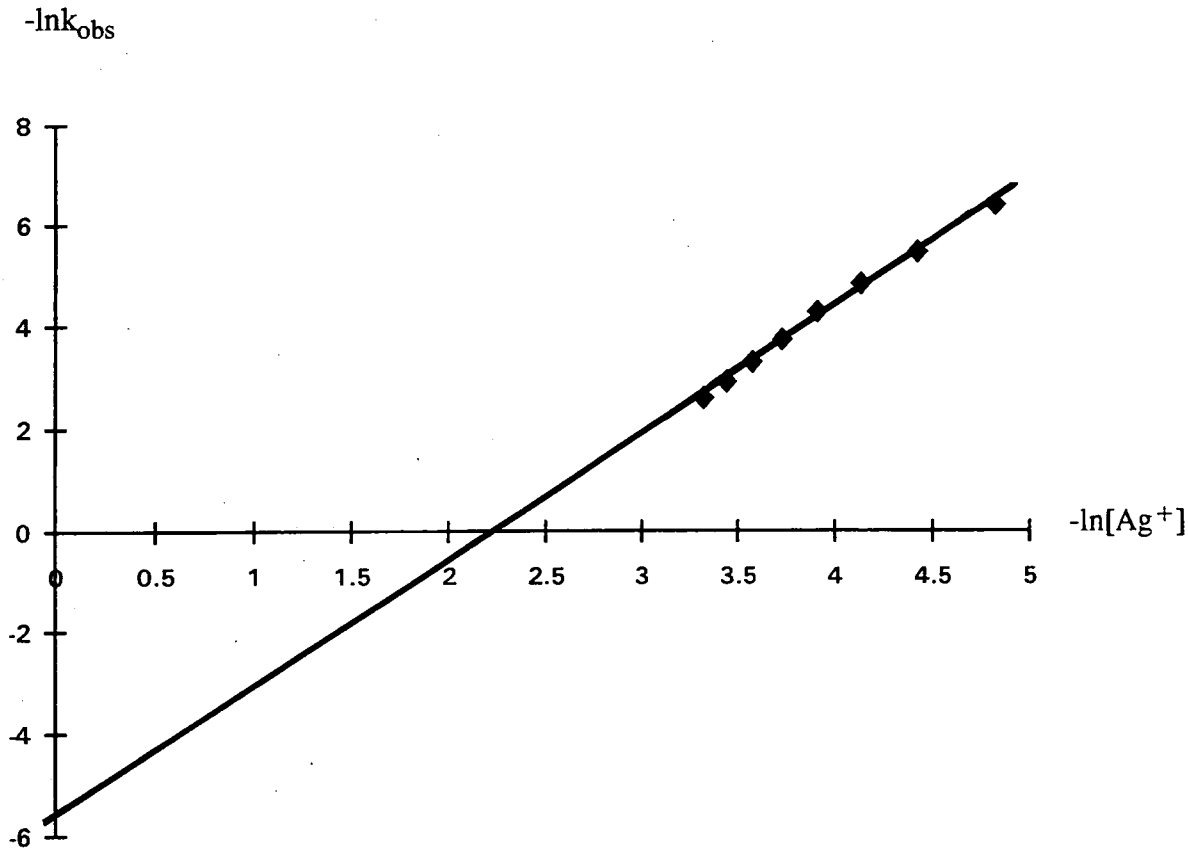

Hence, for the reaction of SNOCAP, n=2.5±0.1 and lnk= 5.8±0.3. The order and value of lnk for GSNO denitrosation were obtained in a similar fashion and results tabulated in table 5.1.

Table 5.1

Rate data for the denitrosation of S-nitrosoglutathione ($4x10^{-4}M$).

$10^2[Ag^+](moldm^{-3})$	$10^{-2}k_{obs}(s^{-1})$
0.8	0.23±0.01
1.2	0.58±0.01
1.6	1.02±0.45
2.0	1.98±0.74
2.4	3.39±0.28
2.8	5.57±0.13
3.2	7.35±0.29
3.6	10.60±3.01

$n = 2.6 \pm 0.1$, $\ln k = 6.2 \pm 0.3$

Hence

$$k_{obs} = k[Ag^+]^{5/2}$$

And therefore the rate of Ag^+ induced denitrosation of SNOCAP and GSNO can be described by eqn. 5.3.

$$\frac{-d[RSNO]}{dt} = k[RSNO][Ag^+]^{5/2}$$

(eqn. 5.3)

The timescale of the reaction was similar to that of Cu^{2+} [5]. To ensure that observed decomposition was as a result of Ag^+ only and not a combination of Ag^+ and Cu^{2+} present naturally in solution, nitrosothiols which showed none or very little reaction (k_2~0 $mol^{-1}dm^3s^{-1}$) with Cu^{2+} were explored. The reaction of Ag^+ with S-nitrosohomocysteine proved unfruitful due to precipitation of the insoluble RSH:Ag^+ complex. Similarly, rate constants for the reaction of Ag^+ with S-nitroso-N-acetylcysteine, S-nitrosocysteamine, S-nitrosomercaptopropionic acid and S-nitrosomethylmercaptopropoinate could not be obtained. Hence an investigation into the substrate structural dependency of the reaction could not be carried out.

5.4 Mechanism of Denitrosation

The products of the reaction were identified as HNO_2 and a RSH:Ag^+ complex. GSNO and SNOCAP are highly soluble in aqueous solution due to the large number of polar groups they possess. The surprising solubility of the GSH:Ag^+ and CAP:Ag^+ complexes was a reflection of this. Denitrosation via Ag^+ took minutes to complete and hence was much slower than the Hg^{2+} induced reaction where denitrosation was over in a fraction of a second. Eqn. 5.4 gives the stoichiometric reaction of RSNO with Ag^+ as determined by the rate equation (eqn. 5.3).

$$2RSNO + 5Ag^+ \xrightarrow[2H_2O]{k} [(RS)_2 Ag_5]^{3+} + 2HNO_2 + 2H^+$$

(eqn. 5.4)

The mechanism of this reaction could not be determined from these results. However, several points about the nature of the mechanism can be made.

Nitric oxide was not released by this reaction and hence nitrous acid formation was as a result of the reaction of NO^+ with H_2O. The release of NO^+ implied that the S-NO bond was heterolytically cleaved during the reaction. This suggested a mechanism similar to that observed by Hg^{2+} (as opposed to Cu^{2+} induced decomposition) where the metal ion directly attacks the sulfur atom of the nitroso group. Hence, the lower reactivity of the silver ion towards nitrosothiols could be a reflection of its lower affinity for the sulfur atom compared to that of Hg^{2+}.

Ag^+ generally forms univalent complexes with thiols. Coordination is via the SH group only and bonding is somewhat covalent in nature. Studies of these complexes has not been extensive due to their insolubility. However ^1H NMR studies of Ag^+ and cysteine in acidic solution[6] showed the formation of a 1:1 complex where Ag^+ displaced the proton from the thiol group as shown in (5.3).

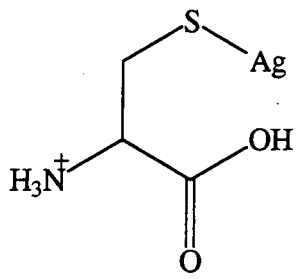

(5.3)

This complex has recently been used to inhibit HIV virus replication[7]. However, eqn. 5.3 does not suggest the formation of a 1:1 RSH:Ag^+ complex in this case.

Further work is required to identify the nature and stoichiometry of the thiol-silver product of this reaction and the $[NO^+]$ quantitatively determined by a more applicable method than the Griess Test. For example, oxidation of 2,2'-azinobis (3-ethylbenzothiazoline-6-sulfonic acid) (ABTS) produces a species which strongly absorbs in the visible region and has been used to determine $[HNO_2]$ in rainwater[8]. The study of a greater number of nitrosothiols to investigate the substrate structural requirements of the reaction would be useful and may confirm the order of reaction with respect to Ag^+. Due to the insolubility of the RSH:Ag^+ complex, studies should be limited to nitroso derivaties of the di and tripeptide sulfhydryl amino acids which possess a large number of polar groups.

5.5 Conclusion

NO is not released from nitrosothiol denitrosation induced by Ag^{+}. The mechanism of this reaction could not be elucidated but is reminiscent of the mechanism proposed for Hg^{2+} induced denitrosation and demonstrates the high affinity of this metal towards the SH group compared to copper.

References

1. N.N.Greenwood, A.Earnshaw, *Chemistry of the Elements*, Pergamon Press, Oxford, 1989, Chap. 28, p.p. 1388.

2. P.C.Jocelyn, *Biochemistry of the SH Group*, Academic Press Inc. Ltd., 1972, Chap.3, p.p. 78.

3. J.McAninly, Ph.D. Thesis, University of Durham, 1994.

4. G.Wilkinson, *Comprehensive Coordination Chemistry*, Vol 5, Pergamon Books Ltd., 1987, Chap. 54, p.p. 776

5. S.C.Askew, D.J.Barnett, J.McAninly, D.L.H.Williams, *J. Chem. Soc. Perkin Trans. 2*, 1995, 741.

6. D.F.S.Natusch, L.J.Porter, *J. Chem. Soc. (A)*, 1971, 2527.

7. S.Hussain, R.F.Anner, B.M.Anner, *Biochem. Biophys. Res. Comm.*, 1992, **189**, 1444.

8. T.Okutani, A.Sakuragawa, S.Kamikura, M.Shimura, S.Azuchi, *Analytical Sciences*, 1991, **7**, 793.

Chapter 6:

Iron Induced Decomposition of S-Nitroso-N-acetylpenicillamine

6.1 Introduction

In vitro studies[1,2] have shown that Fe(II) ions catalyse nitrosothiol decomposition at a similar rate to that of Cu(I). This may also be of physiological importance in the release of NO from these compounds. Therefore a kinetic investigation into the Fe(II) decomposition of S-nitroso-N-acetylpenicillamine (SNAP) was carried out and compared to that of Cu(I) catalysis.

6.2 Synthesis of S-Nitroso-N-acetylpenicillamine

SNAP (6.1) was synthesised and isolated as a green solid as described by Field *et al*[3]. It was convenient to use this solid sample as a source of nitrosothiol.

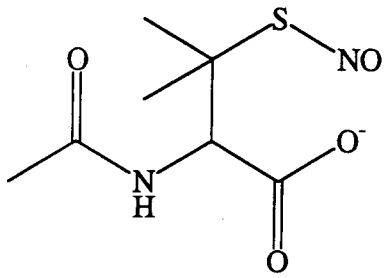

(6.1)

The yield based on weight of product was 45% with a melting point of 149-151^{0}C (c.f. 152-154^{0}C)[3]. Elemental analysis requires C; 38.2, H; 5.5, N; 12.7 and C; 38.2, H; 5.1, N; 12.6 were obtained. The UV-Vis spectrum was characterised by an absorption peak at 340nm (ε= 795±8 mol^{-1}dm^{3}cm^{-1}, c.f. 825 mol^{-1}dm^{3}cm^{-1} [4]).

The NMR spectrum of both N-acetylpenicillamine (NAP) and SNAP were obtained in deuterated dimethylsulfoxide using a 200MHz ^{1}H NMR instrument (see fig. 6.1 and 6.2)

Figure 6.1

^1H NMR spectrum of NAP in $(CD_3)_2SO$

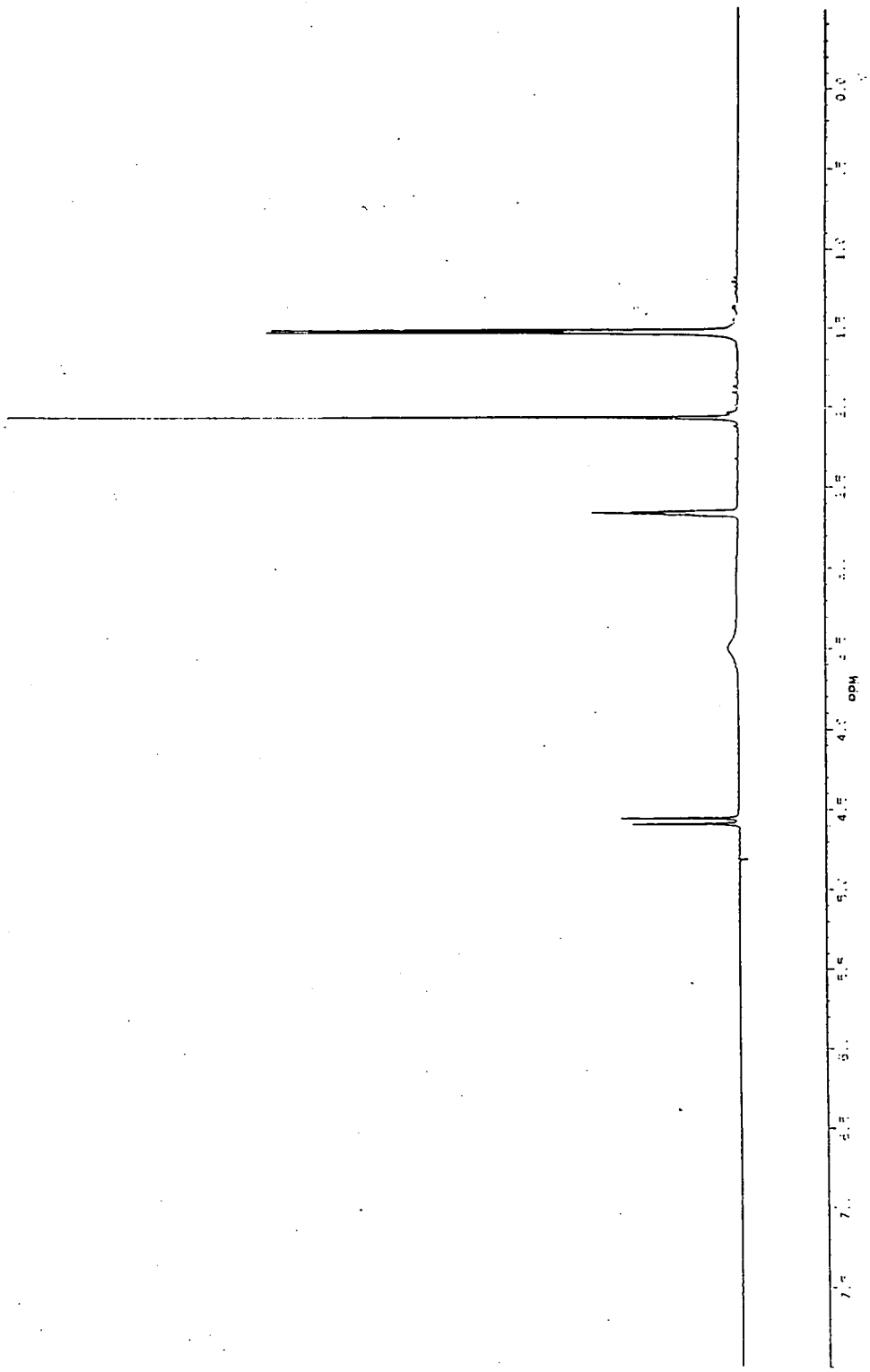

Figure 6.2

^{1}H NMR spectrum of SNAP in $(CD_3)_2SO$

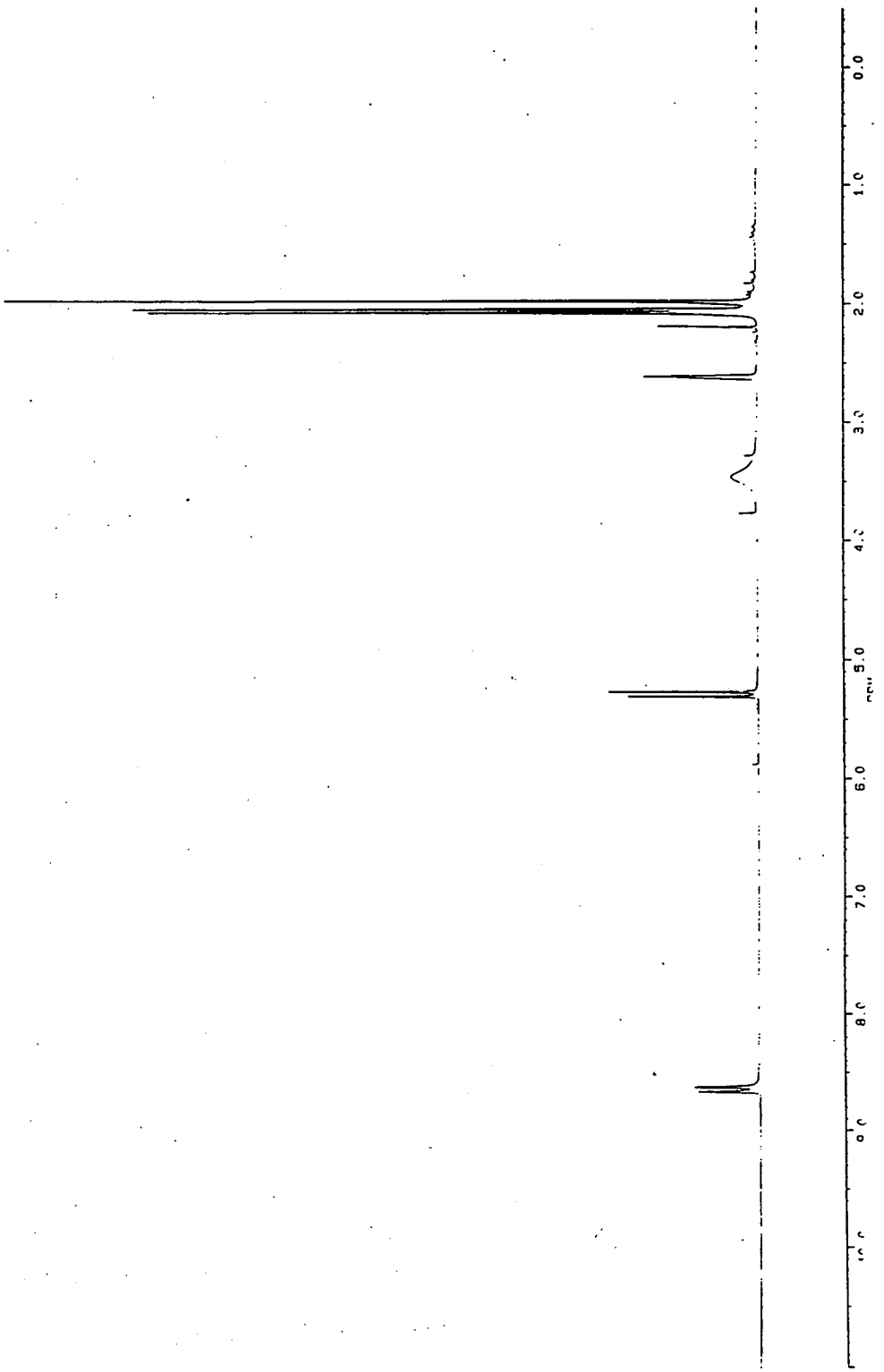

Using (6.2) the proton resonances can be assigned as follows:

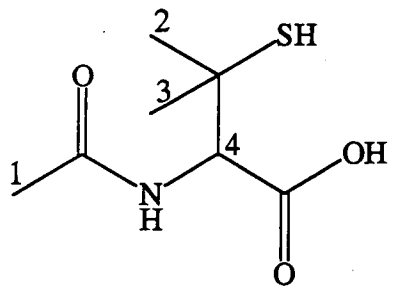

(6.2)

The C-1 methyl ester protons gave a singlet at 2.10ppm, C-2 and C-3 methyl protons gave singlets at 1.52ppm and 1.54ppm, and the C-4 proton gave a doublet at 4.50ppm (J= 9.0Hz). The quintet at 2.70ppm was due to solvent. Nitrosation affected the chemical shift of protons adjacent to the SH group only; the chemical shifts of the C-2 and C-3 methyl protons, and the C-4 proton shifted downfield by 0.50ppm due to the greater electron withdrawing ability of the SNO group. The doublet at 8.51ppm (J= 9.1Hz) is attributed to the amide proton, split by the C-4 proton.

6.3 Kinetic Studies

Oxygen is a sufficiently strong oxidising agent to render $Fe^{2+}_{(aq)}$ unstable to oxidation[5]. However, oxidation at low pH is slow. Therefore Fe^{2+} was produced in acidic solution, under anaerobic conditions, via reduction of Fe^{3+} by $Na_2S_2O_4$. Before reaction, the solution was tested for ferric ions using a 1% solution of ammonium thiocyanate[6]. If Fe^{3+} was present, a red colour resulted. Stock solutions of SNAP (5.2×10^{-4}M) in pH 7.4 phosphate buffer and $Fe_2(SO_4)_3$ (7.8×10^{-4}M) in 0.1M perchloric acid were purged with N_2 for 15mins prior to reaction. 0.05g $Na_2S_2O_4$ was then added to $Fe_2(SO_4)_3$. The reaction of SNAP (5×10^{-4}M) with Fe^{2+} (3×10^{-5}M) was monitored by observing the disappearance of the nitrosothiol at 340nm as a function of time. Reactions took ~1hr. to complete and good first order behaviour was found in each individual kinetic run showing the reaction to be catalytic. However rate constants were irreproducible (see table 6.1 which shows some 14 measurements of k_{obs}) and reactions sometimes did not go to completion.

Table 6.1

k_{obs} for the decomposition of SNAP ($5x10^{-4}M$) by Fe^{2+} ($3x10^{-5}M$) at pH 7.4 and 25^0C.

10^3k_{obs} (s^{-1})	10^3k_{obs} (s^{-1}) contd.
1.54±0.09	5.67±0.14
3.70±0.08	9.43±0.16
4.70±0.02	2.76±0.11
2.91±0.14	2.85±0.14
4.21±0.13	3.38±0.14
3.42±0.06	4.57±0.08
2.61±0.06	7.67±0.15

k_{obs} values ranged from $1.5\text{-}9.4x10^{-3}$ s^{-1}. The cause of this was unknown but was probably due to inconsistencies in the method. However, k_{obs} was greater than the value of k_{obs} for the same reaction with Cu^{2+} (see table 6.2).

Table 6.2

Comparison of k_{obs} for the decomposition of SNAP ($5x10^{-4}M$) via Cu^{2+} and Fe^{2+} ($3x10^{-5}M$) at pH 7.4 and 25^0C.

Metal Ion	10^3k_{obs} (s^{-1})
Cu^{2+}	0.12±0.01*
Fe^{2+}	1.54-9.43±0.06-0.14

* Results obtained by D.J.Barnett[3].

This implied that Fe^{2+} was more reactive than Cu^{2+}.

A control experiment was then undertaken to check no decomposition occurred in the absence of Fe^{2+}. Unfortunately, decomposition was observed due to small amounts of copper ions present naturally in solution. k_{obs} was calculated to be (7.31± 0.11)x10^{-4} s^{-1}. Therefore the observed rate constants shown in table 6.1 seemed to be k_{obs} for the decomposition of SNAP by Fe^{2+} *and* Cu^{2+}.

In an attempt to stop copper catalysed decomposition, the reaction was carried out in the presence of two copper chelating agents.

6.4 Decomposition In The Presence of Two Chelating Agents

SNAP decomposition via Fe^{2+} was carried out as previously described in the presence of two copper chelating agents, cuprizone and neocuproine.

6.4.1 Cuprizone Chelation

Cuprizone is a specific Cu^{2+} chelator[7] (see section 2.4.3). However, decomposition of SNAP was negligible in the presence of cuprizone (3x10^{-5}M). This implied cuprizone chelated Fe^{2+} as well as Cu^{2+}. On the basis of their desired coordination geometry[5], the ability of cuprizone to chelate Fe^{2+} as well as Cu^{2+} is unsurprising.

6.4.2 Neocuproine Chelation

The true catalytic species in copper ion catalysis of RSNO decomposition is known to be Cu^{+} [8] (see section 1.2.5.4). Therefore a second attempt at eliminating decomposition induced by copper was carried out using neocuproine, a Cu^{+} specific chelator[9] (see section 2.4.2). Due to the difference in preferred coordination geometry it was assumed that Cu^{+} only would be chelated and Fe^{2+} left to react with the nitrosothiol. Neocuproine (5x10^{-4}M) was added to a solution of SNAP (1x10^{-3}M), Fe^{2+} (5x10^{-5}M) and Cu^{2+} (5x10^{-6}M) and a reaction was observed, k_{obs}= (2.49 ±0.04)x10^{-3} s^{-1}. However, when repeated, no decomposition occurred at all and in fact the first experiment was never reproduced.

6.5 Conclusion

The apparent Fe^{2+} decomposition of SNAP has been shown to be catalytic. However, problems of reproducibility of k_{obs} values were encountered. Ideally, there should be no oxygen present in solution as Fe^{2+} is susceptible to aerial oxidation. Anaerobiosis obtained by N_2 purging solutions prior to reaction proved to be an ineffective way of eliminating all oxygen. This method could also not ensure that the $[O_2]$ (and hence the $[Fe^{2+}]$) was constant for each kinetic run, and therefore a range of values for k_{obs} were observed.

Decomposition via copper ions naturally present in the aqueous medium was a problem. Chelation via cuprizone proved ineffectual probably due to chelation of the ferrous ion by the agent. The use of the neocuproine chelating agent needs to be further investigated. Perhaps if the concentration of neocuproine was reduced to only a five fold excess over Cu^{2+} (the generally required ratio to obtain all chelation of copper) then decomposition due to Fe^{2+} only may be observed.

Fe^{3+} shows no reactivity towards SNAP[1]. However, GSNO decomposition has been shown to occur upon the addition of GSH and Fe^{3+} [10]. Rate constants were reported to be 0.3-0.4 times those observed with Cu^{2+} in the same conditions. In the latter case, it seems probable that, analogous to Cu^{2+}/GSH induced decomposition, Fe^{2+} was generated by the reduction of Fe^{3+} by the added thiol. However, unlike Cu^{2+}, the amount of thiol, present as unreacted starting material was insufficient to reduce Fe^{3+} and thus SNAP decomposition did not occur. Anaerobic studies[11] of the reaction of ferric salts with glutathione have shown that thiol reduction of Fe^{3+} occurs via an electron transfer reaction. This required the formation of an intermediate complex involving octahedral coordination of the thiol to Fe^{3+} by the thiolate group, the carboxylate groups and intervening -NH groups as shown in (6.3).

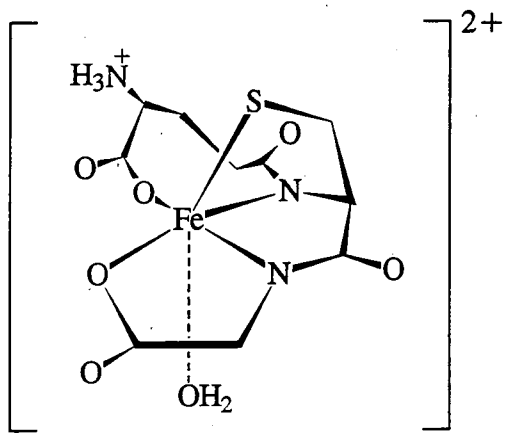

(6.3)

In summary, to calculate the rate constant for this reaction the following improvements have been suggested:

1) A better method of excluding oxygen, such as the glucose/glucose oxidase method[10] (see section 2.5.3), is required.

2) Neocuproine (~5 fold excess over copper) is required to eliminate decomposition via adventitious copper ions but reduce the possibilty of iron chelation.

Vanin *et al*[2] have suggested a homolytic mechanism for Fe^{2+} induced RSNO decomposition. To prove this mechanism, NO release from this reaction must be detected via the NO specific electrode and quantified via the Griess test (see section 2.3.1). The disulfide must be identified via capillary zone electrophoresis[12] or via the glutathione reductase-TNB recycling method[13]. The reaction of thiol with Fe^{3+} should be investigated and the effect of adding thiol to a solution of Fe^{3+} and RSNO observed. Only then may conclusions be drawn about the relative reactivities of Fe^{2+} and Cu^{+} towards nitrosothiols, and related to the mechanism of NO release from these compounds, *in vivo*.

References

1. J.McAninly, D.L.H.Williams, S.C.Askew, A.R.Butler, C.Russell, *J. Chem. Soc. Chem. Commun.*, 1993, 1758.

2. A.F.Vanin, *Biochemistry (Moscow)*, 1995, **60**, 441.

3. L.Field, R.V.Dilts, R.Ravichandran, P.G.Lenhert, G.E.Carnahan, *J.Chem. Soc. Chem. Commun.*, 1978, 249.

4. B.Roy, A.duMoulinet d'Hardemare, M.Fontecave, *J. Org. Chem.*, 1994, **59**, 7019.

5. N.N.Greenwood, A.Earnshaw, *Chemistry of the Elements*, Pergamon Press, Oxford, 1989, Chap. 25, p.p. 1269.

6. *Vogel's Textbook of Quantitative Inorganic Analysis*, Sixth Ed., Longman, New York, 1990, p.p. 106.

7. R.E.Peterson, M.E.Bollier, *Anal. Chem.*, 1955, **27**, 1195.

8. A.P.Dicks, H.R.Swift, D.L.H.Williams, A.R.Butler, H.H.Al Sa'doni, B.G.Cox, *J. Chem. Soc. Perkin Trans. 2*, 1996, 481.

9. G.F.Smith, W.H.McCurdy, *Anal. Chem.*, 1952, **24**, 371.

10. A.C.F.Gorren, A.Schrammel, K.Schmidt, B.Mayer, *Arch. Biochem. Biophys*, 1996, **330**, 219.

11. M.Y.Hamed, J.Silver, M.T.Wilson, *Inorg. Chim. Acta.*, 1983, **78**, 1.

12. J.S.Stamler, J.Loscalzo, *Anal. Chem.*, 1992, **64**, 779.

13.O.W.Griffin, *Anal. Biochem.*, 1980, **106**, 207.

Chapter 7:

Experimental Details

Chapter 7: Experimental Details

7.1 Experimental Techniques

7.1.1 UV-Vis Spectrophotometry

All UV-Vis spectra were obtained from solutions in 1cm path length quartz cells on either a Perkin-Elmer Lambda 2 or a Shimadzu 2102-PC instrument. The same instruments were used when measuring reactions kinetically. For rapid reactions ($t_{1/2} \geq 2 \times 10^{-3}$ s) a stopped flow technique was used (section 7.1.2).

Kinetic measurements were made under pseudo first order conditions. The observed rate constants (k_{obs}) were calculated from the change in absorbance with time at a fixed wavelength. The absorbance/time data from the Lambda 2 were used in a program designed for rate constant calculation on an Epson AX2 personal computer. Similarly for the data from the Shimadzu instrument, a program run on an Opus 386 DX was used to determine rate constants. These programs' calculation of k_{obs} was based on the following derivation.

For a first order process

$$A \xrightarrow{k_{obs}} B$$

the rate of formation of B or the loss of A can be described by eqn. 7.1

$$-\frac{d[A]}{dt} = \frac{d[B]}{dt} = k_{obs}[A]$$

(eqn. 7.1)

and

$$-\int_{[A]_0}^{[A]_t} \frac{1}{[A]}\, d[A] = \int_0^t k_{obs}\, dt$$

hence

$$\ln[A]_0 - \ln[A]_t = k_{obs}t$$

(eqn. 7.2)

where $[A]_o$ and $[A]_t$ are the concentrations of A at times t = 0 and t respectively.

Using the Beer-Lambert law ($A = \varepsilon cl$, where A is the absorbance, ε is the molar extinction coefficient, c is the concentration and l, the path length, is 1cm) the

expression of the absorbance at t = 0 and t can be described by eqns. 7.3 and 7.4 respectively.

$$A_0 = \varepsilon_A[A]_0$$

(eqn. 7.3)

$$A_t = \varepsilon_A[A]_t + \varepsilon_B[B]_t$$

(eqn. 7.4)

As $[B]_t = [A]_o - [A]_t$, substituting for $[B]_t$ into equation 7.4 gives

$$A_t = \varepsilon_A[A]_t + \varepsilon_B[A]_0 - \varepsilon_B[A]_t$$

(eqn. 7.5)

At the end of the reaction, $t=\infty$ and $[B]_\infty = [A]_0$, so

$$A_\infty = \varepsilon_B[A]_0$$

(eqn. 7.6)

Substituting into eqn. 7.5

$$A_t = \varepsilon_A[A]_t + A_\infty - \varepsilon_B[A]_t$$

thus

$$[A]_t = \frac{(A_t - A_\infty)}{(\varepsilon_A - \varepsilon_B)}$$

(eqn. 7.7)

Similarly, at time t=0

$$A_0 = \varepsilon_A[A]_0$$

(eqn. 7.8)

therefore subtracting eqn. 7.8 from eqn. 7.6;

$$(A_0 - A_\infty) = \varepsilon_A[A]_0 - \varepsilon_B[A]_0$$

and

$$[A]_0 = \frac{(A_0 - A_\infty)}{(\varepsilon_A - \varepsilon_B)}$$

(eqn. 7.9)

Substituting eqns. 7.7 and 7.9 into eqn 7.2 gives

$$k_{obs} = \frac{1}{t} \ln \frac{(A_0 - A_\infty)}{(A_t - A_\infty)}$$

(eqn. 7.10)

Rearranging gives

$$\ln(A_t - A_\infty) = -k_{obs}t + \ln(A_0 - A_\infty)$$

(eqn. 7.11)

Therefore a plot of $\ln(A_t - A_\infty)$ against t should be linear with a slope of $- k_{obs}$. The infinity values A_∞, were determined after a period of ten half lives and the disappearance of absorbance followed for at least two half lives.

7.1.2 Stopped Flow Spectrophotometry

For measurement of rate constants of reactions too fast to measure by conventional machines, an Applied Photophysics SX17MV Spectrophotometer was used to measure rate constants of reactions with half lives of <2 mins. Again, kinetics were carried out under pseudo first order conditions except in the case of the reactions of $Hg(NO_3)_2$ with nitrosothiols (see section 4.3.1). A schematic diagram of the stopped-flow spectrophotometer is shown in fig. 7.1. Reactant solutions, A and B, are stored in reservoirs and are drawn into two identical syringes so that equal volumes are mixed. Using a compressed air supply, the syringes are compressed simultaneously, and mixing occurs at point M extremely rapidly (< 1ms). The mixture flows into a thermostatted 2mm path length quartz cell at point O causing the plunger of the third syringe to hit a stop and the flow of solution to cease. The acquisition of data from the reaction is triggered by the third syringe hitting the stop. The reaction is observed by passing a beam of monochromatic light of the appropriate wavelength through the cell by fibre optic cable. The light is passed through a photomultiplier and the change in voltage measured due to a change in absorbance of the solution is observed. Software on the computer that runs the stopped flow machine can transform voltage/time data into absorbance/time data and also calculate the observed rate constants.

Figure 7.1
Schematic Diagram of a Stopped-flow Spectrophotometer.

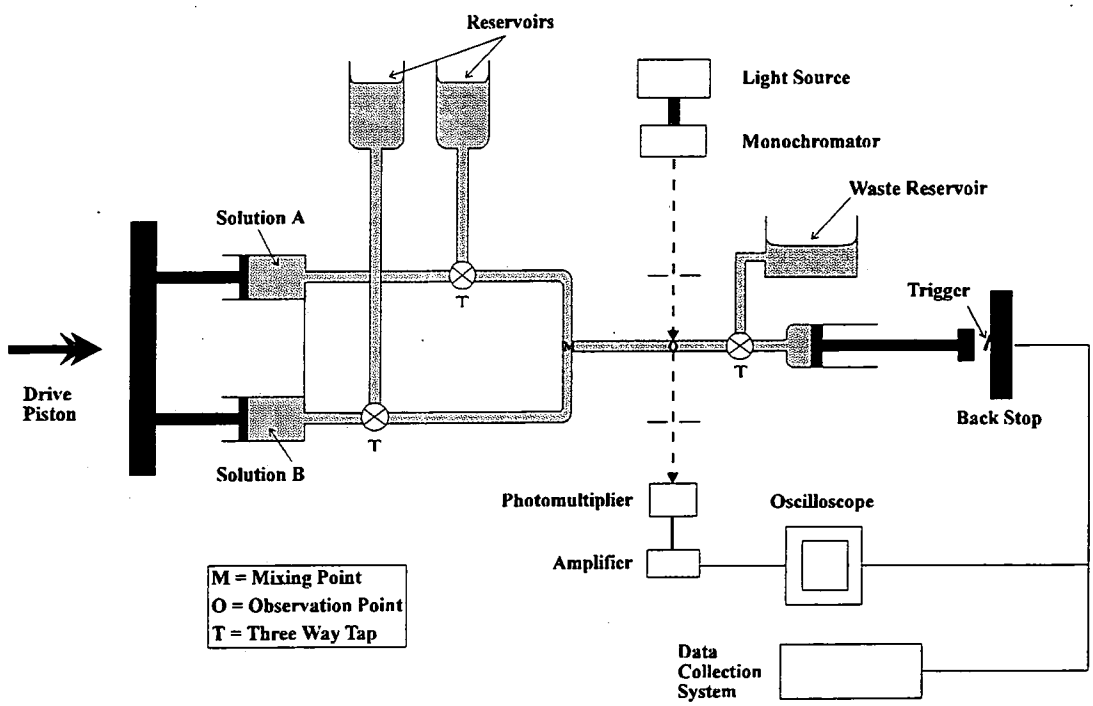

7.2 pH Measurements

All pH measurements were carried out using a Jenway digital 3020 pH meter (accurate to ± 0.02 pH units). The pH meter was calibrated over the range pH 4.0 to 7.0 or pH 7.0 to 10.0 depending on the solution to be measured.

7.3 Nitric Oxide Electrode Calibration

A World Precision ISO-NO nitric oxide specific electrode was used to measure NO release in aqueous solutions. Calibration was carried out with ascorbic acid (0.1M) and sodium nitrite ($2.5x10^{-3}M$) stock solutions. Solutions were thermostatted at 25^0C as passage of NO across the membrane is temperature dependent. The tip of the electrode was immersed 10mm below the surface of the ascorbic acid solution and the reading allowed to stabilise before adjusting to zero. O_2 was rigourously excluded by purging the solution with N_2 such that no NO was lost due to the reaction of NO with O_2 producing NO_3^-. It was assumed that NO was produced quantitatively by the reaction and a calibration curve of current (nA) against concentration of NO produced (μM) was constructed.

7.4 Reagents

All reagents of the highest grade were purchased commercially. Nitrosothiols were produced in solution from the commercially available thiols. The potassium dihydrogen orthophosphate used for preparing buffer solutions was purchased commercially and used as supplied. The perchloric acid solutions were prepared by dilution of concentrated perchloric acid which had been standardised by standard sodium hydroxide solution using phenol red as an indicator.

7.5 GSNO Synthesis

GSNO was synthesised following the method of Hart[1]. Glutathione (1.5344g) was dissolved in water ($8cm^3$) containing 2M HCl ($2.5cm^3$). The reaction vessel was covered in silver foil to avoid photolytic decomposition of the nitrosothiol and 0.3456g sodium nitrite was added in one portion. After stirring for 40 mins at 2^0C the red solution was treated with acetone ($10cm^3$) and stirred for a further 10mins. The resulting red precipitate was filtered and then washed successively with ice cold water ($5x1cm^3$), acetone ($3x10cm^3$) and ether ($3x10cm^3$).

7.6 SNAP Synthesis

SNAP was synthesised following the method of Field *et al*[2]. N-acetylpenicillamine (4.78g) was dissolved in a 1:1 mixture (300ml) of methanol and 1M HCl with concentrated sulfuric acid (20ml). The reaction vessel was covered in silver foil to avoid photolytic decomposition and cooled to 2^0C in an ice bath. A solution of

sodium nitrite (3.45g) was added over 10 mins while stirring. After leaving to warm to room temperature, the green solid was filtered and dried under vacuum in a dessicator.

7.7 Analysis

Analysis of perchloric acid and buffer solutions for trace quantities of copper were carried out on a Perkin Elmer 5000 Atomic Absorption Spectrophotometer by Miss J.Magee. Elemental analysis was performed on samples using a Carlo Erba Elemental Analyser by Mrs J.Dostal.

7.8 Derivation of Rate Equations

7.8.1 Thiol Induced S-Nitrosothiol Decomposition

The mechanism for thiol induced nitrosothiol decomposition is given in scheme 7.1

$$RSH + 1/2O_2 \xrightarrow{k} RS^{\cdot} + 1/2H_2O_2$$

$$RS^{\cdot} + RSNO \xrightarrow{k_3} RSSR + NO$$

$$RS^{\cdot} \xrightarrow{k_4} 1/2RSSR$$

scheme 7.1

where

$$\frac{-d[RSNO]}{dt} = k_3[RSNO][RS^{\cdot}]$$

(eqn. 7.12)

and

$$\frac{d[RS^{\cdot}]}{dt} = k[O_2]^{1/2}[RSH] - k_3[RSNO][RS^{\cdot}] - k_4[RS^{\cdot}]$$

Using the steady state approximation,

$$\frac{d[RS^{\cdot}]}{dt} = 0$$

therefore,

$$0 = k[O_2]^{1/2}[RSH] - k_3[RSNO][RS^{\cdot}] - k_4[RS^{\cdot}]$$

Rearranging gives,

$$[RS^{\cdot}] = \frac{k[O_2]^{1/2}[RSH]}{k_4 + k_3[RSNO]}$$

(eqn. 7.13)

Substituting eqn. 7.13 into eqn. 7.12 gives

$$\frac{-d[RSNO]}{dt} = \frac{kk_3[O_2]^{1/2}[RSH][RSNO]}{k_4 + k_3[RSNO]}$$

7.8.2 Hg^{2+} Induced S-Nitrosothiol Decomposition

The mechanism for Hg^{2+} induced nitrosothiol decomposition is given in scheme 7.2

$$RSNO + Hg^{2+} \underset{}{\overset{K}{\rightleftharpoons}} RS(Hg^{+})NO \xrightarrow[H_2O]{k} RSHg^{+} + HNO_2 + H^{+}$$

scheme 7.2

$$\frac{-d[RSNO]_{total}}{dt} = k[C]$$

(eqn. 7.14)

where C represents the Hg^{2+} complex

$$K = \frac{[C]}{[Hg^{2+}][RSNO]}$$

(eqn. 7.15)

Substituting eqn. 7.15 into eqn. 7.14 gives

$$\frac{-d[RSNO]_{total}}{dt} = kK[Hg^{2+}][RSNO]$$

(eqn. 7.16)

If

$$[RSNO]_{total} = [RSNO] + [C]$$

then

$$[RSNO]_{total} = [RSNO] + K[Hg^{2+}][RSNO]$$

Rearranging gives

$$[RSNO]_{total} = [RSNO]\{ 1 + K[Hg^{2+}] \}$$

(eqn. 7.17)

Substituting eqn. 7.17 into eqn. 7.16 gives

$$\frac{-d[RSNO]_{total}}{dt} = \frac{kK[Hg^{2+}][RSNO]_{total}}{1 + K[Hg^{2+}]}$$

References

1. T.W.Hart, *Tet. Lett.*, 1985, **26**, 2013.

2. L.Field, R.V.Dilts, R.Ravichandran, P.G.Lenhert, G.E.Carnahan, *J. Chem. Soc. Chem. Commun.*, 1978, 249.8

Appendix

Research Colloquia, Seminars, Lectures and Conferences

The Board of Studies in Chemistry requires that each postgraduate research thesis contains an appendix listing:

A. all research colloquia, seminars and lectures arranged by the Department of Chemistry and by the Durham University Chemical Society during the period of the author's residence as a postgraduate student;

B. all research conferences attended and posters presented by the author during the period when research for the thesis was carried out;

C. details of the postgradute induction course.

A. Colloquia, Lectures and Seminars from Invited Speakers Organised by the Durham University Chemistry Department.

1993 - 1996

(* denotes lectures attended)

1993

September 13	Prof. Dr. A.D. Schlüter, Freie Universität Berlin, Germany Synthesis and Characterisation of Molecular Rods and Ribbons
September 13	Dr. K.J. Wynne, Office of Naval Research, Washington, USA Polymer Surface Design for Minimal Adhesion
September 14	Prof. J.M. DeSimone, University of North Carolina, Chapel Hill, USA Homogeneous and Heterogeneous Polymerisations in Environmentally Responsible Carbon Dioxide
September 28	Prof. H. Ila, North Eastern Hill University, India Synthetic Strategies for Cyclopentanoids via Oxoketene Dithioacetals
October 4	Prof. F.J. Feher, University of California, Irvine, USA Bridging the Gap between Surfaces and Solution with Sessilquioxanes
October 14	Dr. P. Hubberstey, University of Nottingham Alkali Metals: Alchemist's Nightmare, Biochemist's Puzzle and Technologist's Dream
October 20	Dr. P. Quayle, University of Manchester Aspects of Aqueous ROMP Chemistry*
October 21	Prof. R. Adams, University of South Carolina, USA Chemistry of Metal Carbonyl Cluster Complexes : Development of Cluster Based Alkyne Hydrogenation Catalysts*
October 27	Dr. R.A.L. Jones, Cavendish Laboratory, Cambridge Perambulating Polymers
November 10	Prof. M.N.R. Ashfold, University of Bristol High Resolution Photofragment Translational Spectroscopy : A New Way to Watch Photodissociation
November 17	Dr. A. Parker, Rutherford Appleton Laboratory, Didcot Applications of Time Resolved Resonance Raman Spectroscopy to Chemical and Biochemical Problems*
November 24	Dr. P.G. Bruce, University of St. Andrews Structure and Properties of Inorganic Solids and Polymers*

November 25	Dr. R.P. Wayne, University of Oxford The Origin and Evolution of the Atmosphere
December 1	Prof. M.A. McKervey, Queen's University, Belfast Synthesis and Applications of Chemically Modified Calixarenes*
December 8	Prof. O. Meth-Cohn, University of Sunderland Friedel's Folly Revisited - A Super Way to Fused Pyridines*
December 16	Prof. R.F. Hudson, University of Kent Close Encounters of the Second Kind

1994

January 26	Prof. J. Evans, University of Southampton Shining Light on Catalysts
February 2	Dr. A. Masters, University of Manchester Modelling Water Without Using Pair Potentials
February 9	Prof. D. Young, University of Sussex Chemical and Biological Studies on the Coenzyme Tetrahydrofolic Acid*
February 16	Prof. K.H. Theopold, University of Delaware, USA Paramagnetic Chromium Alkyls : Synthesis and Reactivity
February 23	Prof. P.M. Maitlis, University of Sheffield Across the Border : From Homogeneous to Heterogeneous Catalysis
March 2	Dr. C. Hunter, University of Sheffield Noncovalent Interactions between Aromatic Molecules*
March 9	Prof. F. Wilkinson, Loughborough University of Technology Nanosecond and Picosecond Laser Flash Photolysis
March 10	Prof. S.V. Ley, University of Cambridge New Methods for Organic Synthesis
March 25	Dr. J. Dilworth, University of Essex Technetium and Rhenium Compounds with Applications as Imaging Agents
April 28	Prof. R. J. Gillespie, McMaster University, Canada The Molecular Structure of some Metal Fluorides and Oxofluorides: Apparent Exceptions to the VSEPR Model.

May 12	Prof. D. A. Humphreys, McMaster University, Canada Bringing Knowledge to Life
October 5	Prof. N. L. Owen, Brigham Young University, Utah, USA Determining Molecular Structure - the INADEQUATE NMR way
October 19	Prof. N. Bartlett, University of California Some Aspects of Ag(II) and Ag(III) Chemistry*
November 2	Dr P. G. Edwards, University of Wales, Cardiff The Manipulation of Electronic and Structural Diversity in Metal Complexes - New Ligands
November 3	Prof. B. F. G. Johnson, Edinburgh University Arene-metal Clusters
November 9	Dr G. Hogarth, University College, London New Vistas in Metal-imido Chemistry
November 10	Dr M. Block, Zeneca Pharmaceuticals, Macclesfield Large-scale Manufacture of ZD 1542, a Thromboxane Antagonist Synthase Inhibitor
November 16	Prof. M. Page, University of Huddersfield Four-membered Rings and b-Lactamase*
November 23	Dr J. M. J. Williams, University of Loughborough New Approaches to Asymmetric Catalysis*
December 7	Prof. D. Briggs, ICI and University of Durham Surface Mass Spectrometry
1995	
January 11	Prof. P. Parsons, University of Reading Applications of Tandem Reactions in Organic Synthesis*
January 18	Dr G. Rumbles, Imperial College, London Real or Imaginary Third Order Non-linear Optical Materials
January 25	Dr D. A. Roberts, Zeneca Pharmaceuticals The Design and Synthesis of Inhibitors of the Renin-angiotensin System
February 1	Dr T. Cosgrove, Bristol University Polymers do it at Interfaces

February 8	Dr D. O'Hare, Oxford University Synthesis and Solid-state Properties of Poly-, Oligo- and Multidecker Metallocenes
February 22	Prof. E. Schaumann, University of Clausthal Silicon- and Sulphur-mediated Ring-opening Reactions of Epoxide
March 1	Dr M. Rosseinsky, Oxford University Fullerene Intercalation Chemistry
March 22	Dr M. Taylor, University of Auckland, New Zealand Structural Methods in Main-group Chemistry
April 26	Dr M. Schroder, University of Edinburgh Redox-active Macrocyclic Complexes : Rings, Stacks and Liquid Crystals
May 4	Prof. A. J. Kresge, University of Toronto The Ingold Lecture Reactive Intermediates : Carboxylic-acid Enols and Other Unstable Species*
October 11	Prof. P. Lugar, Frei Univ Berlin, FRG Low Temperature Crystallography
October 13	Prof. R. Schmultzer, Univ Braunschwieg, FRG. Calixarene-Phosphorus Chemistry: A New Dimension in Phosphorus Chemistry
October 18	Prof. A. Alexakis, Univ. Pierre et Marie Curie, Paris, Synthetic and Analytical Uses of Chiral Diamines*
October 25	Dr.D.Martin Davies, University of Northumbria Chemical reactions in organised systems*
November 1	Prof. W. Motherwell, UCL London New Reactions for Organic Synthesis*
November 3	Dr B. Langlois, University Claude Bernard-Lyon Radical Anionic and Psuedo Cationic Trifluoromethylation*
November 8	Dr. D. Craig, Imperial College, London New Stategies for the Assembly of Heterocyclic Systems
November 15	Dr Andrea Sella, UCL, London Chemistry of Lanthanides with Polypyrazoylborate Ligands
November 17	Prof. David Bergbreiter, Texas A&M, USA Design of Smart Catalysts, Substrates and Surfaces from Simple Polymers

November 22	Prof. I Soutar, Lancaster University A Water of Glass? Luminescence Studies of Water-Soluble Polymers.
November 29	Prof. Dennis Tuck, University of Windsor, Ontario, Canada New Indium Coordination Chemistry
December 8	Professor M.T. Reetz, Max Planck Institut, Mulheim Perkin Regional Meeting

1996

January 10	Dr Bill Henderson, Waikato University, NZ Electrospray Mass Spectrometry - a new sporting technique
January 17	Prof. J. W. Emsley , Southampton University Liquid Crystals: More than Meets the Eye
January 24	Dr Alan Armstrong, Nottingham Univesity Alkene Oxidation and Natural Product Synthesis*
January 31	Dr J. Penfold, Rutherford Appleton Laboratory, Soft Soap and Surfaces
February 7	Dr R.B. Moody, Exeter University Nitrosations, Nitrations and Oxidations with Nitrous Acid*
February 12	Dr Paul Pringle, University of Bristol Catalytic Self-Replication of Phosphines on Platinum(O)
February 14	Dr J. Rohr, Univ Gottingen, FRG Goals and Aspects of Biosynthetic Studies on Low Molecular Weight Natural Products
February 21	Dr C R Pulham , Univ. Edinburgh Heavy Metal Hydrides - an exploration of the chemistry of stannanes and plumbanes
February 28	Prof. E. W. Randall, Queen Mary & Westfield College New Perspectives in NMR Imaging
March 6	Dr Richard Whitby, Univ of Southampton New approaches to chiral catalysts: Induction of planar and metal centred asymmetry*
March 7	Dr D.S. Wright, University of Cambridge Synthetic Applications of Me2N-p-Block Metal Reagents
March 12	RSC Endowed Lecture - Prof. V. Balzani, Univ of Bologna Supramolecular Photochemistry

March 13	Prof. Dave Garner, Manchester University Mushrooming in Chemistry
April 30	Dr L.D.Pettit, Chairman, IUPAC Commission of Equilibrium Data pH-metric studies using very small quantities of uncertain purity

B. Conferences Attended

The 12th I.U.P.A.C. Conference on Physical Organic Chemistry in Padova, Italy, September, 1994.

Poster presented: "The Reaction of S-Nitrosothiols With The Mercury (II) Ion"

The Postgraduate Winter School on Organic Reactivity-Wisor V, Bressanone, Italy, January, 1996.

Poster presented: "Nitric Oxide Release From Slow Reacting S-Nitrosothiols"

The Royal Society of Chemistry 6th International Meeting on Reaction Mechanisms, University of Kent at Canterbury, UK, July, 1996.

Poster presented: "Nitric Oxide And The Decomposition Of S-Nitrosoglutathione"

C. First Year Induction Course, October 1991

The course consists of a series of one hour lectures on the services available in the department.

1. Introduction, research resources and practicalities
2. Safety matters
3. Electrical appliances and hands-on spectroscopic services
4. Departmental computing
5. Chromatography and high pressure operations
6. Elemental Analysis
7. Mass spectrometry
8. Nuclear magnetic resonance spectroscopy
9. Glassblowing techniques